Cranial anatomy of the Late Jurassic dwarf sauropod Europasaurus holgeri (Dinosauria, Camarasauromorpha): ontogenetic changes and size dimorphism

Jean Sebastian Marpmann, José Luis Carballido, P. Martin Sander & Nils Knötschke

[+] View supplementary material 🗗

📅 Published online: 27 Mar 2014.

✏️ Submit your article to this journal 🗗

📊 Article views: 1962

🔍 View related articles 🗗

CrossMark View Crossmark data 🗗

Taylor & Francis
Taylor & Francis Group

Cranial anatomy of the Late Jurassic dwarf sauropod *Europasaurus holgeri* (Dinosauria, Camarasauromorpha): ontogenetic changes and size dimorphism

Jean Sebastian Marpmann[a], José Luis Carballido[b]*, P. Martin Sander[a] and Nils Knötschke[c]

[a]*Steinmann Institute, Division of Palaeontology, University of Bonn, Nussallee 8, 53115 Bonn, Germany;* [b]*Consejo Nacional de Investigaciones Científicas y Técnicas, Museo Paleontológico Egidio Feruglio, Fontana 140, 29100 Trelew, Argentina;* [c]*Dinosaurier-Freilichtmuseum Münchehagen, Alte Zollstrasse 5, 31547 Rehburg-Loccum, Germany*

Sauropods were the most successful herbivorous group of dinosaurs during the Mesozoic era. Despite their supremacy as reflected in the fossil record, sauropod skulls are very rare and current knowledge of skull anatomy is based on just a few taxa. Juvenile skull bones are even rarer than adult skulls; thus, our understanding of their morphology and ontogenetic changes is limited. The recent discovery of several adult and juvenile specimens of a Late Jurassic taxon from Germany, *Europasaurus holgeri*, extends our knowledge of sauropod skull anatomy. A total of 123 skull bones, representing at least 14 skulls, were examined, described and compared to other taxa. The skull material includes several individuals of various ontogenetic stages. Because size alone is not sufficient to determine the morphological ontogenetic stage (MOS), size-independent characters were used to stage the bone elements. Detailed studies of the skull bones proved that the material represents two morphotypes, independent of ontogenetic stage. Since the original description of *Europasaurus*, new skull material has been found, and an updated skull reconstruction of an adult individual is presented here. All the autapomorphic characters of *Europasaurus* recognized in the skull (i.e. anteroposteriorly long and lateromedially narrow frontal; presence of postparietal fenestra; large participation of the jugal to the ventral rim of the skull and the orbit; presence of a postparietal foramen and single optic foramen) are plesiomorphic characters of basal sauropodomorphs and/or present in embryos and juvenile sauropods. Therefore, we consider that in *Europasaurus* these characters evolved through paedomorphosis, which resulted in the dwarf condition of this taxon.

Keywords: Macronaria; ontogeny; maturity; dimorphism; dwarfism; island rule; heterocrony; Late Jurassic

Introduction

Sauropods are the largest terrestrial vertebrates and most successful herbivorous non-avian dinosaurs to have ever existed (e.g. Upchurch *et al.* 2004; Sander *et al.* 2010; Clauss 2011; Hummel & Clauss 2011). They achieved a global distribution and spanned the Late Triassic (Buffetaut *et al.* 2000; Yates & Kitching 2003) to the very end of the Cretaceous (Fastovsky & Weishampel 2005; Schulte *et al.* 2010). These colossal animals, which could attain body lengths of more than 40 m (Sander & Clauss 2008; Sander *et al.* 2010) and weigh 100 tonnes (Upchurch *et al.* 2004; Sander & Clauss 2008; Sander *et al.* 2010), are characterized by massive bodies with pillar-like limbs, extremely elongated necks and tails, and small skulls (Upchurch *et al.* 2004; Fastovsky & Weishampel 2005, Chure *et al.* 2010).

Approximately 175 valid sauropod genera are known to date (Upchurch *et al.* 2011), with few specimens preserving cranial remains (Mannion & Upchurch 2010). Findings of sauropod embryos, hatchlings or juveniles are even less common (Carpenter & McIntosh 1994; Upchurch *et al.* 2004; Foster 2005). So far, young sauropod individuals are known from only a few specimens worldwide, yet a large number of descriptions have been made in the 21st century (see Table 1). Due to the lack of juvenile sauropod skulls, no extensive growth series exists for their cranial bones. Thus, morphological changes in ontogeny are not fully understood, and major morphological transformations are difficult to interpret (e.g. Carballido & Sander 2014; Wedel & Taylor 2013). Additional difficulties include evaluating the phylogenetic affinities of juvenile specimens (Schwarz *et al.* 2007; Carballido *et al.* 2012).

Usually, small bones of sauropod dinosaurs are considered parts of juvenile specimens. But the diminutive *Europasaurus holgeri* from Kimmeridgian shallow marine sediments of northern Germany (Sander *et al.* 2006, fig. 1) is a classical example of an island dwarf or phyletic nanoid (Sander *et al.* 2006; Benton *et al.* 2010; Stein *et al.* 2010), which most likely evolved by a heterochronic process (Sander *et al.* 2006; Benton *et al.* 2010; Stein *et al.*

Table 1. List of better-documented juvenile sauropods and preserved regions (skull, axial, appendicular). Juvenile material is tentatively staged as Em (embryonic), EJ (early juvenile) and LJ (late juvenile), mainly based on referred publications.

Taxon	Ontogenetic stage	Material	Most relevant references
Sauropoda			
Tazoudasaurus	EJ	Axial and appendicular	Allain & Aquesbi (2008)
Eusauropoda			
Barapasaurus	LJ	Appendicular bones	Bandyopadhyay *et al.* (2010)
Patagosaurus	LJ	Skull, axial and appendicular	Coria (1994)
Chebsaurus	LJ	Skull, axial and appendicular	Mahammed *et al.* (2005)
Neosauropoda			
Haplocanthosaurus	LJ	Axial and appendicular bones	Hatcher (1903)
Macronaria			
Bellusaurus	LJ	Skull, axial and appendicular	Dong (1990)
Europasaurus	EJ–LJ	Skull, axial and appendicular	Klein & Sander (2008); Carballido & Sander (2014)
Camarasaurus	LJ	Complete specimen	Gilmore (1925)
Camarasaurus	Em	Premaxilla	Britt & Naylor (1994)
Camarasaurus	LJ	Skull, axial and appendicular	Ikejiri *et al.* (2005)
Camarasaurus	LJ	Axial and appendicular	Foster (2005)
Titanosauriformes			
Brachiosaurus?	EJ	Almost complete postcranial skeleton	Schwarz *et al.* (2007); Carballido *et al.* (2011)
Titanosauria			
Titanosauria indet.	Em	Skull (rest mainly un-ossified)	Salgado *et al.* (2005); García *et al.* (2010)
Phuwiangosaurus	EJ–LJ	Axial and appendicular	Martin (1994); Martin *et al.* (1994); Martin *et al.* (1999)
'Astrodon'	LJ	Skull, axial and appendicular	Carpenter & Tidwell (2005); D'Emic (2012)
Alamosaurus	LJ	Axial and appendicular	Lehman & Coulson (2002)
Rocasaurus	LJ	Axial and appendicular	Salgado & Azpilicueta, 2000
Rincosaurus	LJ	Axial and appendicular	Calvo & Gonzáles Riga (2003)
Bonitasaura	LJ	Skull, axial and appendicular	Apesteguía (2004); Gallina (2011); Gallina & Apesteguía (2011)
Bonatitan	LJ	Skull, axial and appendicular	Martinelli & Forasiepi (2004)
Rapetosaurus	LJ	Skull, axial and appendicular	Curry Rogers & Forster (2001, 2004, 2009)
Lirainosaurus	?	Isolated teeth	Díez Díaz *et al.* (2012)
Saltasaurus	LJ	Skull, axial and appendicular	Powell (1992)
Diplodocoidea			
Diplodocidae			
Diplodocidae indet.	EJ–LJ	Axial	Woodruff & Fowler (2012); Wedel & Taylor (2013)
Diplodocus	LJ	Almost complete skull	Whitlock *et al.* (2010)
Diplodocus?	LJ	Caudal vertebrae	Foster (2005)
Apatosaurus	LJ	Axial and appendicular bones	Foster (2005)
Rebbachisauridae			
cf. *Zapalasaurus*		Axial and appendicular bones	Sagado *et al.* (2012)

2010). An heterochrony resulted in miniaturization is known as paedomorphosis, i.e. the retention of juvenile characters of ancestors (Alberch *et al.* 1979). Evidence to support the dwarf status of *Europasaurus* was provided by the histological study of several long bones carried out by Sander *et al.* (2006). The histology revealed different growth stages including juveniles, subadults and fully grown individuals.

Europasaurus is the only sauropod with several individuals that have skull elements representing various ontogenetic stages. Recently, a complete description and re-evaluation of the axial skeleton suggested the presence of two different morphotypes, which mainly differ in size and stage of skeletal maturity (Carballido & Sander

2014). Here we provide a detailed description of each skull bone recovered to date, as well as the ontogenetic stage for each of these bones. The focus of this study is to evaluate the cranial material of the most complete collection of disarticulated skull bones of a single sauropod taxon and to establish a detailed growth series to ascertain the morphological changes during sauropod cranial ontogeny, as well as potentially to detect postcranial dimorphism in the skull material. Furthermore, the presence of new autapomorphic characters are discussed as well as the recognition of three different morphological ontogenetic stages (MOS) in both morphotypes (see Carballido & Sander 2014) and the presence of numerous paedomorphic characters that result from dwarfing. *Europasaurus*

holgeri has been described as a basal macronarian (Sander *et al.* 2006), a position recently recovered by Ksepka & Norell (2010), Carballido *et al.* (2011a, b) and Carballido & Sander (2014). Nevertheless, *Europasaurus* was recovered by D'Emic (2012) as a basal brachiosaurid due to the presence of some synapomorphic characters of this group in this taxon, but noting that the missing data could strongly influence this position (see also Mannion *et al.* 2013). Although a new phylogenetic analysis lies outside the scope of this contribution, detailed comparisons with basal macronarians (e.g. *Camarasaurus*) and brachiosaurids (e.g. *Giraffatitan*, *Abydosaurus*) are here provided.

Institutional abbreviations

CM: Carnegie Museum of Natural History, Pittsburgh, PA, USA; **CLH**: Cuesta Lonsal Herrero, Galve, Spain; **DFMMh/FV**: Dinosaurier-Freilichtmuseum Münchehagen/Verein zur Förderung der Niedersächsischen Paläontologie e.V., Rehburg – Loccum, OT Münchehagen, Germany; **MACN**: Museo Argentino de Ciencias Naturales 'Bernardino Rivadavia,' Buenos Aires, Argentina; **MfN**: Museum für Naturkunde – Leibniz-Institut für Evolutions und Biodiversitätsforschung an der Humboldt-Universität zu Berlin, Germany; **MNN GAD**: Musee National du Níger, Níger; **NMB**: Staatliches Naturhistorisches Museum Braunschweig, Braunschweig, Germany; **PMU**: Palaeontological Museum, Uppsala, Sweden; **SMA**: auriermuseum Aathal, Aathal-Seegräben, near Zurich, Switzerland; **BYUVP**: Brigham Young University Vertebrate Palaeontology, Provo, UT, USA; **YPM**: Yale Peabody Museum of Natural History, New Haven, CT, USA.

Systematic palaeontology

Saurischia Seeley, 1887
Sauropodomorpha von Huene, 1932
Eusauropoda Upchurch, 1995
Neosauropoda Bonaparte, 1986
Macronaria Wilson & Sereno, 1998
Camarasauromorpha Salgado *et al.*, 1997
Genus *Europasaurus* Mateus *et al.* in Sander *et al.* 2006
Europasaurus holgeri Mateus *et al.* in Sander *et al.* 2006
(Figs 1–14)

Holotype. DFMMh/FV 291: disarticulated left premaxilla (DFMMh/FV 291.18), right maxilla (DFMMh/FV 291.17); right quadratojugal (DFMMh/FV 291.25), fragment of a braincase (DFMMh/FV 291.15), left laterosphenoid–orbitosphenoid complex (DFMMh/FV 291.16), right surangular (DFMMh/FV 291.10), left prearticular (DFMMh/FV 291.24), left dentary (DFMMh/FV 291.11),

teeth (DFMMh/FV 291), cervical and sacral vertebrae, and cervical and dorsal ribs assigned to one individual.

Referred material. The referred material represents at least 14 individuals, but probably several more. The minimum number of individuals is based on the number of single dentary rami and size differences.

Horizon and locality. Late Jurassic, middle Kimmeridgian marine carbonate rocks, bed 93 of section at Langenberg Quarry, Lower Saxony basin, Oker near Goslar, Lower Saxony, Germany.

Emended diagnosis. *Europasaurus holgeri* is diagnosed from the following characters based on the holotype and referred specimens: (1) anteroposteriorly long and lateromedially narrow frontal with a very deep orbital rim causing an extreme reduction of the frontal–prefrontal and frontal–nasal articulations; (2) absence of quadratojugal–maxilla contact and large participation of the jugal to form the ventral margin of the skull; (3) extensive ventral participation of the jugal to the orbit; (4) presence of postparietal foramen (convergently acquired in some diplodocoids); (5) single optic foramen; (6) anterior cervical vertebrae without an anterior centrodiapophyseal lamina; (7) cervical vertebrae with well-developed prespinal and postspinal laminae (convergent with *Isisaurus*; Wilson & Upchurch 2003); (8) scapular acromion with a prominent posterior projection; and (9) transverse width of astragalus twice its dorsoventral height and anteroposterior length.

Remarks. The present emended diagnosis is fairly similar to that proposed by Carballido & Sander (2014) with the addition of two autapomorphic characters (characters 3 and 5). Autapomorphic characters 8 and 9 were listed as autapomorphies by Mateus *et al.* in Sander *et al.* (2006), and are included here as well. The new materials revealed that the nasal process of the premaxilla is not anterolaterally oriented (see below), whereas the presence of a notch is a widespread character (Carballido & Sander 2014). Therefore, these two characters are no longer considered as autapomorphies of *Europasaurus*.

Description
Ontogenetic stages and morphotypes
A reliable method to determine the ontogenetic age of an individual is to histologically sample long bones and ribs (e.g. Klein & Sander 2008; Sander *et al.* 2011; Cerda *et al.* 2014); size alone is not a good proxy for age (e.g. Brochu 1996; Sander & Klein 2005; Wedel & Taylor 2013). However, this method is not applicable to the relatively narrow and delicate skull bones. Like the axial elements described by Carballido & Sander (2014), the skull elements of *Europasaurus* cannot be properly linked to certain long bones (either ribs or limbs). Therefore,

different ontogenetic information than that offered by histology must be used. Following Carballido & Sander (2014), size-independent characters were used for determining the different MOS of each skull bone. Bone surface texture has proven to be a useful criterion to stage the bones and determine a relative age (see Varricchio 1997; Tumarkin-Deratzian 2009). Bones of an ontogenetically young individual, as studied in other dinosaur groups (Sampson *et al.* 1997), have rough, very porous and possibly striated bone surfaces (Varricchio 1997), which is typical for a fast-growing tissue. As an individual ages, the porosity or vascularity of the bone surface decreases; therefore, changes in bone texture can be applied to ontogenetic stages (Varricchio 1997; Tumarkin-Deratzian 2009). Other size-independent characters are used, but are specific for each skull bone and will be mentioned with the description of their respective skull element.

The MOS corresponds to the relative age class of the individual bone element. As the degree of vascularization is used for all the elements, this character allows standardization of the MOS amongst different skull bones. Three main MOS were defined for *Europasaurus*: MOS 1 represents the youngest stage, presumably of juvenile animals; MOS 2 is used for intermediate stages; and MOS 3 is the oldest recognized stage, which, at least for most of the elements, indicates that the animal reached adulthood. These three MOS are applicable to all bones in this study, and are comparable amongst all bone types. In addition, because some skull elements could be staged into more than three MOS, sub-stages were introduced (e.g. MOS 1.1, MOS 1.2). Not all of the three MOS are always represented in every bone type. See Online Supplementary Material for a complete list of the skull material and its principal measurements.

MOS 1. This is characterized by a highly vascularized bone surface (hvbs) with small canals penetrating the bone surface at a low angle. It is typical for individuals still actively growing (e.g. Benton *et al.* 2010). A similar surface texture is present in the actively growing pleurocoels of juvenile sauropods (Carballido *et al.* 2012; Carballido & Sander 2014). Bones of very young individuals also show well-defined striations on the bone surface. Only material from the DFMMh/FV collection is referable to this growth stage. A total of 25 skull bones were assigned to MOS 1.

MOS 2. The intermediate growth stage shows a partially vascularized bone surface combined with characters of presumably fully grown individuals (e.g. distinctive structures for articulations with other bones). This growth stage is represented in at least 22 skull bones.

MOS 3. This is characterized by a generally smooth bone surface with pronounced, rugose articular facets. Further secondary characters are bone specific and will therefore be described individually for each bone type. This stage is exemplified in at least 62 skull bones, presumably representing the adult growth stage of *Europasaurus*.

Different morphotypes. Examining the material and recognizing different MOS have revealed that two different morphotypes are present amongst the *Europasaurus* samples, the presence of which was also recognized in the axial skeleton (Carballido & Sander 2014) and is identified when size differences are observed amongst elements that share the same MOS. Therefore, the two morphotypes found within the *Europasaurus* material represent two size classes. The morphotypes were distinguished as morphotype A (small) and morphotype B (large). In general, morphotype B elements are 30–55% larger than those of morphotype A. Independent of ontogenetic stage, bones of morphotype A are more 'gracile', whereas those of morphotype B are more 'robust' in appearance. Bones of morphotype B, with 27 elements, are under-represented, while material of morphotype A is represented by 65 elements.

Skull reconstruction. Based on the complete information provided here, it was possible to reassemble bone elements, presumably of adult growth stages, graphically into a new skull reconstruction of *Europasaurus holgeri* (Fig. 1). This reconstruction attempts to account for the different MOS as well as the two different morphotypes. The method used for reconstructing the skull is discussed at the end of the following description.

Skull roof bones

Of the bones of the skull roof, only the prefrontal and scleral ossicles are missing (Fig. 1). Furthermore, several elements cannot be compared due to the fact that they are too fragmented. These elements are one complete maxilla and four maxillary fragments from the DFMMh/FV collection; one maxilla from the NMB collection; one complete nasal and two fragments from the DFMMh/FV collection; and five lacrimal fragments, three from the DFMMh/FV collection and two elements from the NMB collection.

Premaxilla. Eight premaxillae (Fig. 2) have been identified amongst the *Europasaurus* material (DFMMh/FV 032, 061, 291.18, 652.2, 831, 703.5, 890.8, 982). None is completely preserved; nevertheless, DFMMh/FV 032 (which only lacks most of the nasal process) and DFMMh/FV 831 (of which the ventral body of the premaxilla is not preserved but all of its nasal process is present) provide the most complete information on the premaxillary anatomy of *Europasaurus* (Fig. 2A–D). The following description is mainly based on these last two elements, except when explicitly mentioned.

In lateral view, the premaxilla of *Europasaurus* has a rectangular shape, which gives the skull a bulldog-like
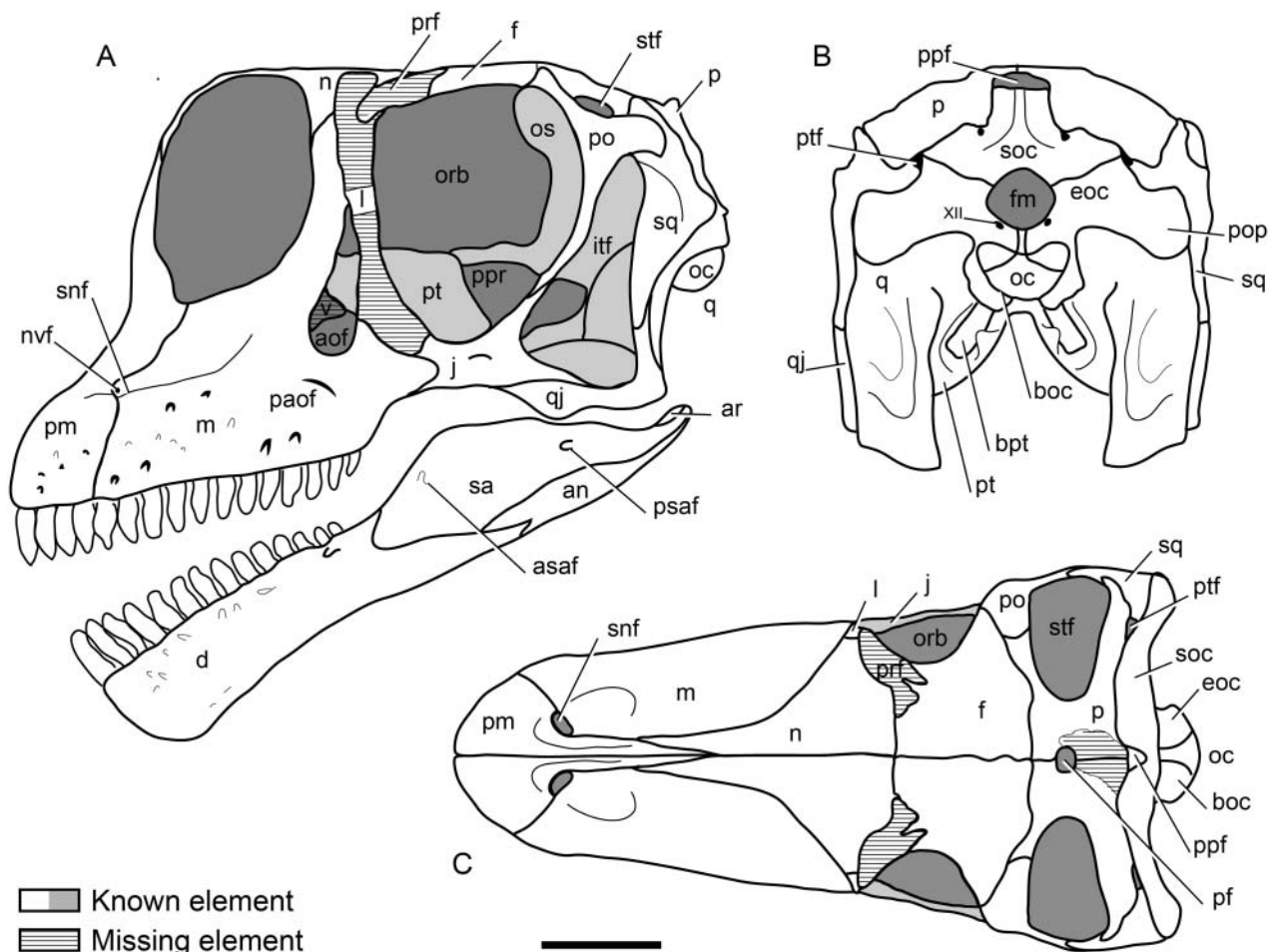
Figure 1. *Europasaurus holgeri* skull reconstruction in **A,** left lateral; **B,** occipital; and **C,** dorsal views. Reconstruction modified from Sander *et al.* (2006) on the basis of the new bones recently recovered and new observations. White bones correspond to known elements, whereas missing elements are lined. See text for a complete discussion on modified regions with respect to the previous skull reconstruction. Abbreviations: an, angular; aof, antorbital fenestra; ar, articular; asaf, anterior surangular foramen; boc, basioccipital; bpt, basipterygoid process; d, dentary; en, external naris; eoc, exoccipital; f, frontal; itf, infratemporal fenestra; j, jugal; l, lacrimal; m, maxilla; n, nasal, nvf, neurovascular foramen; orb, orbit; oc, occipital condyle; os, orbitosphenoid; p, parietal; paof, preantorbital fenestra; pf, parietal fenestra; pt, palatine; pm, premaxilla; po, postorbital; pop, paroccipital process; ppf, postparietal fenestra; prf, prefrontal; ppr, parasphenoid rostrum; psaf, posterior surangular foramen; pt, pterygoid; ptf, post-temporal fenestra; q, quadrate, qj, quadratojugal; sa, surangular; snf, subnarial foramen; soc, supraoccipital; sq, squamosal; stf, supratemporal fenestra; v, vomer. Scale bar represents 5 cm.

muzzle shape similar to that of *Camarasaurus* (Madsen *et al.* 1995), although the muzzle is more elongated dorsoventrally (Fig. 1). The nasal process of the premaxilla was initially restored as inclined anteriorly (Sander *et al.* 2006), and therefore considered an autapomorphic character of this taxon. Based on new and better-preserved premaxillae, the new reconstruction presented here (Figs 1, 2) indicates that the nasal process is oriented with a more vertical inclination, similar to that of *Camarasaurus* but not as posteriorly inclined as in *Euhelopus*. Therefore, the former autapomorphic character was excluded from the diagnosis of this taxon (see Emended diagnosis above). The ventral starting point of the nasal process is posterodorsally oriented whereas, at the height of the subnarial

foramen, the nasal process points in the dorsal direction until it contacts the nasal. This orientation gives the nasal process a step-like shape. When observed in lateral view, the nasal process starts turning dorsally at the same height of the fourth premaxillary and first maxillary tooth (Fig. 2A, C). The development of the step in the premaxilla of *Europasaurus* is thus similar to the condition observed in some specimens of *Camarasaurus* (e.g. Madsen *et al.* 1995, fig. 1; SMA 0002/02) and in *Euhelopus* (Mateer & McIntosh 1985; PMU 233). Nevertheless, this step is less developed in some specimens of *Camarasaurus*, such as the complete juvenile skull (CM 11338). In contrast, the premaxilla of the brachiosaurids *Giraffatitan* and *Abydosaurus*, as well as the premaxilla of the skull
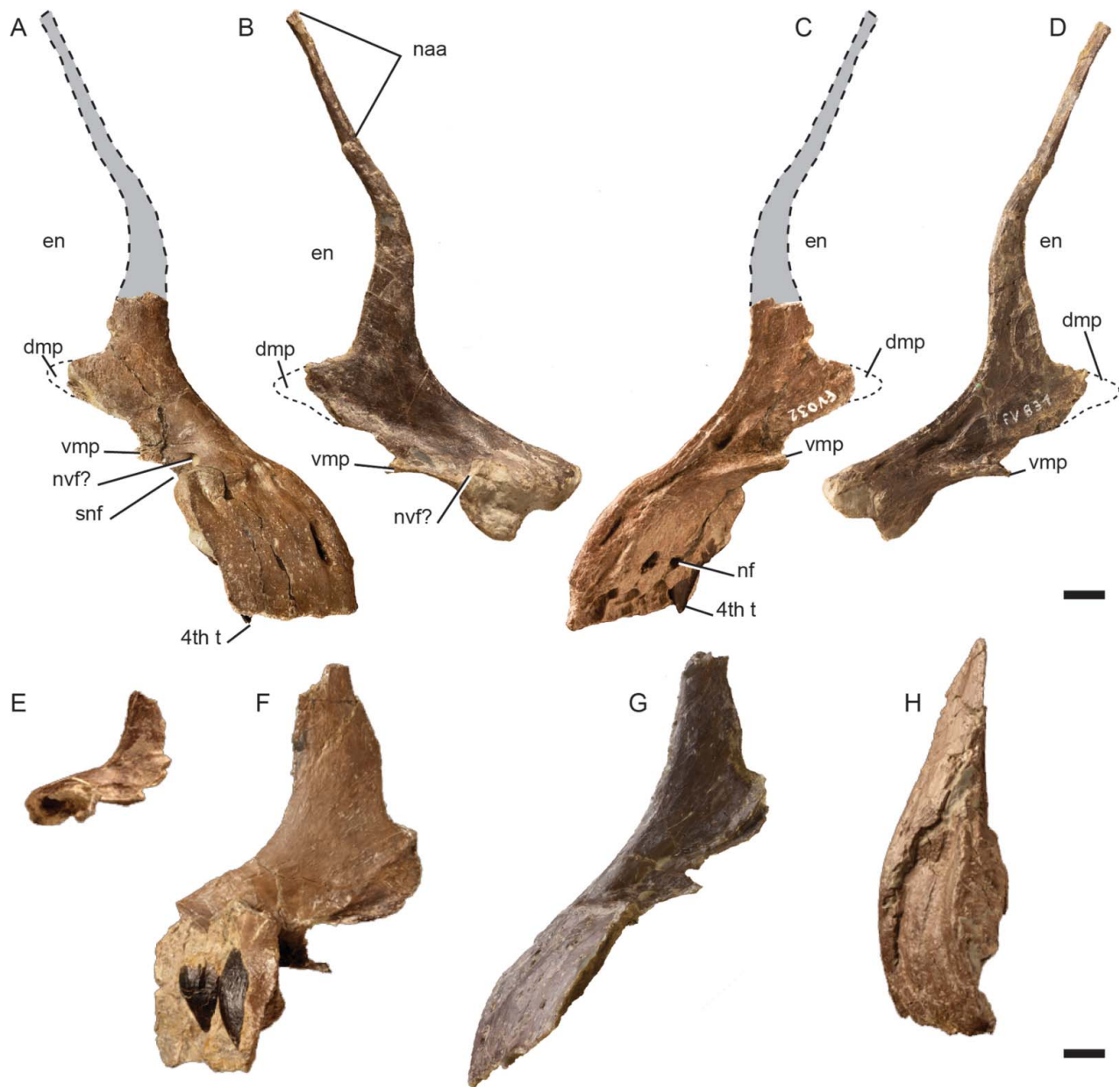
Figure 2. *Europasaurus holgeri* premaxillae. **A, C,** DFMMh/FV 032 (right) in **A,** lateral and **C,** medial views. **B, D,** DFMMh/FV 831 (right) in **B,** lateral and **D,** medial views. **E–H,** lateral views of the elements; **E,** DFMMh/FV 982 (reversed left); **F,** DFMMh/FV 291.18; **G,** DFMMh/FV 831 (reversed left); **H,** DFMMh/FV 061 (reversed left). Abbreviations: 4th t, fourth premaxillary tooth; dmp, dorsomedial process; en, external naris; naa, nasal articulation; nf, nutrient foramen; nvf, neurovascular foramen; snf, subnarial foramen; vmp, ventromedial process. Scale bars represent 2 cm.

referred to as *Brachiosaurus* sp. by Carpenter & Tidwell (1998), have a well-developed step. In these taxa, the inflection point of the nasal process is at the height of the last maxillary tooth, which is positioned further posteriorly than in *Europasaurus*, *Camarasaurus* or *Euhelopus* (MB.R. 2223.1; Chure *et al.* 2010; USNM 5730; PMU 233). As a consequence, the external narial fenestra in the aforementioned brachiosaurids is retracted and its posterior edge exceeds the last maxillary tooth. In *Europasaurus*, the external narial fenestra was reconstructed as larger than the antorbital fenestra, being almost as large as the orbit. This character is also present in other basal camarasauromorphs (*Camarasaurus*, *Giraffatitan*, *Abydosaurus*, *Malawisaurus*; Janensch 1935–1936; Madsen *et al.* 1995; Gomani 2005; Chure *et al.* 2010) and differs from the reduced and extremely retracted external narial fenestra of titanosaurs (*Rapetosaurus*, *Nemegtosaurus*, *Tapuiasaurus*; Curry Rogers & Forster 2004; Wilson

2005; Zaher *et al.* 2011). A small but well-developed fora-men is present in all premaxillae of *Europasaurus*. This foramen lies below the ventromedial process of the pre-maxilla, next to the subnarial foramen. We interpret it as a neurovascular foramen, which is well developed in *Europasaurus* (Fig. 2A).

In medial view, four large alveoli can be observed with their nutrition foramina preserved beneath them. The interdental plate union forms the nutrition foramina. Through the nutrition foramina a second generation of replacement teeth can be observed in the second and fourth alveolus of specimen DFMMh/FV 032. The teeth of *Europasaurus* are D-shaped and spatulate, although to a lesser extent than those of *Camarasaurus* and more basal sauropods. The general morphology seems to be an intermediate between the teeth of *Camarasaurus* and that observed amongst titanosauriforms. The mesial sides of the teeth show small denticles. A complete and detailed description of the teeth lies outside the scope of this publi-cation and is being prepared by V. Régent and P. M. Sander (Régent 2011). The premaxilla symphysis is not as broad as in *Camarasaurus* and is rather dorsoventrally long and anteroposteriorly narrow. The articular facet of the premaxilla for the maxilla is wider dorsally than ven-trally and becomes thinner ventrally (Fig. 2A–D). In medial view a concave articular facet is developed between the ventromedial and dorsomedial processes of the premaxilla. This facet serves as an articular facet for the premaxillary process of the maxilla, which is not pre-served in any of the recovered maxillae.

Ontogenetic changes. The MOS are identified by several size-independent characters: bone surface structure, the increasingly erect nasal process and anterior snout region, and the tendency for the muzzle to become relatively wider during ontogeny (the last character is also used for other sauropods; Whitlock *et al.* 2010). Relative muzzle width is measured as the anteroposterior length of the pre-maxillary body divided by its lateromedial width (mea-sured at the premaxillary–maxillary suture); note that in this ratio lower values indicate greater relative width. The anteroposterior length of the vertical part of the nasal pro-cess decreases in relation to the premaxillary body (Britt & Naylor 1994). Except for specimen DFMMh/FV 831, all premaxillae lack most of the dorsal part of the nasal process. The three recognized MOS are present in the pre-served premaxillae.

DFMMh/FV 982 represents MOS 1 (Fig. 2E). The tiny and incomplete bone shows an hvbs structure. The pre-maxillary body inclines at a shallow angle before it bends dorsally towards the nasal process. The muzzle region is relatively short and, notably, is relatively slender. The proximal end of the nasal process is relatively long com-pared to the premaxillary body. This premaxilla is pre-sumed to be a juvenile of morphotype A.

DFMMh/FV 291.18 represents the MOS 2 (Fig. 2F). The second oldest premaxilla is much larger than the aforementioned specimen. The lateral side is striated, while the medial side still shows an hvbs structure. As in DFMMh/FV 982, the muzzle region is relatively short and lateromedially slender. The nasal process is slightly elongated posterodorsally, and its ventral region is rela-tively long, compared to the preserved premaxillary body. This premaxilla is assigned to morphotype A.

DFMMh/FV 061 represents an intermediate MOS (2–3) (Fig. 2H). This premaxilla has a remarkable overall resemblance to the premaxilla of an embryonic specimen of *Camarasaurus* sp. (Britt & Naylor 1994, figs 16.1– 16.2; BYUVP 8967), but is also highly reminiscent of the premaxillae of *Tornieria africana* (Remes 2009, fig. 2; MB.R. 2343 and MB.R. 2346). CT scanning revealed that the premaxilla DFMMh/FV 061 bears the distinct *Europa-saurus* premature replacement teeth, and not the more cylindrical teeth of diplodocids. The bone surface is mostly fully developed with little vascularization laterally and medially to the nasal process. Its premaxillary body is much more robust than that of the other elements. Based on the MOS of this element and the significantly different shape, DFMMh/FV 061 is considered a premaxilla of morphotype B.

Five elements, which show some variation, are pre-served of MOS 3. DFMMh/FV 831 (MOS 3.1; Fig. 2B, D) has the most completely preserved nasal process, but most of its premaxillary body is missing. Bone surface texture is smooth. The erectness of the nasal process extends more posteriorly. The proximal end of the nasal process is anteroposteriorly short relative to the premaxil-lary body. DFMMh/FV 831 represents a presumed adult stage of morphotype A. DFMMh/FV 032 (MOS 3.2; Fig. 2A, C) has the most complete premaxilla body, with a decreasing anteroposterior length of the nasal process to the premaxillary body. Its bone surface structure looks fully developed, lacking any vascularization. The nasal process becomes steeper, and the muzzle becomes rela-tively wider compared to the younger elements of mor-photype A, with which this element is associated. Three specimens represent MOS 3.3. DFMMh/FV 652.2 is the largest of these, with parts of the nasal process preserved as well as its premaxilla body. The nasal process is antero-posteriorly short compared to the premaxilla body, which is the widest amongst all elements. Bone surface structure is overall very smooth and the nasal process shifts even more posterodorsally. It represents the largest known pre-maxilla of morphotype A. DFMMh/FV 703.5 is repre-sented only by the vertical rim of the nasal process and is still embedded in the rock matrix. The curvature of the nasal process is almost identical to that of DFMMh/FV 652.2 and shows a smooth bone surface structure. There-fore, DFMMh/FV 703.5 might be of the same ontogenetic stage of morphotype A. Element DFMMh/FV 890.8 is a

fragment of the anterolateral margin of the premaxilla body. The bone surface is comparable to that of DFMMh/ FV 652.2 and might be of morphotype A as well.

Maxilla. Six maxillae were discovered amongst the *Europasaurus* material (Fig. 3). DFMMh/FV 291.17 is the best preserved, corresponding to the holotype material (Fig. 3). Therefore, the maxilla description is mainly based on this specimen. A small anterodorsal part is missing, which articulates with the premaxilla and builds the posterior rim of the subnarial foramen. The maxilla has a large body with two main processes, the nasal process and a dichotomous posterior process, formed by the lacrimal process in dorsal direction and the jugal process in the posterior direction (Fig. 3B). The maxilla of *Europasaurus*, like most sauropods, has a short and weakly developed lacrimal process, except *Rapetosaurus* (Curry Rogers & Forster 2004). The nasal process is long and well developed. The posterior edge of the nasal process, up to the beginning of the lacrimal articulation (Fig. 3), surrounds the anteroventral part of the antorbital fenestra (Fig. 1). The posterodorsally oriented nasal process forms an angle of 120° with the tooth row. The lacrimal process is well developed and is pointed dorsally, strongly resembling the lacrimal process development of *Euhelopus* (PMU 233; Mateer & McIntosh 1985, fig. 5). In some specimens of *Camarasaurus* and *Abydosaurus* the lacrimal process is expanded dorsally and is not as pointed as is in *Europasaurus* and *Euhelopus* (Madsen *et al.* 1995, fig. 9; Chure *et al.* 2010, fig. 3). In contrast, the subadult specimens of *Camarasaurus* (CM 11338) and *Giraffatitan*

(Janensch 1935–1936, fig. 42; MB.R.2233.1) have a lacrimal process that is neither pointed nor expanded. In *Europasaurus* the lacrimal and nasal processes are close to each other, resulting in an anteroposteriorly short tear-shaped antorbital fenestra (Figs 1, 3). This fenestra is approximately three times as high as it is wide. Those of *Camarasaurus*, *Giraffatitan*, *Abydosaurus* and *Euhelopus* are about twice as high as they are wide. The antorbital fenestra is positioned anteriorly to the last maxillary tooth, as is common for basal sauropods (*Patagosaurus*, *Jobaria*; MACN 934; MNNTIG 5) and some camarasauromorphs like *Camarasaurus* (Madsen *et al.* 1995; CM 11338; SMA 0002/02) and *Euhelopus* (PMU 233). The brachiosaurids *Giraffatitan*, *Abydosaurus* and *Brachiosaurus* sp. have a posteriorly retracted antorbital fenestra. In these taxa, the posterior edge of the antorbital fenestra is positioned posteriorly to the last maxillary tooth (MB. R.2223.1; Chure *et al.* 2010; USNM 5730). In derived titanosaurs the antorbital fenestra is positioned even further posteriorly from the last maxillary teeth (e.g. *Rapetosaurus*, *Tapuiasaurus*; Curry Rogers & Forster 2004; Zaher *et al.* 2011). In *Europasaurus* a small and lateromedial flat opening can be seen below the antorbital fenestra, which is interpreted as the preantorbital fenestra, a synapomorphic character of Neosauropoda (Wilson & Sereno 1998). The preantorbital fenestra is completely opened in derived titanosaurs and diplodocoids (e.g. *Diplodocus*, *Tapuiasaurus*), while in *Europasaurus* (Fig. 3A), as well as *Camarasaurus* and *Euhelopus*, the preantorbital fenestra is located beneath the antorbital fenestra; in

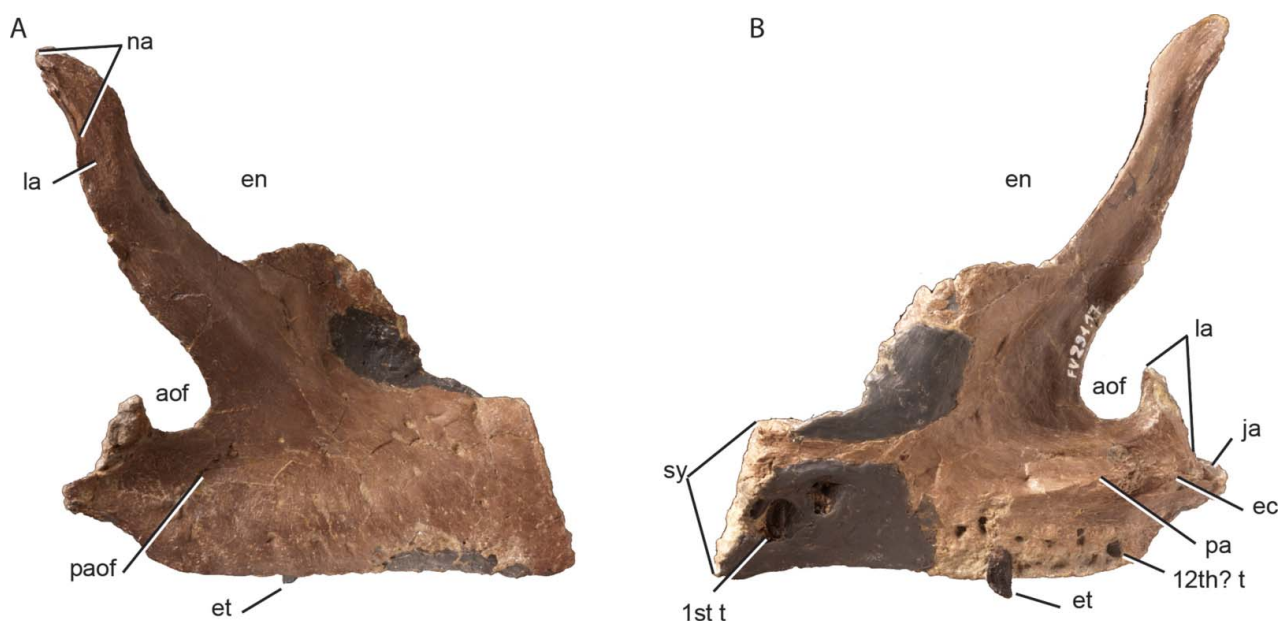**Figure 3.** *Europasaurus holgeri* right maxilla (DFMMh/FV 291.17) in **A,** lateral and **B,** medial views. Abbreviations: 1st t, first tooth; 12th? t, twelfth tooth; aof, antorbital fenestra; ec, ectopterygoid articulation; en, external naris; et, erupted tooth (eighth?); ja, jugal articulation; la, lacrimal articulation; na, nasal articulation; paof, preantorbital fenestra; sy, symphysys. Scale bar represents 1 cm.

Giraffatitan and *Abydosaurus* the preantorbital fenestra is more anteriorly positioned with respect to the antorbital fenestra, but in a similar position with respect to the tooth row.

In medial view, the tooth row is poorly preserved, so the number of maxillary teeth present in *Europasaurus* is difficult to ascertain (Fig. 3B). Based on visible teeth and the alveolus, and the distance between them, the estimated number of teeth for the maxilla is 12–13. Basal sauropods usually have more than 12 teeth (16 in *Jobaria*: Sereno *et al.* 1999; 14–15 in *Atlasaurus*: Monbaron *et al.* 1999). Some macronarians, such as *Camarasaurus* and *Euhelopus*, have between nine and 10 maxillary teeth (Madsen *et al.* 1995; Wilson & Upchurch 2009). Brachiosaurids have a variable number of teeth (12 in *Giraffatitan*: Janensch 1935–1936; 14–15 in *Brachiosaurus* sp.: Carpenter & Tidwell 1998; 10 in *Abydosaurus*: Chure *et al.* 2010). The tooth row of *Europasaurus* takes up more than 70% of the total length of the maxillary body. Only replacement teeth can be observed in the element DFMMh/FV 291.17, visible through the nutrition foramina and broken surfaces. All show three or four small denticles on their mesial sides. While the anterior (non-erupted) teeth seem to be aligned vertically with respect to the tooth row, the single erupted tooth is slightly posteriorly inclined. The crown shape of this tooth is slightly posteriorly twisted (around 15°), much less than *Abydosaurus* or *Giraffatitan* (30–45°; D'Emic 2012; Mannion *et al.* 2013). In fact, most of the preserved teeth of *Europasaurus* have straight crowns, and only a few having marginally twisted crowns (Régent 2011).

Ontogenetic changes. Of the six preserved maxillae, the large specimen DFMMh/FV 291.17 is nearly complete, and is classified as MOS 3 due to its smooth bone surface structure and well-developed processes and articular facets. The element is attributed to morphotype A. The MOS and the morphotype are the same for the incomplete maxilla NMB-2207-R. Although the position of these maxillary bone fragments (DFMMh/FV 077, DFMMh/FV 218, DFMMh/FV 911 and DFMMh/FV 1046) can be determined, they cannot be staged or assigned to any morphotype.

Nasal. Three nasals are preserved amongst the *Europasaurus* material (Fig. 4). One almost complete and undeformed left nasal was recently discovered (DFMMh/FV 1150.1; Fig. 4), and is the basis for most of the description. Two nasal fragments were identified as the posterior part of a right nasal (DFMMh/FV 1037.13), and as the anterior section of another right nasal (DFMMh/FV 867.4).

Posteriorly the nasal becomes overlapped by the frontal, both bones being extremely narrow in this section. Neither of the nasals is complete in this section, although a small facet for the articulation with the frontal and the
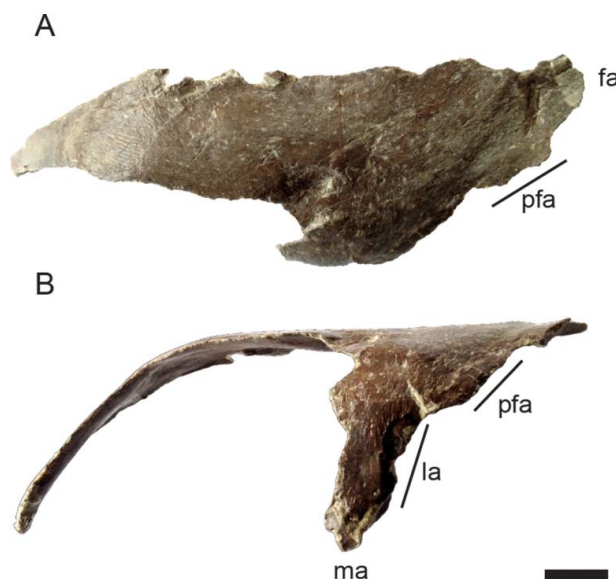

Figure 4. *Europasaurus holgeri* right nasal (DFMMh/FV 1150.1) in **A,** lateral and **B,** dorsal views. Abbreviations: fa, frontal articulation; la, lacrimal articulation; ma, maxilla articulation; pfa, prefrontal articulation. Scale bar represents 1 cm.

prefrontal is observed in DFMMh/FV 1150.1 (Fig. 4A). The nasal–frontal articulation is mediolaterally narrow, evident in both the frontal and the nasal (Fig. 4; see below). The dorsolateral edge of the nasal has a rough surface, which is interpreted as the contact of the nasal with the prefrontal. The ventrolateral process, which articulates with the lacrimal and the nasal process of the maxilla (e.g. *Camarasaurus*; Madsen *et al.* 1995; Figs 1, 4), is almost completely intact. The nasal–lacrimal articulation is discernible in lateral view and covers most of the posterior edge of the ventrolateral process (Fig. 4A, B), whereas the articulation for the nasal process of the maxilla is slightly preserved on the ventral edge of the ventrolateral process of the nasal (Fig. 4B). If the lateroventral process is almost vertically oriented, as in Figures 1 and 4 and follows the orientation of this process in other sauropods (e.g. *Camarasaurus*, *Giraffatitan*; Janensch 1935–1936, supplement 7; Madsen *et al.* 1995, figs 1, 5), the premaxillary process of the nasal is horizontally directed before turning ventrally. In contrast, in *Giraffatitan* the nasal is dorsally directed. The morphology of the newly recovered nasal is clearly different from that previously reconstructed by Sander *et al.* (2006, fig. 1b), which seems to follow the nasal morphology of *Giraffatitan*.

Ontogenetic changes. The three preserved nasals probably belong to fully grown individuals, as indicated by their smooth bone surface structure, and they are accordingly staged as MOS 3. The nasals fit perfectly into the above-mentioned premaxillary process and the frontal of
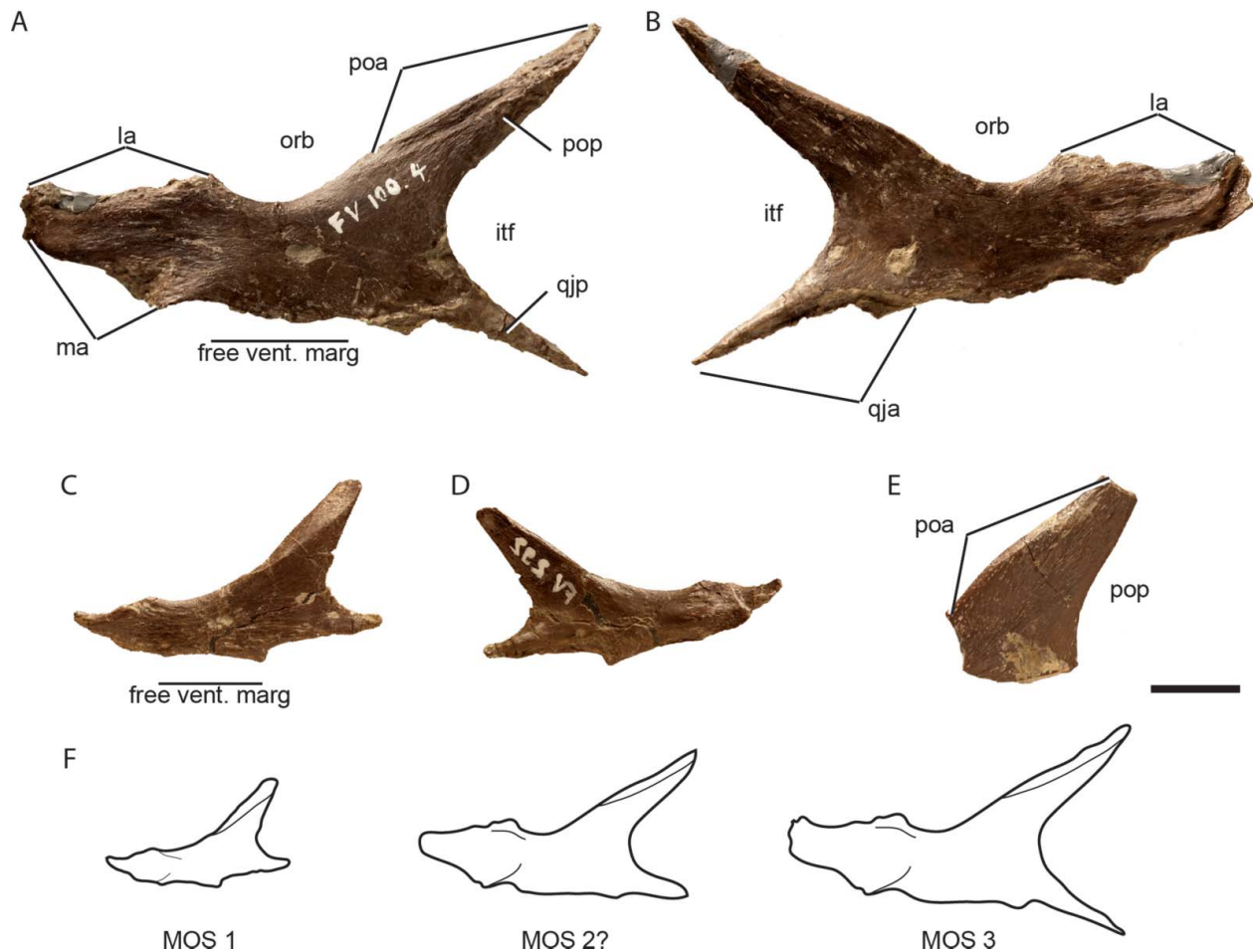
Figure 5. *Europasaurus holgeri* jugals. **A, B,** DFMMh/FV 100.4 (left) in **A,** lateral and **B,** medial views. **C, D,** DFMMh/FV 292 (reversed right) in **C,** lateral and **D,** medial views. **E,** DFMMh/FV 908 (reversed right) in lateral view. **F,** reconstruction of the different MOS detected amongst preserved jugals in lateral view; white line indicates free ventral margin of the element. Abbreviations: itf, infratemporal fenestra; la, lacrimal articulation; ma, maxilla articulation; orb, orbit; poa, postorbital articulation; pop, postorbital process; qjp, quadratojugal process. Scale bar represents 1 cm.

DFMMh/FV 552, which further underlines the assumption that they belong to fully grown individuals, and possibly the same morphotype (A). Further comparisons and ontogenetic inferences are not possible.

Jugal. Three jugals are preserved amongst the *Europasaurus* material (Fig. 5): two are almost complete (DFMMh/FV 292 and 100.4) and the third is preserved as the basal part of the postorbital process (DFMMh/FV 908). The following description is mainly based on element DFMMh/FV 100.4, a nearly complete specimen that only lacks a small anterior part of the maxillary process and the tip of the quadatojugal process (Fig. 5A, B).

The jugal, which is greatly reduced in camarasauromorphs, is a long and well-developed bone in *Europasaurus*. Comparing this element to other related sauropods (e.g. *Camarasaurus*, *Giraffatitan* and *Abydosaurus*) is difficult because the jugal of *Europasaurus* is more

reminiscent of those of basal sauropodomorphs. The jugal of *Europasaurus* contributes to the infratemporal fenestra, the orbit and the ventral margin of the skull, but does not contribute to the antorbital fenestra.

The posteroventral or quadratojugal process of the jugal is extremely fragile and narrow, showing an articular scar along its ventromedial side, which extends from the posterior acute tip to almost the mid-length of the maxillar process, just below the anteroventral side of the posterodorsal or postorbital process. The quadratojugal process and the postorbital process diverge from each other at an angle of 75°, forming the anteroventral margin of the infratemporal fenestra (Figs 1, 5A, B).

The postorbital process articulates with the postorbital through an anteriorly long surface, which extends along the third dorsal edge of the postorbital process of the jugal. The centre between the dorsal part of the postorbital process and the posterodorsal edge of the maxillary

process forms a rounded concavity, which contributes to the ventral margin of the orbit. In this respect the jugal of *Europasaurus* is also more similar to those of basal sauropodomorphs (e.g. *Riojasaurus*, *Massospondylus*; Gow *et al.* 1990; Bonaparte & Pumares 1995), compared to the jugals with reduced ventral participation in the orbit of most sauropods (e.g. *Camarasaurus*, *Giraffatitan*; Janensch 1935–1936; Madsen *et al.* 1995). Similarly, a large participation of the jugal to the orbit was recently described for titanosaur embryos (Salgado *et al.* 2005; García *et al.* 2010), but has not been observed in any adult titanosaur described so far (e.g. *Rapetosaurus*, *Nemgtosaurus*, *Tapuiasaurus*; Nowinski 1971; Curry Rogers & Forster 2004; Zaher *et al.* 2011).

The well-developed maxillary process of the jugal contacts both the maxilla and the lacrimal. The anterolateral side of the maxillary process of the jugal contacts the medial side of the maxilla. Therefore, about half of the maxillary process of the jugal is covered by the maxilla (Fig. 5A). The medial side of the maxillary process of the jugal shows a small sigmoidal scar. The indented lateral side of the maxillary process of the jugal fits perfectly in the medial side of the jugal process of the maxilla, resulting in a stiffer articulation between the elements.

The jugal–quadratojugal articulation occurs solely on the ventral margin of the jugal (Fig. 5B), and not on its posterior margin (as is seen in *Camarasaurus*). Therefore, *Europasaurus* has the derived state that is characteristic of macronarians more derived than *Camarasaurus* (Curry Rogers 2005; Mannion *et al.* 2013). The jugal–quadratojugal and jugal–maxilla articulations leave a wide gap in the centre of the jugal bone. Thus, the jugal contributes to the ventral rim of the skull (Figs 1, 5A, B). In the adult, the length of this free ventral margin is at least a quarter of its total anteroposterior length. A large participation of the jugal to the ventral margin of the skull is a widespread character amongst sauropods more basal than *Shunosaurus* (Chatterjee & Zheng 2002; e.g. *Plateosaurus*, *Massospondylus*, *Mussaurus*, *Melanorosaurus*; Galton 1984, 1985; Sues *et al.* 2004; Pol & Powell 2007; Yates 2007). In more derived forms jugal participation to the ventral margin of the skull is precluded by the direct maxilla–quadratojugal contact (e.g. *Mamenchisaurus*, *Turiasaurus*, *Camarasaurus*, *Nemegtosaurus*; Nowinski 1971; Madsen *et al.* 1995; Ouyang & Ye 2002; Royo Torres & Upchurch 2012), or is extremely reduced as in *Giraffatitan* (Janensch 1935–1936). Amongst camarasauromorphs a reduced participation of the jugal has been described only for *Giraffatitan* and reconstructed for *Malawisaurus* (Gomani 2005; Royo Torres & Upchurch 2012) and *Abydosaurus* (Chure *et al.* 2010, fig. 3B). Of these taxa only *Giraffatitan* has an undoubted minor participation of the jugal to the ventral margin of the skull (MB.R. 2223.1). For *Malawisaurus*, Gomani (2005, fig. 31) published only a general reconstruction, and this character was not

specified. In *Abydosaurus*, this participation could be the result of breakage, as it is observed in the right lateral view, but absent in left lateral view (Chure *et al.* 2010, fig. 3). If present the contribution of the jugal to the ventral margin of the skull in *Abydosaurus* is as reduced as in *Giraffatitan*. Therefore, the large participation of the jugal to the ventral rim of the skull is here interpreted as an autapomorphic character of *Europasaurus*, resulting in a reversion to the plesiomorphic character of basal sauropodomorphs.

As in *Camarasaurus* (Madsen *et al.* 1995) and most camarasauromorphs, the jugal does not contribute to the antorbital fenestra in *Europasaurus* (Figs 1, 5A, B), differing from the large participation of the jugal in the antorbital fenestra of diplodocoid sauropods (e.g. *Diplodocus*; CM 11255; Upchurch 1998; Whitlock 2011) and the titanosaur *Tapuiasaurus* (Zaher *et al.* 2011). A reduced participation of the jugal to the antorbital fenestra was described for some titanosauriforms such as *Giraffatitan* (Janensch 1935–1936), *Abydosaurus* (Chure *et al.* 2010) and *Rapetosaurus* (Curry Rogers & Forster 2004). In *Europasaurus* the jugal is completely excluded from the antorbital fenestra, as in *Nemegtosaurus* (Nowinski 1971) and *Camarasaurus* (Madsen *et al.* 1995).

Ontogenetic changes. Two elements are of MOS 1 (DFMMh/FV 292 and 908) and one element is of MOS 3 (DFMMh/FV 100.4). No intermediate MOS have been identified yet amongst the preserved jugals of *Europasaurus*. Size-independent characters are the structure of the bone surface, the articular facets on the processes, the length and ratio of the free space of the ventral margin of the jugal that contributes to the ventral rim of the skull, the shape of the curvature between postorbital and quadratojugal process, and the angle of the curvature of the dorsal margin that forms the ventral margin of the orbit.

The bone surface structure of DFMMh/FV 292 (Fig. 5C, D), which is only a few centimetres long, is highly vascularized with striations showing small grooves and canals penetrating the bone surface at a low angle, and is therefore staged as MOS 1. The articular facets of the maxillary, the postorbital as well as the quadratojugal process are not yet well developed. The postorbital process has a small and smooth edge on its lateral side. The free ventral margin has a length of 11.3 mm and contributes 33% to the total length of the jugal. The curvature between the postorbital and the quadratojugal processes is J-shaped and the angle of the dorsal margin shows an inclination of 20°. DFMMh/FV 292 is associated with morphotype A.

DFMMh/FV 908 (Fig. 5E) has the same bone surface structure as DFMMh/FV 292, including a pronounced edge on the lateral side of the postorbital process. Even though the postorbital process is about 55% larger in DFMMh/FV 908 than in DFMMh/FV 292, both have

typical bone surface structures of juveniles (Fig. 5). Given the similar size of the basal postorbital process of the jugal of DFMMh/FV 292 and DFMMh/FV 100.4 (described below), the surface structure of this jugal is considered to be a bone of the larger morphotype B.

DFMMh/FV 100.4 is assigned to MOS 3 (Fig. 5A, B). Bone surface structure is rather plain on the lateral side and rugose on the articular facets of all processes, especially the maxillary and postorbital ones. This jugal shows a small ridge for the articulation with the lacrimal along the anterodorsal margin. The free ventral margin is 18.8 mm long and contributes 25% to the total length of the jugal (Fig. 5A, B); therefore, it contributes proportionally less than the jugal staged as MOS 1. The curvature between the postorbital and the quadratojugal processes is more L-shaped, and the angle of the dorsal margin shows an inclination of about 40°. This bone seems to be an adult specimen of morphotype A.

Lacrimal. There can be no detailed description of the lacrimal because only fragments have been found, in both the DFMMh/FV and NMB collections. The correct position within the skull is only known for specimen DFMMh/FV 994 and the two elements of NMB-2207-R. The correct position of the other specimens (DFMMh/FV 521, DFMMh/FV 858.2) remains unknown.

Ontogenetic changes. Judging by the bone surfaces of DFMMh/FV 994, DFMMh/FV 521 and DFMMh/FV 858.2, they seem to belong to fully grown animals and are attributed to MOS 3. However, due to their fragmentary nature, the association of DFMMh/FV 521 and DFMMh/FV 858.2 is highly uncertain. The lacrimal elements associated with other bones in the NMB-2207-R specimen are of morphotype A, but the morphotype for the DFMMh/FV lacrimals cannot be determined with certainty.

Frontal. The frontal of *Europasaurus* (Fig. 6) is known from four individuals (DFMMh/FV 162, 552, 389 and 907, all being left except for 552 which corresponds to a right frontal). Whereas in *Camarasaurus* the paired frontals and parietals are rarely found disarticulated (Madsen *et al.* 1995), this is not true for *Europasaurus* in which all the frontals were found disarticulated and were probably never tightly sutured or fused with any other skull bone (see Discussion). As can be inferred from the visible articulation surfaces of the frontals, and by comparison to other sauropods (e.g. *Giraffatitan*, *Camarasaurus*; MB.R.2223.1; CM 11338), the frontal contacts the parietal posteriorly and posterolaterally, the postorbital posterolaterally, the prefrontal anterolaterally, the nasal anteromedially, and the laterosphenoid and orbitosphenoid ventrally (Figs 1, 6A, B). The smooth interdigitating frontal–frontal suture is transversely long. This suture determines the longest axis of the frontal. The frontal is anteroposteriorly longer than it is lateromedially wide.

This is an unusual character for a eusauropod dinosaur (Wilson 2002) and is therefore interpreted as an additional autapomorphic character. Similar proportions were recently described for a titanosaur embryo (García *et al.* 2010).

The frontal–frontal contact is completely preserved in two of the frontals (DFMMh/FV 162, 552; Fig. 6), and both have an edge that is completely straight, without any sign of fenestration, even in their posterior ends. Thus the planar frontal–frontal articulation differs from the interdigitated shape of *Giraffatitan* or *Camarasaurus*. Additionally, the frontals are excluded from the so-called frontoparietal fenestra (also the pineal fenestra; Madsen *et al.* 1995), which in *Europasaurus* is only surrounded by the parietals and here referred to as the parietal fenestra. The presence of a similar fenestra was reported for the dicraeosaurids *Amargasaurus* and *Dicraeosaurus* (Salgado & Calvo 1992; Paulina Carabajal *et al.* in press), the diplodocid *Apatosaurus* (Balanoff *et al.* 2010), some specimens of *Camarasaurus* (Madsen *et al.* 1995), and recently for titanosaur embryos (Salgado *et al.* 2005; García *et al.* 2010). The posterior surface of the frontal, which mainly articulates with the parietal, forms an angle of about 100° with the frontal–frontal suture axis. Additionally, the frontal also articulates with the parietal throughout half of its posterolateral edge, whereas the distal half of this surface articulates with the frontal process of the postorbital (not preserved), as is also observed in other sauropods (e.g. *Camarasaurus*, *Giraffatitan*; CM 11338; MB.R.2223.1). Therefore, the posterior edge of the frontal does not form the anterior margin of the supratemporal fenestra because the parietal and postorbital precludes its participation, a widespread character amongst sauropods more derived than *Shunosaurus* (e.g. Wilson 2002), with a reversion probably in *Turiasaurus* (Royo Torres & Upchurch 2012).

The orbital margin is not very long and does not bear any sign of ornamentation. While some camarasauromorphs (e.g. *Camarasaurus*, *Nemegtosaurus*; Madsen *et al.* 1995; Wilson 2005) show an ornamented margin, *Europasaurus* is more similar to the completely smooth frontal of *Giraffatitan* (MB.R.2223.1). The orbital rim deeply penetrates the frontal. This concavity is well visible in dorsal or ventral view (Fig. 6). The deep penetration of the orbital rim into the skull roof results in very reduced contacts for the prefrontal and the nasal. The general condition in sauropods is that the anterior edge of the frontal contacts the nasal and the prefrontal, forming an anterior articulation surface that is almost equally wide as the widest section of this bone. In contrast, in the frontals of *Europasaurus*, the articulation surface for the nasal and prefrontal is about half the width of the widest area of the bone (Fig. 6). The prefrontal (not preserved) was firmly interdigitated by a deep articular facet with the frontal. Although the frontal–prefrontal articulation is extremely
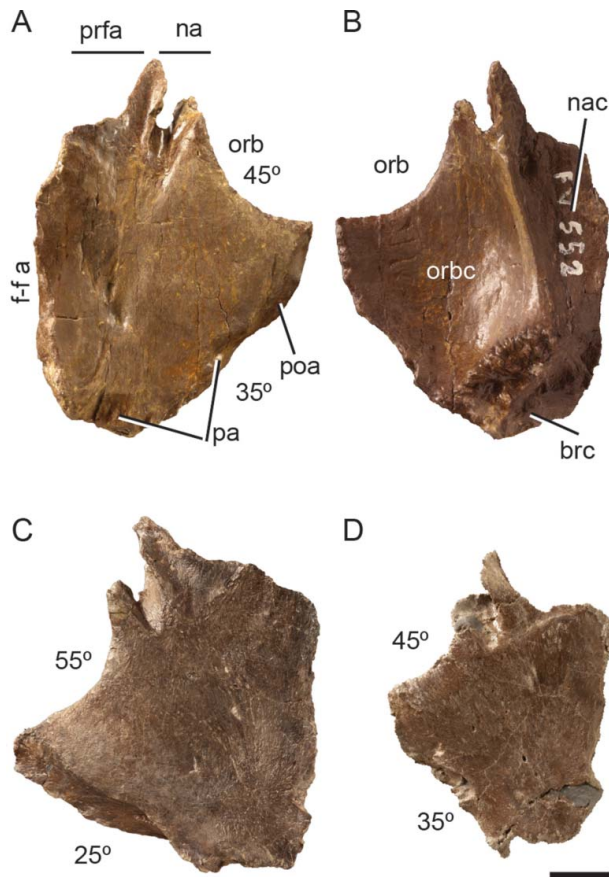
Figure 6. *Europasaurus holgeri* frontals. **A, B,** DFMMh/FV 552 (right) in **A,** dorsal and **B,** ventral views. **C, D,** dorsal views of the elements; **C,** DFMMh/FV 162 (left); **D,** DFMMh/FV 389 (right). Abbreviations: brc, brain cavity; f-f a, frontal–frontal articulation surface; na, nasal articulation; nac, narial cavity; orb, orbit; orbc, orbital cavity; pa, parietal articulation; poa, postorbital articulation; prfa, prefrontal surface articulation. Scale bar represents 1 cm.

reduced in *Europasaurus*, and thus has previously been regarded as an autapomorphic character of this taxon (Sander *et al.* 2006), the frontal–nasal articulation is also very reduced. This reduction is the result of the deep indentation of the rim of the orbit into the frontal. The combination of a long and narrow frontal with a deep orbital rim and narrow articulation surface for the prefrontal and nasal is considered here to be an autapomorphic character of *Europasaurus*.

In ventral view three separated concavities can be distinguished: the orbital, nasal and cranial cavities (Fig. 6B). The orbital cavity is separated from the nasal cavity by a well-developed ridge that extends posteriorly from the deep insertion of the prefrontal to the anterior end of the rugose articular surface for the laterosphenoid–orbitosphenoid. This crest diverges from the frontal–frontal axis articulation in an angle that varies between 20° (in DFFMh/FV 552) and almost 45° (in DFFMh/FV162). The

articulation between the frontal and the laterosphenoid–orbitosphenoid precludes any connection between the cranial cavity and the orbital cavity. The cranial cavity is connected with the nasal cavity by a small gap, which is slightly convex ventrally. This gap leads to a dorsal cavity that gives way for the olfactory bulb, which is separated from the brain cavity. Besides their position, these cavities also differ from each other in their size, the orbital cavity being the largest as in other sauropods (e.g. *Nigersaurus*, *Camarasaurus*, *Giraffatitan*, *Phuwiangosaurus*, *Rapetosaurus*; Janensch 1935–1936; Madsen *et al.* 1995; Curry Rogers & Forster 2004; Sereno *et al.* 2007; Suteethorn *et al.* 2009). In *Europasaurus* the cranial cavity is small and shallow, while the orbital cavity is about twice the size. Whereas the large size of the orbital cavity seems to be a widespread character amongst sauropods, the sizes of the brain cavity and nasal cavity in the frontal show some variation amongst taxa. The frontal of *Europasaurus*, with a small brain cavity and middle-sized nasal cavity, resembles other non-titanosaur camarasauromorphs such as *Camarasaurus* and *Phuwiangosaurus* (Madsen et al. 1995; Suteethorn *et al.* 2009). However, as the cranial cavity forms, the frontals of titanosaurs seem to have an extensive participation that covers more than half of the anteroposterior region of the frontal (e.g. *Rapetosaurus*, *Bonitasaura*; Curry Rogers & Forster 2004; Gallina & Apesteguía 2011). In titanosaurs the nasal cavity is reduced and confined to the anteriormost part of the frontal (e.g. *Rapetosaurus*; Curry Rogers & Forster 2004), whereas in diplodocoids (e.g. *Nigersaurus*; Sereno *et al.* 2007) the nasal cavity seems to be equally as large as the cranial cavity. Thus, the relative size of these cavities in *Europasaurus*, as well as other basal camarasauromorphs (e.g. *Camarasaurus*, *Giraffatitan*, *Phuwiangosaurus*), is provisionally regarded as a plesiomorphic character for basal camarasauromorphs, since the same shape is observed in non-neosauropod sauropods (e.g. *Spinophorosaurus*; Knoll *et al.* 2012; GCP-CV-4229).

Ontogenetic changes. Of the four frontals preserved, three are MOS 1 and one is MOS 3, and no intermediate stage could be determined. Size-independent characters used are: the structure of the bone surface; the sharpness of the orbitonasal ridge separating the posterior part of the orbital cavity, nasal cavity and braincase region on the ventral side; and the bending depth of the curvature of the posterior part of the orbital cavity on the ventral side. The morphotypes are differentiated by the difference in the angle in which the orbital rim opens laterally. The angle is measured from the medial suture to the central point of the orbital rim (Fig. 6). Importantly, both morphotypes are distinguished from all other sauropods in which the orbital rim does not open as much anterolaterally (an autapomorphic character of *Europasaurus*).

Currently two stages are recognized amongst the elements assigned to MOS 1. DFMMh/FV 907 (MOS 1.1) preserves the anterior region between the medial suture and the medial process for the prefrontal. Ontogenetically, this element is the youngest *Europasaurus* frontal to have been found. The dorsal and the ventral bone surface show an hvbs structure. The orbitonasal ridge is not very prominent but rather rounded, and shows a relatively flat bulge. The curvature of the orbital cavity appears very shallow. Determining the morphotype is not as obvious as with the other three elements because of its fragmentary state. Given its small size in combination with the described size-independent characters, this fragmentary frontal probably belongs to morphotype B (see DFMMh/FV 162).

MOS 1.2 is represented by two elements (DFMMh/FV 162 and 389). DFMMh/FV 162 is an almost complete frontal (Fig. 6C); the dorsal side consists mainly of an hvbs structure with several striations. The orbitonasal ridge is sharper and more developed than in DFMMh/FV 907 and is very similar to DFMMh/FV 389. The posterior part of the orbital cavity is deeper than in DFMMh/FV 907, but still quite shallow. Despite the autapomorphic characters of *Europasaurus* being present, some aspects of the morphology of the frontal are different. In DFMMh/FV 389 and DFMMh/FV 552 the orbital rim opens at 45° anterolaterally, measured between the margin of the medial suture and the middle of the lateral orbital opening, whereas the orbital rim opens slightly more laterally in DFMMh/FV 162; the contact with the nasal is more lateromedially extended; and the articular facet for the anterolateral process of the parietal opens at 25° anterolaterally, measured from the posterior margin, and is inclined at a shallow angle posteroventrally. The most lateral point extends further laterally than in DFMMh/FV 389, leading to a larger posterior section of the orbital cavity. No hook-shaped structure is visible on the posterolateral margin. The angle at which the orbital rim opens laterally, the articular facet for the parietal, and the missing hook-shaped structure are characteristics that differ exceedingly from DFMMh/FV 389 and DFMMh/FV 552. Therefore, this frontal is not assigned to morphotype A but to morphotype B. DFMMh/FV 389 only lacks the lateral process for the prefrontal and was reconstructed on the posteromedial margin (Fig. 6D). The bone surface structure, the sharpness of the ridge, and the depth of the posterior part of the orbital cavity are very similar to DFMMh/FV 162. The size-independent characteristics lead to the assumption that DFMMh/FV 389 and DFMMh/FV 162 are of a similar age but of different size (Fig. 6C, D). Their morphology is very different from each other; however, the orbital rim opens at 45° in the anterolateral direction, and therefore more anterior than in DFMMh/FV 162. Furthermore, the contact for the nasal is short, and the articular facet for the anterolateral process of the parietal opens at 35° anterolaterally, and is inclined

at a steep angle posteroventrally. The most lateral point does not extend as far laterally as in DFMMh/FV 162, leading to a smaller posterior part of the orbital cavity. A hook-shaped structure is visible on the posterolateral margin that would fit the depression of the anteromedial process of a parietal. The morphotype for this frontal is A.

DFMMh/FV 552 represents MOS 3 (Fig. 5A, B). Bone surface structure shows almost no striation and no visible vascularization, and has an overall smooth appearance. The ventral ridge is very sharp and strongly pronounced, and the depression of the posterior part of the orbital cavity is very deep, as is expected in an adult individual. Except for its similar large size to DFMMh/FV 162, morphology is the same as in DFMMh/FV 389 with the same angles and morphological characteristics that define morphotype A.

Parietal. Five isolated parietals identified as *Europasaurus* have been found (Fig. 7), including a left and right parietal (DFMMh/FV 581.2 and 581.3) that undoubtedly belong to the most complete braincase DFMMh/FV 581.1, representing a single specimen. These two parietals are nearly complete, except for a small medial portion that would prevent their middle sections from contacting each other. The following description is mainly based on these two osteologically mature parietals (see below), because they are not only the most complete elements but also articulate with the complete preserved braincase as mentioned above.

In dorsal view the parietals are anteroposteriorly narrow (Fig. 7A, B), whereas in posterior view they have a rectangular shape. Their height is almost half of the length of their total lateromedial width (Fig. 1B). The dorsoventral height of the parietals is slightly larger than the height of the foramen magnum. This difference is not as major as it is in most sauropods (e.g. *Camarasaurus*, *Giraffatitan*), but it is clearly different from the dorsoventrally short parietals of derived titanosaurs (*Nemegtosaurus*, *Rapetosaurus*; Nowinski 1971; Curry Rogers & Forster 2004).

The ventral side of the posterolateral process of the parietal articulates with the supraoccipital at its medial half and therefore covers all the dorsolateral margin of the supraoccipital. The ventral margin of the posterolateral process expands further laterally beyond the supraoccipital–exoccipital contact. This condition prevents any contact of the squamosal with the supraoccipital and differs from the condition seen in diplodocids (Calvo & Salgado 1995; Upchurch 1998; Remes 2006). The parietal forms the dorsolateral part of the post-temporal fenestra (Fig. 1B). Medioventrally, the post-temporal fenestra is surrounded by the exoccipital and laterally by the squamosal (Fig. 1B), a widespread character amongst nonflagelicaudatan sauropods (Upchurch 1998; Wilson 2002; Upchurch *et al.* 2004; Whitlock 2011). Amongst macronarian neosauropods, the exclusion of the parietal from
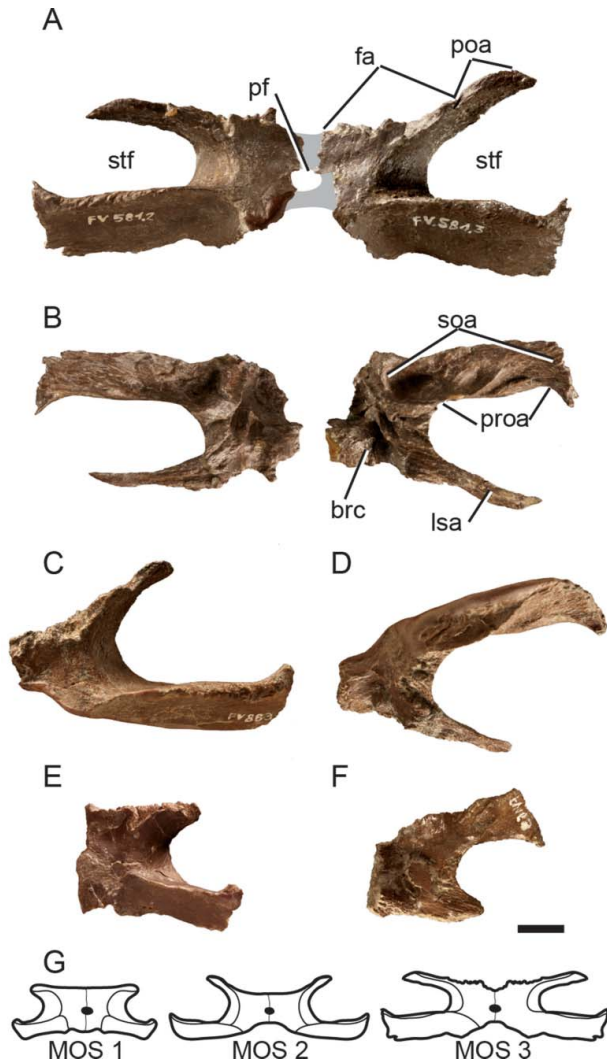
Figure 7. *Europasaurus holgeri* parietals. **A, B,** DFMMh/FV 291.2 (left) and DFMMh/FV 291.3 (right) in **A,** dorsal and **B,** ventral views. **C, D,** right parietal (DFFNh/FV 883) in **C,** dorsal and **D,** ventral views. **E, F,** reversed left parietal (DFMMh/FV 169) in **E,** dorsal and **F,** ventral views. **G,** reconstruction of the different MOS detected amongst preserved parietals in dorsal view. Grey zone in A corresponds to broken surface, reconstructed in the base of broken edged and articulation of parietals into the braincase (DFMMh/FV 291.1). Abbreviations: brc, brain cavity; fa, frontal articulation; lsa, laterosphenoid articulation; pf, parietal fenestra; poa, postorbital articulation; proa, prootic articulation; soa, supraoccipital articulation; stf, supratemporal fenestra. Scale bar represents 1 cm.

the post-temporal fenestra has been reported only for some titanosaurs such as *Nemegtosaurus* and *Malawisaurus* (Wilson 2005). The anterior planes of the posterolateral processes of the parietals articulate with the prootics ventrally; these processes form the posterior wall of the supratemporal fenestrae. The medial and anterior margins of the supratemporal fenestrae are formed dorsally by the parietals and ventrally by the laterosphenoid. The left

parietal (DFMMh/FV 581.2) contacts the left laterosphenoid on the medial side of the parietal, whereas the anterolateral process of the parietal matches the lateral process of the laterosphenoid. The supratemporal fenestra of *Europasaurus* is around 2.5 times wider lateromedially than long anteroposteriorly (Fig. 7A, B). Therefore, the supratemporal fenestra is anteroposteriorly short, as can be seen in most sauropods (e.g. *Spinophorosaurus*, *Camarasaurus*, *Giraffatitan*), but differs from *Shunosaurus* (Chatterjee & Zheng 2002) and basal sauropodomorphs. The dorsal distance that separates the supratemporal fenestrae is only slightly larger (1.1) than the long axis of the fenestra. Similar proportions are observed in some specimens of *Camarasaurus* (Madsen *et al.* 1995, fig. 25; SMA 0002/02). The dorsal distance between the supratemporal fenestrae observed in the juvenile specimen of *Camarasaurus* (CM 11338) is proportionally larger than that observed in *Europasaurus* and other *Camarasaurus* specimens. This difference amongst *Camarasaurus* specimens indicates that there must be some ontogenetic or even specific variations amongst this taxon, although based on *Europasaurus* ontogenetic evidence the former hypothesis is supported. In flagellicaudatan diplodocoids, the supratemporal fenestrae are separated from each other (with a distance that is around as twice as long as the longest axis of the fenestrae); however, a supratemporal fenestra in rebbachisaurids seems to be absent, as in *Nigersaurus* (Sereno *et al.* 2007), or very reduced, as in *Limaysaurus* (Calvo & Salgado 1995; Salgado *et al.* 2004). Similar proportions to those observed in *Europasaurus* appear to be present in basal sauropods (*Spinophorosaurus*, *Mamenchisaurus*, *Jobaria*; GCP-CV-4229; Ouyang & Ye 2002, Fig. 5, MNNTIG4). In contrast, the distance that separates both supratemporal fenestrae in *Giraffatitan* is just half of the length of the long axis of the supratemporal fenestra (MB.R.2223.1). This also holds true for *Abydosaurus* (Chure *et al.* 2010). The distance between both supratemporal fenestrae in the skull referred to as *Brachiosaurus* sp. (Carpenter & Tidwell 1998; USNM5730) is almost the same as the lateromedial length, and is thus relatively wider than in *Giraffatitan*. Therefore, the shape of the parietals in *Europasaurus* is more reminiscent of other sauropods, but not of *Giraffatitan* or *Abydosaurus*.

Besides the supratemporal fenestra, two other fenestrae are surrounded by the parietals, the parietal fenestra and the postparietal fenestra. The parietal fenestra is discernible as a small concavity, especially in dorsal view of the left parietal. The exact size or shape of this fenestra is unknown because of missing bone fragments that prevent the parietals from contacting medially (Fig. 7A). The presence of another fenestra, the postparietal fenestra, is also evident when both parietals are manually articulated with the braincase. In dicraeosaurid sauropods (e.g. *Suuwassea*, *Amargasaurus*; Salgado & Calvo 1992; Harris

2006), this fenestra is surrounded by the parietals dorsally and the supraoccipital ventrally, as in *Europasaurus*. The postparietal fenestra is easily visible in posterior view of the skull (see Fig. 1 and below). The occurrence of a postparietal fenestra is an unusual character for a non-dicraeosaurid sauropod (e.g. Salgado & Calvo 1992; Upchurch 1998; Wilson 2002). Its presence was recognized as a synapomorphic character of dicraeosaurids (e.g. Salgado & Calvo 1992; Upchurch 1998; Wilson 2002; Whitlock 2011). Amongst non-dicraeosaurid sauropods, the postparietal fenestra was only described for the basal sauropod *Spinophorosaurus* (Knoll *et al.* 2012) and an indeterminate titanosaur from the Late Cretaceous of Argentina (Paulina-Carabajal & Salgado 2007). Therefore, its presence in *Europasaurus* is interpreted as an autapomorphic character of this taxon, convergently acquired in *Spinophorosaurus* and, amongst neosauropods, in dicraeosaurids and probably some derived titanosaurs.

Ontogenetic changes. Recognized size-independent characters include the structure of the bone surface, the structure of the articular facet of the distal part on the anteroventral plane of the posterolateral process, the absence or presence of a depression at the proximal end of the anteroventral plane of the posterolateral process, the development of the frontoparietal contact, the width of the supratemporal fenestra in relation to the total width of the parietal (both measured lateromedially), and the depth of the brain cavity. The width (lateromedially measured) of the supratemporal fenestra in relation to the length (anteroposteriorly measured) is not a distinctive character since the openings differ greatly from each other even in the two parietals that belong to the same braincase.

Two elements are interpreted as being MOS 1 (DFMMh/FV 1078 and 169; Fig. 7G, H). DFMMh/FV 1078 is the smallest parietal with an hvbs structure, and on the ventral side the part that encloses the brain cavity is very shallow and shows no ridges. The laterally longer posterolateral process has a rugose structure. The articular facet for the squamosal does not seem to be well developed in the distal part on the anteroventral plane of the posterolateral process, and neither is the articular facet for the laterosphenoid. The development of these articular facets is a sign for a rather loose connection of these bones. The lack of a depression at the proximal end of the anteroventral plane of the posterolateral process also shows that there was a very loose connection with the supraoccipital–prootic notch, which explains the disarticulated nature of the specimen. No depression for the hook of the frontal is visible, either because it is still in a juvenile stage or because it belongs to morphotype B, in which the frontal does not have the hook-shaped structure. Considering this specimen undoubtedly belongs to an ontogenetically young individual, determining the morphotype is rather difficult. The size difference with

DFMMh/FV 169 is not significant, and the morphology is very similar in the two specimens, except for the slightly more developed articular facet for the squamosal in the parietal DFMMh/FV 1078. Therefore, the parietal DFMMh/FV 1078 cannot be associated with either morphotype.

The other element, staged MOS 1 as well, is DFMMh/FV 169 (Fig. 7G, H). This very fragile parietal is slightly larger than DFMMh/FV 1078, yet both have the same bone surface structure, as well as the incomplete anterolateral process. Additionally, this specimen lacks parts of the posterior region of the medial margin. The articular facet on the posterolateral process is less rugose than on the smallest parietal of DFMMh/FV 1078, making it even more loosely connected to the squamosal. A depression for the supraoccipital cannot be found at the ventral side of the parietal (Fig. 7). The anterior side for the contact to the frontal also lacks a depression. The width of the supratemporal fenestra is slightly larger than half the width of the parietal. Parietal DFMMh/FV 169 probably represents a diminutive specimen of morphotype A but, as in DFMMh/FV 1078, the characters are not reliable enough to determine the morphotype.

DFMMh/FV 883 represents the MOS 2 (Fig. 7E, F). This partially incomplete parietal is the largest and most robust parietal, especially in its posterolateral process. Some spots with a vascularized bone surface structure are visible in the medial region on the ventral side. The rest of the bone surface is very rugose and the articulation for the squamosal shows well-pronounced facets to allow a tight connection. The anterolateral process is short, as in DFMMh/FV 169 and DFMMh/FV 1078, but the distal part of the process is almost complete. Compared to the posterolateral process, the anterolateral process is rather short. Parietal DFMMh/FV 883 lacks the depression on the ventral side, and judging by the preserved parts, it seems that there was none, which is similar to the potentially juvenile specimens. The parts enclosing the brain cavity are shallow, as in DFMMh/FV 169 and DFMMh/FV 1078. The frontoparietal contact is not well developed. The width of the supratemporal fenestra is slightly smaller than half the width of the parietal, and therefore the supratemporal fenestra is relatively wider than that measured in the parietals staged as MOS 1. This large parietal, which had not finished growing, is probably a subadult of morphotype B and would have become even larger.

Two elements are assigned to MOS 3: DFMMh/FV 581.2 and DFMMh/FV 581.3 (Fig. 7A–D). Both parietals have a highly rugose bone surface structure lacking any vascularization. The only differences between the specimens are the stouter appearance of DFMMh/FV 581.3 in the lateromedial direction and the different shapes of the supratemporal openings. Both have relatively long anterolateral processes compared to the more juvenile stages above. These processes seem to have had a good

articulation with the laterosphenoids. The articular facets on the posterolateral processes are well developed, showing ridges and grooves for a strong connection to the squamosals. Both show deep depressions at the proximal ends of the anteroventral plane of the posterolateral processes, which are needed for a firm contact with the notch of the supraoccipital–prootic region. The sections that contribute to the brain cavity are deep and winding, giving the brain more space. This corresponds to the ontogenetic change from juvenile to adult, although the brain cavity is proportionally larger in juveniles. This specimen has a comparatively wider supratemporal fenestra, indicating that the relative distance that separates the supratemporal fenestrae tend to decrease through ontogeny. The anterior regions for the frontoparietal contact show well-developed contacts for the hook-shaped structures described in morphotype A of the frontals, suggesting that DFMMh/FV 581.2 (Fig. 7) and DFMMh/FV 581.3 are both part of morphotype A. When parietals DFMMh/FV 581.2 and DFMMh/FV 581.3 are put together, the presence of the postparietal foramen in the skull can be regarded as an autapomorphic character.

Postorbital. Five right postorbitals (DFMMh/FV 095, 097, 098, 380, 555/1) and one left postorbital (DFMMh/FV 096) from *Europasaurus* were studied (Fig. 8). This triradiate bone is interpreted as a fused postorbital and postfrontal (Upchurch *et al.* 2004), also described as postorbital + postfrontal by Janensch (1935–1936). As in other sauropods, the postorbital participates in forming the lateral margin of the supratemporal fenestra, the anterior edge of the infratemporal fenestra, and the posterior border of the orbit (Fig. 1A). The postorbital has three processes: the ventral or jugal process, which is the longest and most gracile process; the posterior or squamosal process; and the anterior or parietal–laterosphenoid process, which is the most robust of the processes (Fig. 8A).

The maximum anteroposterior length of this element is measured from the anterior to the posterior process in dorsal view. This distance is slightly longer than half of the dorsoventral height of the jugal process of the postorbital. A postorbital of similar robustness is present in *Camarasaurus* (Madsen *et al.* 1995; CM11338) and *Euhelopus* (Mateer & McIntosh 1985; PMU 233). The postorbital of *Giraffatitan* is more gracile (anteroposterior length is less than half of the dorsoventral height; Janensch 1935–1936; MB.R. 2223.1). The squamosal process is tapered at its distal end and contacts the concave sulcus of the squamosal medially. The anterior process is deflected medially to support the lateral process of the laterosphenoid and the anterolateral process of the parietal. The gracile jugal process is anteroventrally oriented and articulates with the postorbital process of the jugal.

Ontogenetic changes. Size-independent characters used are the bone surface structure and the depression on the
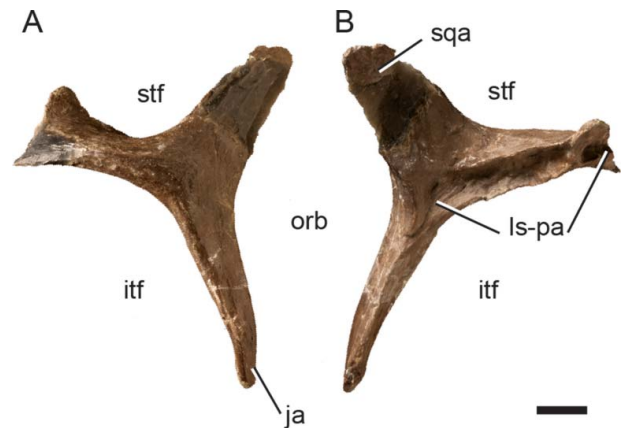

Figure 8. *Europasaurus holgeri* left postorbital (DFMMh/FV 96) in **A,** lateral and **B,** medial views. Abbreviations: itf, infratemporal fenestra; ja, jugal articulation; ls-pa, laterosphenoid and parietal articulation surface; orb, orbit; sqa, squamosal articulation; stf, supratemporal fenestra. Scale bar represents 1 cm.

medial side, where the three processes come together, which is very deep in adult specimens. Nonetheless, the shape of the jugal process, a contribution of the postorbital to the orbital opening, is not a reliable character in *Europasaurus*, because the orbit remains relatively large throughout ontogeny. Two elements are considered MOS 1 and four elements MOS 3. The postorbitals contain no intermediate MOS.

MOS 1 is observed in DFMMh/FV 555/1. This element is rather gracile in appearance compared to the more robust, presumably adult elements. As DFMMh/FV 555/1 is rather small with an hvbs structure and no depression on the medial side, it probably is a juvenile. Overall morphology is similar to morphotype A adult specimens DFMMh/FV 095 and DFMMh/FV 096; thus, we assign the same morphotype to DFMMh/FV 555/1. DFMMh/FV 380 is of about the same size as the ontogenetically older DFMMh/FV 095 and DFMMh/FV 096, but shows juvenile characters such as an hvbs structure and the absence of the depression on the medial side. Therefore, it is assigned to MOS 1 of the larger morphotype B.

DFMMh/FV 095 and DFMMh/FV 096 are associated with MOS 3.1. These two elements vary only slightly in morphology, and both show a finished surface structure with medial depressions. Specimen DFMMh/FV 096 attaches very well to the other skull bones of the adult morphotype A, which are all visualized in the new skull reconstruction. DFMMh/FV 097 and DFMMh/FV 098 represent MOS 3.2. These two elements show a very rugose surface. While DFMMh/FV 097 has the rugose surface predominantly on its medial side, DFMMh/FV 098 also has a rugose surface on the ventral side down toward the base of the jugal process, which is mostly absent. Both show an extensive deep depression situated medially in DFMMh/FV 097. Element DFMMh/FV 097

varies the most from the other postorbitals, but seems to be deformed diagenetically rather than representing another morphotype. Since DFMMh/FV 097 is deformed and broken and DFMMh/FV 098 is incomplete, it is difficult to determine the morphotype beyond the staging.

Squamosal. Four isolated squamosals have been discovered (DFMMh/FV 657 is a right element, while 993, 1004 and 712.2 are left squamosals), but only one specimen (DFMMh/FV 712.2) is almost complete (Fig. 9). The latter only lacks a small distal fragment of the ventral process, and the following description is mainly based on this nearly complete element. The squamosal is a triradiate bone with a large ventral process that contacts the quadrate, an anterior process in which the postorbital is inserted, and a medial process that mainly articulates with the parietal and exoccipital–paroccipital–opisthotic complex. In size and shape, the squamosal fits very well with the complete braincase DFMMh/FV 581.1.

As described by Madsen et al. (1995) for *Camarasaurus*, the squamosal has the shape of a question mark in lateral view. Its anterior process supports the posterior process of the postorbital and both form the temporal bar. The articular facet for the postorbital is broad, with a maximum length of around 2.27 cm and a maximum height of 1.36 cm. The ventral margin of this articular facet is well marked by a lateral expansion that serves as ventral support for the postorbital. The squamosal forms a small posterolateral margin of the supratemporal fenestra, which is mainly formed by the parietal and postorbital (Fig. 1).
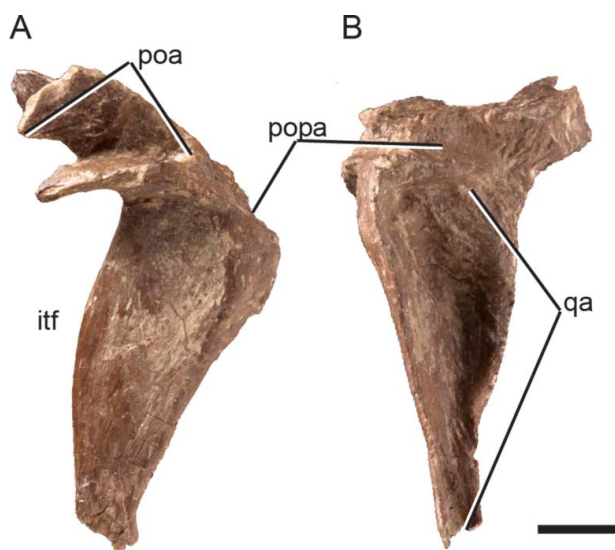

Figure 9. *Europasaurus holgeri* left squamosal (DFMMh/FV 712.2) in **A,** lateral and **B,** medial views. Abbreviations: itf, infratemporal fenestra; poa, postorbital articulation; popa, paraoccipital process articulation; qa, quadrate articulation. Scale bar represents 1 cm.

The medial process of the squamosal is robust and articulates mainly with the exoccipital–paroccipital–opisthotic complex through its entire posteroventral margin. It is also completely inset in the concave dorsal margin of the exoccipital–paroccipital–opisthotic complex, covering most of the complex and laterally bounding the post-temporal fenestra. The exact position and size of the post-temporal fenestra remains unknown because no squamosal was found in articulation with the almost completely preserved braincase. Posteromedially, the squamosal contacts the posterolateral process of the parietal, forming a broad overlapping surface. The parietals are included in forming the post-temporal fenestra (see above), since the squamosal does not expand medially. If present, this medial expansion would exclude the parietals from the post-temporal fenestrae, observed in other sauropods (e.g. *Negmetosaurus*, *Apatosaurus*; Wilson 2005; Balanoff *et al.* 2010).

The ventral process of the squamosal is long and gracile. In lateral view, its anterior edge is slightly convex, whereas its posterior border is mainly straight and only curves posteriorly at the ventral end. The anterior margin of the ventral process of the squamosal builds the upper posterior part of the infratemporal fenestra. The squamosal is, besides the postorbital, the element that contributes most to the shape of the infratemporal fenestra (Fig. 1).

Ontogenetic changes. Size-independent characters consist of the bone surface structure and the shape of the articular facets. Morphotype determination depends on the size in correlation with the bone surface structure, especially of the medial process. Three elements are MOS 1 and one element is MOS 3. The squamosal has no intermediate MOS.

Four specimens represent MOS 1. While specimens DFMMh/FV 657, 993 and 1004 all show an hvbs structure with depressions and articular facets already accentuated, given their surface and size, the first and the third seem to be juveniles of morphotype A. DFMMh/FV 993 also shows an hvbs structure, but with striated articular facets. It is even larger than the MOS 3 squamosal of morphotype A, suggesting that this specimen is a juvenile of the larger morphotype B.

Element DFMMh/FV 712.2 is interpreted as being MOS 3. The bone surface is only slightly vascularized in some spots, but looks mostly finished. The articular facets are very rugose and the squamosal fits very well onto the braincase of DFMMh/FV 581.1. Therefore, this squamosal is assigned to morphotype A.

Quadratojugal. Three quadratojugals have been found. Only a completely preserved right quadratojugal pertains to the holotype material (DFMMh/FV 291.25; Fig. 10). Quadratojugals DFMMh/FV 785.2 and DFMMh/FV 734 each consist of a different right element, preserving the posterior half and the anterior half, respectively. The

complete quadratojugal (DFMMh/FV 291.25) can be manually articulated with the quadrate DFMMh/FV 062, indicating an individual of similar size and proportions. As in other sauropods, when viewed in lateral view, the quadratojugal is L-shaped with a horizontally long process (the anterior process) and a short vertical process (the dorsal process) (Fig. 10). The length of the dorsal process is around three-quarters that of the anterior process. In *Europasaurus* the quadratojugal forms the lateroventral margin of the infratemporal fenestra (Figs 1A, 10). The quadratojugal articulates with the squamosal (dorsolaterally), the quadrate (medially), and the jugal (anteriorly) (Figs 1, 10). Based on the reconstruction of the skull (Fig. 1) and the articulation of the quadratojugal with the surrounding bones, the anterior process of the quadratojugal is horizontally aligned with the tooth row (Fig. 1), as in *Camarasaurus* (Madsen *et al.* 1995), instead of being inclined, as in *Giraffatitan* and *Abydosaurus* (Janensch 1935–1936; Chure *et al.* 2010).
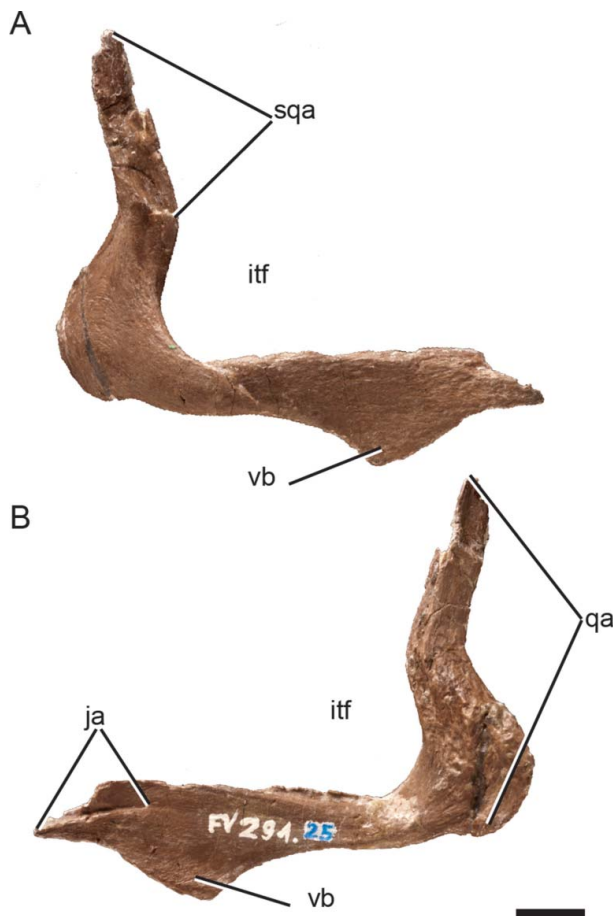

Figure 10. *Europasaurus holgeri* right quadratojugal (DFMMh/FV 291.25) in **A,** lateral and **B,** medial views. Abbreviations: itf, infratemporal fenestra; ja, jugal articulation; qa, quadrate articulation surface; sqa, squamosal articulation surface; vb, ventral bulge. Scale bar represents 1 cm.

The dorsal process is sigmoidal, following the same shape observed in the lateral edge of the quadrate. While the dorsal part of the squamosal process is narrow and delicate, its ventral section is stouter and anteroposteriorly wider. This expansion or wider zone articulates with the lateroventral margin of the lateral outline of the quadrate (Fig. 10B). Half of the lateral surface of the squamosal process of the quadratojugal serves as an articular plane for the squamosal (Fig. 10A). The articulation between these two bones starts at the same point in which the dorsal process changes its orientation, from dorsal towards posterodorsal (Fig. 10A). In medial view, the articulation of the quadratojugal with the quadrate is clearly distinguishable as a rough surface, which extends through almost all the medial surface of the vertical process (Fig. 10). Therefore, as was noted above, the quadratojugal articulates with the quadrate, medially, and with the squamosal, laterally.

The anterior process of the quadratojugal is straight on its dorsal outline, as is observed in most other sauropods (e.g. *Camarasaurus*, *Brachiosaurus*; Janensch 1935–1936; Madsen *et al.* 1995). The ventral margin has a marked ventral expansion that forms a prominent ventral keel (Fig. 10), which is present in both quadratojugals preserving this section of the bone (DFMMh/FV 291.25 and 734). A ventral expansion was recently described as a synapomorphic character of Brachiosauridae (D'Emic 2012), and scored associated with the derived state (presence of ventral projection) only in *Europasaurus*, *Giraffatitan* and *Abydosaurus* (D'Emic 2012, chapter 9). The ventral expansion of the latter two of these taxa has a slightly developed and more rounded ventral expansion than that of *Europasaurus*. A similar ventral rounded expansion to that of *Giraffatitan* (Janensch 1935–1936, fig. 21) and *Abydosaurus* (Chure *et al.* 2010, fig. 3) is present in some specimens of *Camarasaurus* (Madsen *et al.* 1995, fig. 19; SMA 0002/02). In addition, a similar, although much more developed, ventral expansion is present in the anterior ramus of the quadratojugal of *Tapuiasaurus* (Zaher *et al.* 2011, fig. 1). A rounded and slightly developed ventral expansion is also present in *Nemegtosaurus* (Wilson 2005, fig. 3), which is more similar to that of *Giraffatitan* than *Europasaurus* or *Tapuiasaurus*. Therefore, the presence of a ventral expansion in the quadratojugal seems to have a broader distribution amongst camarasauromorph sauropods and is not only restricted to taxa of the clade Brachiosauridae. The articulation for the jugal can be observed in medial view and is formed as a thin scar that extends up to the level of the ventral expansion.

Ontogenetic changes. Size-independent characters used are the bone surface structure and the articular facets. Since the incomplete specimens are both from different parts of the bone, they can only be compared to the complete quadratojugal. It is difficult to predict if the shape of

the keel-like tip on its anteroventral margin and the form of the vertical process are ontogenetic differences or features that differ between morphotypes. Two elements are presumably MOS 2 and one element is MOS 3. No element was determined to be a juvenile.

MOS 2 is represented by two elements (DFMMh/FV 734 and DFMMh/FV 785.2). DFMMh/FV 734 is preserved as the anterior part of the horizontal branch with a smooth bone surface structure, but a rounded tip of the keel. It is the same size as DFMMh/FV 291.25, but the keel does not look complete developed compared to the stage three specimen. DFMMh/FV 785.2 is significantly smaller than DFMMh/FV 291.25, but shows a straight rather than a sigmoidal vertical process (*cf*. Madsen *et al.* 1995, fig. 19; DNM 28 and DNM 975), although the articular facets are well developed and the bone surface structure has a smooth surface. Considering too much material is missing in both elements, it is hard to assign them to a specific stage. But both look slightly younger than the MOS 3 specimen, and thus for now they will be assigned MOS 2. The different features of DFMMh/FV 734 and DFMMh/FV 785.2 probably mean that they are both of the other morphotype.

MOS 3 is assigned to DFMMh/FV 291.25. This complete element fits very well into the squamosal DFMMh/FV 712.2. Bone surface structure is smooth and has a finished appearance. The vertical process is sigmoidal and the horizontal rather straight, while articular facets on both are well accentuated and rugose. The keel-like tip is pointed and lateromedially sharp. It is regarded as being of morphotype A.

Palate

Neither a palatine nor a vomer has been found from the palate area. As the quadrate is most commonly referred to as being part of the palate region, this scheme will be used here, too. Of the 13 preserved palate elements amongst the *Europasaurus* material, the quadrates are listed first, because the quadrate is a bone that connects several skull regions, including the palate region, with those of the skull roof. The description follows an anterior direction starting at the quadrate.

Quadrate. In total, six isolated quadrates from *Europasaurus* were collected (DFMMh/FV 057, 058, 062, 062.1, 972.2, 1032.2) (Fig. 11). The following description is mainly based on the largest and best-preserved element (DFMMh/FV 062), which fits well onto braincase DFMMh/FV 581.1 and squamosal DFMMh/FV 712.2.

Quadrate DFMMh/FV 062 is well preserved and its general shape is reminiscent of quadrates of other relatively basal macronarians (e.g. *Camarasaurus*, *Giraffatitan*; Janensch 1935–1936; Madsen *et al.* 1995). The articular surfaces for the squamosal, quadratojugal and pterygoid are well defined (Fig. 11). A well-developed
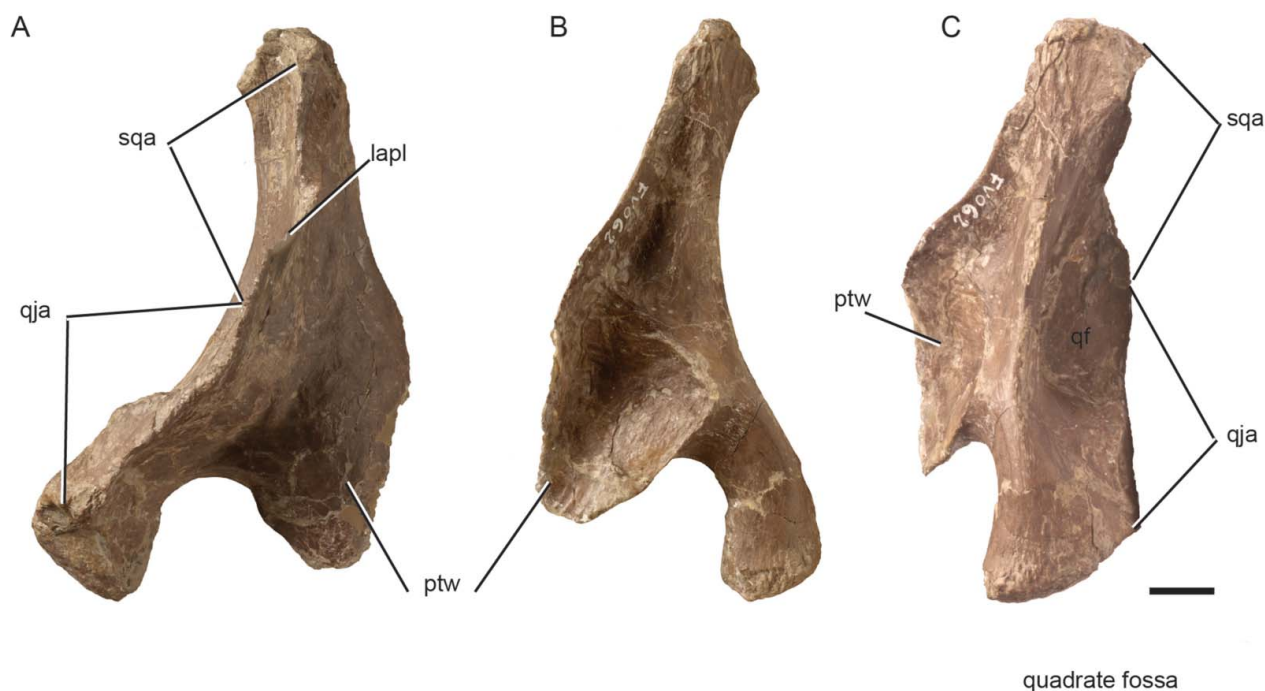

Figure 11. *Europasaurus holgeri* left quadrate (DFMMh/FV 062) in **A,** lateral, **B,** medial and **C,** posterolateral views. Abbreviations: lapl, lateral plate; ptw, pterygoid wing; qf, quadrate fossa; qja, quadratojugal articulation; sqa, squamosal articulation. Scale bar represents 1 cm.

shaft is present along the entire length, which is dorsally and ventrally expanded to form the head as well as the articular surface of the quadrate. The pterygoid wing runs along the medial side of the quadrate in an anterior direction (Fig. 11). A narrow lamina-like process, referred to as the lateral plate, extends laterally from the shaft to contact the squamosal and the quadratojugal (Fig. 11A). The lateral surface of the lateral plate has a scar that extends throughout the surfaces and serves as a contact for the quadratojugal (ventrally) and the squamosal (dorsally). Due to the squamosal–quadratojugal contact along the lateral margin of the quadrate, the quadrate is excluded from the infratemporal fenestra. The dorsal head of the quadrate has a triangular shape in cross section. The posteriorly oriented apex forms the dorsal margin of a robust posterior crest.

The quadrate fossa is deep and posteriorly directed. Ventrally, this fossa begins at the same level as the ventral edge of the pterygoid process. The lateral plate, squamosal and quadratojugal together form the lateral edge of the quadrate fossa. The medial wall is formed by a robust crest, which is posteriorly directed and extends throughout the height of the quadrate. In posterior view, this crest stretches dorsolaterally from the ventromedial corner of the quadrate to the dorsomedial end.

The pterygoid wing is well developed and anteriorly expanded (Fig. 11). Its dorsal edge is anteroventrally directed from the quadrate head down to the middle of the quadrate, where the ventral edge acquires a strong ventral orientation. The single articulation facet for the pterygoid is large and covers most of the medial side of the pterygoid wing except for the more dorsal margin. In posterior view the ventral articular surface of the quadrate, which articulates with the articular in the mandibles, is dorsolaterally oriented (Fig. 11), but forms two almost horizontal facets that are separated by a marked step.

Ontogenetic changes. Size-independent characters for staging the quadrates are bone surface structure, depth of the quadrate fossa, and the curvature between the process for the articular and the pterygoid wing. DFMMh/FV 972.2 is assigned to morphotype B while all the others, apart from DFMMh/FV 062.1, can be assigned to morphotype A. One element is described as MOS 1, three as MOS 2, and two as MOS 3.

DFMMh/FV 062.1 represents MOS 1. Bone surface structure is highly vascularized. The quadrate fossa is shallow. The curvature between the process for the articular and the pterygoid wing is not very pronounced. Although identification as a quadrate is indisputable, its morphology differs from all the other quadrates at the posterodorsal margin. At this margin, there is a crest instead of a concave indentation. Except for this crest, morphology is reminiscent of the other *Europasaurus* quadrates. The crest might be a juvenile character that is

not preserved in older ontogenetic stages. The assignment of the quadrate to *Europasaurus* is currently uncertain but it will be regarded as belonging to *Europasaurus* for the time being.

Three sub-stages were recognized in MOS 2. MOS 2.1 is represented by element DFMMh/FV 1032.2. This complete specimen shows a moderately vascularized bone surface structure. The quadrate fossa and the curvature are both shallow. The second sub-stage (MOS 2.2) is represented by DFMMh/FV 057. This almost complete specimen shows a moderately vascularized bone surface structure with most surfaces finished. The posterior plane of the squamosal process, however, is highly vascularized, showing that this part is still growing. DFMMh/FV 057 has a shallow quadrate fossa, but the curvature cuts in more deeply. The third stage, MOS 2.3, represented by DFMMh/FV 058, has a similar bone surface structure as in DFMMh/FV 057, except for the posterior plane of the squamosal process. The quadrate fossa is deeper, as is the degree of curvature.

The third MOS is represented by two elements (DFMMh/FV 062 and DFMMh/FV 972.2). The bone surface structure of these two elements is smooth and appears finished. The articular facets are well defined and rugose, and the quadrate fossa is very deep, as is the curvature. The quadrate fits very well to squamosal DFMMh/FV 712.2 and quadratojugal DFMMh/FV 291.25. In DFMMh/FV 972.2, the quadrate fossa is very deep, but the curvature here is shallow to almost non-existent. Since one putative diplodocoid dorsal vertebra has also been found in the quarry (JLC pers. obs.), the question arises if DFMMh/FV 972.2 could be assigned to another sauropod taxon. But since the quadrate fossa is really deep in contrast to the condition seen in diplodocoids, such as *Diplodocus* or *Apatosaurus* (Whitlock *et al.* 2010), it is more likely a quadrate of an adult of morphotype B.

Pterygoid. The pterygoid is usually the largest element of the sauropod palate (Fig. 12). Seven pterygoids are preserved, including five left (DFMMh/FV 100.2, 244, 554.6, 748, 965.4) and two right (DFMMh/FV 196, 964) elements. The pterygoid of *Europasaurus* is a large element with three different processes. One of these processes is an anteriorly directed wing that contacts the contralateral pterygoid (the anterior pterygoid wing). A second process is lateroventrally directed for contacting the ectopterygoid (the lateroventral pterygoid process), and the third process is a posteriorly directed wing, which gives support to the basipterygoid process of the braincase and the quadrate (the posterior pterygoid wing). These three processes lead to the characteristic triradiate shape of the pterygoid (Fig. 12).

The anterior pterygoid wing is the longest and most prominent process of the pterygoid. The pterygoid contacts with its contralateral through a medially directed
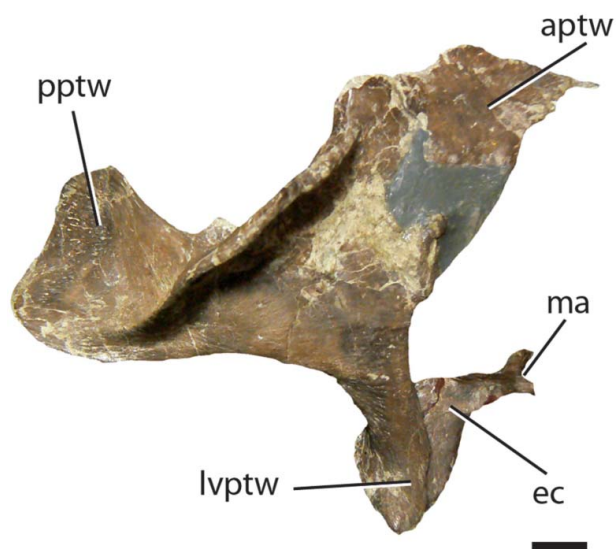
Figure 12. *Europasaurus holgeri* left pterygoid (DFMMh/FV 100.2) and manually articulated ectopterygoid (DFMMh/FV 748) in medial view. Abbreviations: aptw, anterior pterygoid wing; ec, ectopterygoid; lvptx, lateroventral pterygoid wing; ma, maxillar articulation; pptw, posterior pterygoid wing. Scale bar represents 1 cm.

expansion, which starts below the posterior pterygoid wing and diminishes into the dorsal surface of the anterior pterygoid wing. Anteriorly to this expansion the facet for the interpterygoid articulation cannot be clearly distinguished because of the state of preservation. However, as in most sauropods, this facet was probably extended more anteriorly, up to the level of the pterygoid–vomer articulation. The vomer articular facet in the anterior pterygoid wing is well marked and recognized as an anteroventral depression on the lateral side of the anterior pterygoid wing (Fig. 12). The exact place where the palatine articulates on the medial side of the anterior pterygoid wing cannot be defined, but as in most sauropods, this surely covers most of the ventrolateral side of this process except the facet for the vomer.

The lateroventral pterygoid wing is the smallest but most robust of the three processes of the pterygoid. The lateroventral process is a short expansion that supports the ectopterygoid. The articulation surface for the ectopterygoid extends nearly the entire length of the process as a marked longitudinal canal in which the ectopterygoid is inset.

The posterior pterygoid wing (or quadrate process) is a middle-sized process that gives support to the basipterygoid process of the parabasisphenoid, dorsally, and contacts the quadrate lateroventrally. In dorsal view the posterior process and the anterior pterygoid wing diverge from each other at an angle slightly larger than 90°, resulting in a curved shape of the pterygoid (Fig. 12). The basipterygoid pit (fossa basipterygoideus) is a small round

depression observed in the anterodorsal surface of the process. This facet is inset in a medially facing, concave surface of the process. The convex lateral surface of the posterior pterygoid wing has a rugose surface, especially ventrally, that articulates with the medial surface of the pterygoid wing of the quadrate (Fig. 12).

Ontogenetic changes. Size-independent characters used are bone surface structure, elevation of the blunt, tooth-like projection anterior to the basipterygoid pit, curvature of the medial side of the quadrate process, depth of the basipterygoid pit, form of the anterodorsal margin of the quadrate process, and the medial margin of the basipterygoid pit. The absence or presence of the latter is used to define the morphotype. One element is assigned stage 1, two to stage 2, and one to stage 3.

DFMMh/FV 196 (MOS 1) is represented only by a small fragment. The bone has an hvbs structure with striations in the longitudinal direction. The tooth-like projection is moderately developed. There is no curvature on the medial side, but a rather flat surface. The basipterygoid pit is not very deep. The anterodorsal margin is rounded and the medial margin is lacking, suggesting that the element is of morphotype B.

Two different substages are recognized amongst the elements interpreted as MOS 2. The incomplete DFMMh/FV 244 (MOS 2.1) shows a partially vascularized bone surface. The tooth-like projection is small, the curvature is slightly concave, and the basipterygoid pit is shallow. The anterodorsal margin is not as sharp as in stage 3, but the medial margin is still rounded. This pterygoid is the youngest element of morphotype A amongst the pterygoids. DFMMh/FV 554.6 (MOS 2.2) preserves about the same part as DFMMh/FV 244. It has a partially vascularized bone surface, a small tooth-like projection, and a concave curvature. The basipterygoid pit is deep and the anterodorsal margin is not as sharp as in stage 3, while the medial margin is already sharp. This pterygoid is the second oldest element of morphotype A amongst the pterygoids.

The third stage (MOS 3) was recognized in DFMMh/FV 100.2 (Fig. 12). The bone surface structure of this almost complete specimen is smooth, and the articular facets are very rugose. The tooth-like projection is well developed, and the curvature is concave. The basipterygoid pit is very deep. Both the anterodorsal margin and the medial margin are sharp. This pterygoid is of a presumably fully grown animal of morphotype A and fits quite well with the quadrate DFMMh/FV 062.

Ectopterygoid. The ectopterygoid is a rather simple element, which contacts with the pterygoid, palatine and maxilla (Fig. 12). Three ectopterygoids are preserved (DFMMh/FV 748, 965.4, 966). Two processes form the L-shaped ectopterygoid: a narrow anterolaterally directed process which contacts posteriorly with the maxilla, and a

vertically expanded flange which contacts with the ptery-goid. The anterolateral process is mainly oval-shaped in cross section. Its posterior end is expanded to form the facet for the articulation with the palatine process of the maxilla. Two differently positioned articular facets are observed at this posterior end, a posterodistal and an ante-rodistally facet, giving a firm attachment of the palate to the maxilla. This process is posteriorly expanded to form the process that is inserted into the lateroventral pterygoid process of the pterygoid. Through the posterior half of the lateral side of the ectopterygoid, a rugose and slightly expanded surface marks the area of contact with the pala-tine. This area is mainly extended through the posterodor-sal side of the ectopterygoid vertical expansion, and only slightly exposed in the anterolateral process.

Ontogenetic changes. All three preserved elements show rather rugose bone surfaces with little vascularization and well-pronounced articular facets. While DFMMh/FV 748 has an elongated lateral shaft and a claw-like medial flange with a concave medial margin, DFMMh/FV 965.4 shows a rather stout lateral shaft and the blade-like medial flange has a straight medial rim. They probably belong to two morphotypes: DFMMh/FV 748 is presumably mor-photype A, and DFMMh/FV 965.4 morphotype B. The third specimen, DFMMh/FV 966, is rather incomplete, but shows characters that resemble those of morphotype B. Specimen DFMMh/FV 748 fits well in the articular facet of pterygoid DFMMh/FV 100.2 and therefore might be of the same, presumably adult, stage. The morphotype B specimens belong at least to stage 2, but they could pos-sibly be older.

Braincase and occiput

Several bones from the braincase of *Europasaurus holgeri* are preserved, most as isolated elements. Of the braincase and occiput region, only the stapes are missing, which so far have been reported in few sauropods (*Shunosaurus*, *Camarasaurus*; Zheng 1991; Madsen *et al.* 1995). The braincase description is mainly based on a newly pre-pared, almost complete, and excellently preserved speci-men (DFMMh/FV 581.1). Most of the bone sutures of DFMMh/FV 581.1 are completely closed, but some are still discernible. The same specimen preserves both parie-tals (DFMMh/FV 581.2 and 581.3), which are not fused with the braincase or the frontals (see above). For descrip-tive purposes, the braincase is oriented with the dorsal sur-face of the occipital condyle horizontally positioned, which is coincident with a horizontal position of the lat-eral semicircular canal (Schmitt 2012). Further informa-tion from individual braincase bones is based on isolated elements, which also provides evidence of ontogenetic changes.

Supraoccipital. Two of the six preserved supraoccipitals (Fig. 13) are fused with surrounding skull elements in the braincases (DFMMh/FV 581.1 and 1077). The other four supraoccipitals were found isolated (DFMMh/FV 041, 723, 724 and 867.3), all being complete except specimen DFMMh/FV 724. The isolated supraoccipitals do not show enough reliable characters amongst each other to make strong arguments for any staging from the ontoge-netic perspective or to support any kind of morphotype differences. The fused supraoccipitals and surrounding bones likely belong to morphologically mature animals (subadult or adult specimens).

The supraoccipital is a massive single bone that forms the posterior roof of the endocranial cavity. The sutures between this bone and the exoccipitals are closed, but are still visible in occipital view (Fig. 13A). The supraoccipi-tal is only slightly higher (2.71 cm) than the occipital con-dyle (2.36 cm), which seems to be a consequence of the relatively small foramen magnum of *Europasaurus*. Whereas the exoccipitals surround 72% of the external edges of the foramen magnum, the supraoccipital sur-rounds 25% and the basioccipital, 3%. The supraoccipital contacts the prootic anteriorly, leaving a shallow suture at the union. Laterally throughout its height the supraoccipi-tal articulates with the parietal in an almost vertical con-tact, which terminates ventrally in a small but well-marked notch. This notch gives support to the ventral pro-cess of the parietal. A small foramen is present in the deepest part of the notch, which opens internally into the brain cavity. This foramen, the external occipital fenestra for the caudal middle cerebral vein (Witmer & Ridgely 2009), mainly pierces the supraoccipital but its posterior opening is dorsally bounded by the parietal (Fig. 13A). Thus, as in other sauropods (e.g. *Apatosaurus*, *Camara-saurus*; Witmer *et al.* 2008; Balanoff *et al.* 2010), the external occipital fenestra is in the line of the suture between the supraoccipital and the parietals. Laterodor-sally, the supraoccipital is highly fused with the prootic, which forms the ventral support for the parietal. Ventro-laterally, the supraoccipital articulates with the exoccipi-tal–opisthotic complex. The ventral surface of the supraoccipital can be observed in the isolated supraoccipi-tals (e.g. DFMMh/FV 867.3), being square-shaped and with two well-defined facets. The anterior facet articulates with the prootic, whereas the posterior facet articulates with the exoccipital.

A lateromedially narrow but well-developed and poste-riorly projected nuchal crest is present. In occipital view, this crest is triangular (Fig. 13A). Starting as a wide pro-jection, close to the foramen magnum, the crest ends in a thin lamina at its dorsal end. When the parietals of this braincase are articulated with the supraoccipital (see above), a small but well-distinguishable posterior opening is formed between the dorsal margin of the supraoccipital and the ventral edge of the parietals (Fig. 13A). We
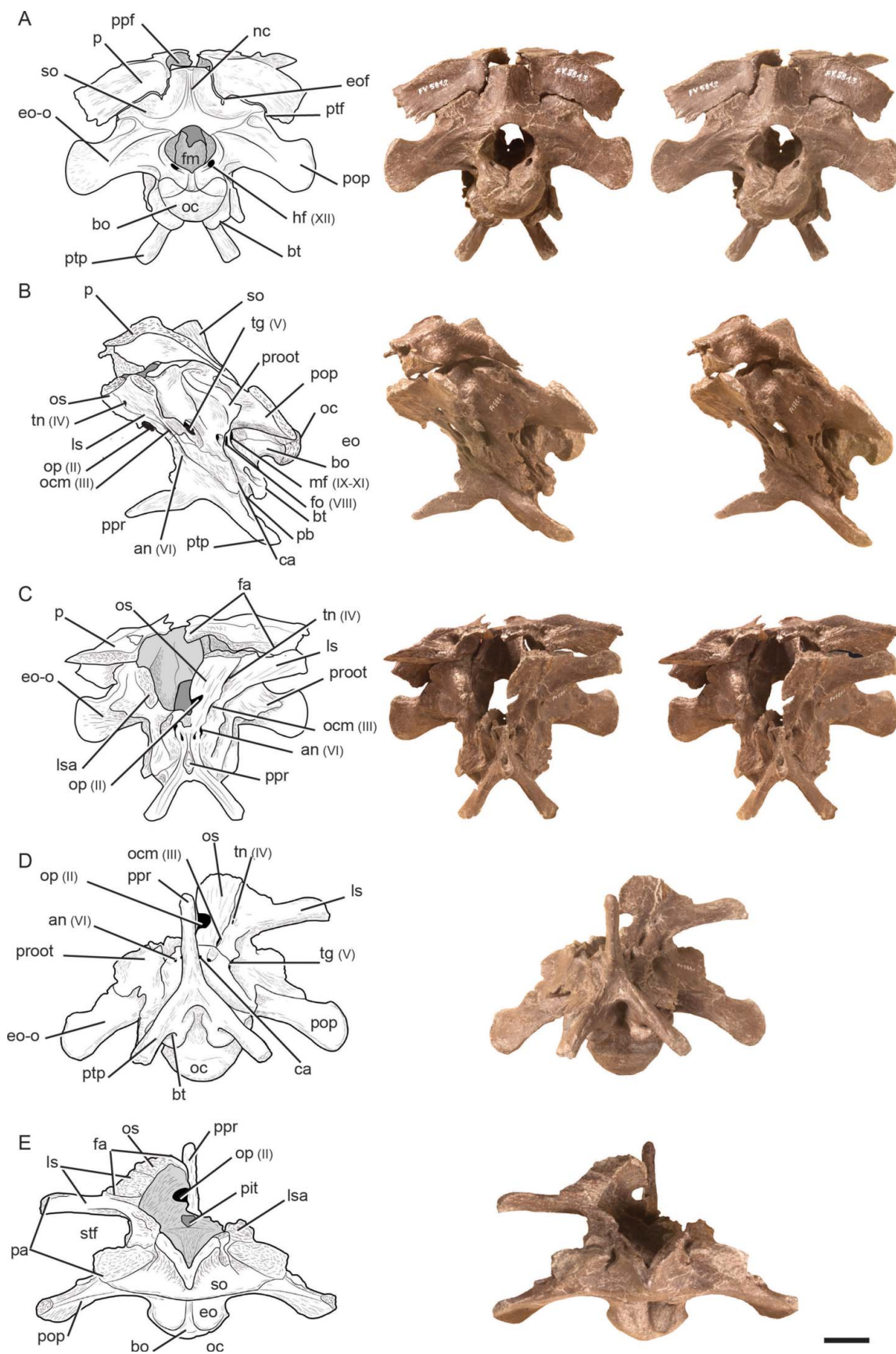
interpret this opening as the postparietal foramen, which is an unusual character for a non-dicraeosaurid sauropod (Salgado & Calvo 1992; Paulina Carabajal *et al.* in press). The presence of the foramen is recovered as a synapomorphic character of dicraeosaurids (Salgado & Calvo 1992; Wilson 2002; Whitlock 2011) and is convergently present in the diplodocids *Apatosaurus* and *Kaatedocus* (Balanoff *et al.* 2010; Tschopp & Mateus 2013) and the basal sauropod *Spinophorosaurus* (Knoll *et al.* 2012). The presence of a postparietal foramen in *Europasaurus* is interpreted as an autapomorphic character of this taxon, convergently acquired in dicraeosaurids amongst neosauropods. In *Europasaurus*, it cannot be known if the postparietal foramen is completely separated from the parietal fenestra (described above with the parietals).

Exoccipital–opisthotic complex. The exoccipital and opisthotic are always fused and found articulated in *Europasaurus* (Fig. 13). Both bones form a single bone complex (e.g. Madsen *et al.* 1995) and therefore, they are described as a simple structure (e.g. Harris 2006; Paulina Carabajal & Salgado 2007; Balanoff *et al.* 2010). The presence of a slight trace above the metotic fissure, which marks the line of union of these two bones, was recently described for *Rapetosaurus* (Curry Rogers & Foster 2004). Therefore, as was previously suggested (Madsen *et al.* 1995), the opisthotic forms the anteromedial face of this complex (Curry Rogers & Foster 2004). In *Europasaurus* this suture is not visible in any of the preserved isolated exoccipital–opisthotic complexes; thus, these bones are described together with the opisthotic representing the anteromedial section of this complex.

The paired exoccipital–opisthotic complex forms the lateral and most of the ventral breadth of the foramen magnum, and extends laterally to form the paroccipital process. In occipital view the complex fits between the supraoccipital (posterodorsally), the basioccipital (posteroventrally) and the parietals (dorsally) (Fig. 13A), whereas in lateral view this complex articulates anteriorly with the prootic (Fig. 13B, C). The suture of the exoccipital–opisthotic with the underlying basioccipital is visible in occipital and lateral views (Fig. 13). The ventral margin of the exoccipital–opisthotic is wide, with both (left and right) complexes almost contacting each other in the midline above the occipital condyle. As a product of this expansion, the exoccipital–opisthotic forms the lateral and most of the ventral margin of the foramen magnum, virtually excluding the basioccipital from this foramen (Fig. 13A, E). The exoccipital–opisthotic is the main bone forming the posterior floor of the brain cavity. The paroccipital process is ventrolaterally directed, at an angle that is higher than in *Giraffatitan* but not as high as *Camarasaurus*. The robustness of the paroccipital process (the ventromedial length in relation with the maximum lateral height) is also intermediate between *Camarasaurus* and *Giraffatitan*. Distally the paroccipital process is dorsally and ventrally expanded, to a similar degree as observed in *Giraffatitan* (Janensch 1935–1936; MB.R.2223.1) and *Camarasaurus* (Madsen *et al.* 1995). As in most sauropods, the paroccipital process is anteroposteriorly compressed, differing from the wider and rounded (in cross section) paroccipital process of *Spinophorosaurus* (Knoll *et al.* 2012). The post-temporal fenestra is reduced and interpreted as being present at the dorsal base of the paroccipital process, at the union of the exoccipital–opisthotic, parietal and supraoccipital (Fig. 13A).

The exoccipital–opisthotic complex is involved, to some degree, in the delineation of three cranial foramina, which are closely positioned towards each other. These foramina are, from posterior to anterior, the XII cranial nerve foramen (the hypoglossal nerve), the metotic fenestra (for the IX–XI cranial nerves), and the fenestra ovalis or vestibuli (for the VIII cranial nerve). The hypoglosal nerve completely pierces the exoccipital–opithotic complex. Whereas basal sauropods have two foramina for the hypoglosal nerve, the presence of a single hypoglosal foramen seems to be a derived character, widespread in camarasauromorph sauropods (Paulina Carabajal 2012). The metotic fenestra is almost as large as the trigeminal foramen, being 2.8 times higher (1.31 cm) than wide (0.46 cm), thus having an oval shape in lateral view (Fig. 13B). This fenestra is completely enclosed by the exoccipital–opisthotic complex. Although the sutures between these two bones are not discernible, the anterior branch (the crista interfenestralis) can be interpreted as part of the opisthotic, which forms the anterior edge of the metotic fenestra, whereas the exoccipital forms its posterior wall. The crista interfenestralis also forms the

Figure 13. *Europasaurus holgeri* braincase (DFMMh/FV 581.1). **A,** occipital view with articulated parietals (DFMMh/FV 581.2 and 581.3); **B,** left lateral with articulated parietals (DFMMh/FV 581.2 and 581.3); **C,** anterior view with articulated parietals (DFMMh/FV 581.2 and 581.3); **D,** ventral view; **E,** dorsal view without the parietals. Abbreviations: an, abducens nerve (VI); bt, basal tuberae; ca, carotid artery; eof, external occipital fenestra for the caudal middle cerebral vein; eo-o, exoccipital–opisthotic complex; fa, frontal articulation; oc, occipital condyle; ocm, oculomotor nerve foramen (III); op, optic foramen (II); fm, foramen magnum; fo, fenestra ovalis (VIII); hf, hypoglosal foramen (XII); ls, laterosphenoid; lsa, laterosphenoid articulation; mf, metotic fenestra (IX–XI); nc, nucal crest; so, supraoccipital; op, optic nerve foramen (II); os, orbitosphenoid; p, parietal; pa, parietal articulation; pb, parabasisphenoid; pit, space for the pituitary gland; pop, paraoccipital process; proot, prootic; ppf, postparietal foramen; ppr, parasphenoid rostrum; ptf, post-temporal fenestra; ptp, pterygoid process; stf, supratemporal fenestra; tg, trigeminal foramen (V); tn, trochlear nerve foramen (IV). Scale bar represents 2 cm.

posterior edge of the fenestra ovalis, which is anteriorly delimited by the crista prootica. The external opening of the fenestra ovalis is as large as the metotic fenestra but reduces rapidly in size, and only a small internal opening links the large external surface with the inner ear.

Ontogenetic changes. Size-independent characters are the bone surface structure, relative size of the paroccipital process, shape of the articular facets, and whether or not the exoccipital–opisthotic complex is fused with other elements. No distinctive morphotype could be identified for the isolated bones. Four disarticulated and five articulated elements are preserved amongst the *Europasaurus* material, comprising four elements of MOS 1 and five fragmentary elements of MOS 3. No intermediate MOS could be determined.

Amongst the first MOS, four different substages were recognized. MOS 1.1 is represented by DFMMh/FV 898, a tiny bone with a very small and thin paroccipital process, which is less than half as long as the total dorsoventral expansion of the bone. It is generally highly vascularized with no rugose structures on the ventral or dorsal sides. A slightly rugose surface is visible at the contact plane where the prootic would attach. The connection with the occipital condyle, supraoccipital and prootic must have been very loose with a lot of cartilage in between. Given this fact in combination with the very small size of this bone and the hvbs structure, the bone likely represents a hatching stage or at least a very young juvenile. DFMMh/FV 981.2 (MOS 1.2) is very similar to DFMMh/FV 898 but slightly larger. Most of the paroccipital process is missing but the preserved proximal part is slightly thicker than in DFMMh/FV 898. MOS 1.3 is represented by DFMMh/FV 249. The paroccipital process is more than half the length of the total dorsoventral expansion of the bone. The contribution to the occipital condyle is elongated posteriorly, but the element is still isolated. It is vascularized but shows rugose articular facets for the occipital condyle and supraoccipital as well as for the prootic. The fourth MOS 1 (MOS 1.4) is recognized in DFMMh/FV 205. This is the largest of the small and isolated specimens, showing a smoother bone surface structure with less vascularization. Although most of the paroccipital process is broken off, enough material is preserved to show that it is developed much more robustly with well-pronounced articular facets.

Three elements are considered to be MOS 3. The distal part of the left paroccipital process is preserved in DFMMh/FV 291.15, as are the most proximal attachments of both left and right sides that contribute to the neck of the occipital condyle. The bone shows a smooth surface structure and a fusion of the epoc with the basioccipital and parabasisphenoid. The second exoccipital–opisthotic element is part of the most complete braincase (DFMMh/FV 581.1). In this braincase, the two exoccipital–

paroccipital–opisthotic complexes (epocs) are preserved in their entirety. They are tightly fused with the surrounding basioccipital, parabasisphenoid, prootics and supraoccipital, and the sutures are still well visible. There are pronounced depressions for the squamosals and a rim at the dorsal side of the paroccipital process on both sides. The bone surface is smooth. The third element (DFMMh/FV 1077) is only preserved on its left side, all characters being similar to 581.1.

Prootic. The prootic (Fig. 13) is usually a difficult bone to study when it is fused with the adjoining elements since most of its posterior, ventral, dorsal and medial sides are covered. In the braincase of *Europasaurus* DFMMh/FV 581.1, the scars of the articular edges of this bone and the adjacent elements (Fig. 13C) can be observed. The prootic posteriorly articulates with the exoccipital–opisthootic complex and the supraoccipital, anteriorly with the laterosphenoid, ventrally with the parabasisphenoid, and dorsally with the parietal. In anterior view the prootic articulates with the paroccipital process covering around half of it and forms, ventrally to this contact, the crista prootica (Fig. 13C), which posteriorly delimits the fenestra ovalis. Anteriorly, the prootic contacts the laterosphenoid, both bounding the trigeminal foramen (for the cranial nerve V).

Ontogenetic changes. Although it is very fragmentary, the smaller size and the vascularized bone surface structure shows that the isolated DFMMh/FV 1042 might be a prootic of a juvenile. Judging by their smooth bone surface, the single bones of DFMMh/FV 466, DFMMh/FV 561 and DFMMh/FV 964 are at least in stage 2 if not stage 3. The same smooth surface is shown in the three prootics of the braincases DFMMh/FV 581.1 and DFMMh/FV 1077. Of the occiput region (DFMMh/FV 291.15) only the two crista prooticae are preserved, thus making comparisons difficult. Morphotypes can only be given to the prootics fused with the associated braincases: DFMMh/FV 291.15 and DFMMh/FV 581.1 are morphotype A; DFMMh/FV 1077 is morphotype B.

Basioccipital. The basioccipital (Fig. 13) is the main bone forming the occipital condyle along with the exoccipital–opisthotic complex. As most of the dorsal surface of the basioccipital contacts the exoccipital, the basioccipital has a minor contribution to the foramen magnum, leaving a narrow sulcus on the dorsal surface of the occipital condyle. A similar narrow sulcus, a product of the extensive lateromedial ventral expansion of the exoccipital, is observed in some basal camarasauromorphs such as *Camarasaurus* (CM 11338) and *Giraffatitan* (MB.R. 22231.1), differing from the broad sulcus formed by the exoccipital–basioccipital contact of *Spinophorosaurus* (GCP-CV-4229; Knoll *et al.* 2012). The ventral depth of this sulcus, which is well marked, is the only contribution

of the basioccipital to the foramen magnum. The suture of the basioccipital with the exoccipital is almost completely closed, but a narrow suture can be recognized in occipital and lateral views (Fig. 13A, B). The occipital is crescent-shaped in occipital view, as is also observed in the anterior articulation of the atlas (Carballido & Sander 2014). The occipital condyle is only slightly wider (3.22 cm) but more than twice as high (Fig. 13A) as the foramen magnum (width = 2.67 cm). The occipital condyle is 1.5 times wider than tall (2.10 cm). This ratio is greater than that of most neosauropods (see Mannion 2011, table 1). Compared to *Giraffatitan* (MB.R.2180.22) or the skull referred to *Brachiosaurus* (Carpenter & Tidwell 1998; USNM 5730), the occipital condyle is anteroposteriorly shorter than in these taxa, having similar proportions to those of *Camarasaurus* (Madsen *et al.* 1995) and basal sauropods (Knoll *et al.* 2012).

The basioccipital forms around the posterior third of the basal tubera, its anterior section formed by the parabasisphenoid. The suture between the parabasisphenoid and the basioccipital is completely closed but is still discernible in ventral and lateral views. Laterally, the union of these two bones is extended from the ventral floor up to the ventral base of the metotic foramen (Fig. 13). The basioccipital forms the posteroventral tip edge of this nerve foramen, which is mainly set into the exoccipital–opisthotic complex (see above). This is the only cranial foramen (apart of the foramen magnum) that is bounded in any degree by the basioccipital. The basal tubera are wide and short, and diverge from each other at an angle of around 45° forming a V-shaped notch. The basal tubera of *Europasaurus* remain separated throughout their length, surpassing the division for half of the total basal tubera length seen in diplodocids (*Apatosaurus*, *Diplodocus*; Mannion *et al.* 2013), *Giraffatitan* (MB.R. 2223.1) and most specimens of *Camarasaurus* (SMA 0002/02; Madsen *et al.* 1995), but not the juvenile specimen CM 11338 in which the basal tubera is undivided. Due to the absence of ontogenetic information, it is not possible to evaluate if the condition of CM 11338 is due to ontogenetic variation, and therefore it is advisable to score this character as ambiguous in *Camarasaurus* (following Mannion *et al.* 2013). The posterior surface of the basal tubera does not exhibit any sign of a fossa, although a small pit is observed in the ventral neck that separates the basal tubera from the occipital condyle. A deep ventral fossa is present on the ventral surface, between the basal tubera and the basipterygoid fossa. The presence of this fossa is widespread amongst macronarians more derived than *Camarasaurus* (Mannion *et al.* 2013). The ratio between the width of the basal tubera and the occipital condyle width is 1.37 (see also Mannion 2011, table 1), which is the plesiomorphic condition for macronarians, differing from Lithostrotia and some specimens of *Camarasaurus*, which have a greater ratio (Mannion *et al.* 2013).

Ontogenetic changes. DFMMh/FV 291.15 seems to have been diagenetically compressed. Although it still shows distinctive sutures with the exoccipitals, the bone surface looks fully developed. Therefore, it is interpreted as MOS 3. The association with a morphotype is difficult, although DFMMh/FV 291.15 is similar to the complete specimen DFMMh/FV 581.1, which is assigned to morphotype A. The basioccipital of DFMMh/FV 581.1 is complete and undeformed and also shows sutures, but is overall fused with most of the other bones that build up the braincase and is therefore described as MOS 3. DFMMh/FV 581.1 presumably represents the adult MOS. In DFMMh/FV 1077 only the left side of the MOS 3 braincase is preserved. The basioccipital alone does not give further hints regarding the morphotype, but the downward angle in which the paroccipital process faces differs radically from the angle in the other paroccipital processes. Therefore, DFMMh/FV 1077 possibly belongs to morphotype B.

Parabasisphenoid. In sauropods the basisphenoid is completely fused with the parasphenoid without any sign of suture, even in immature specimens (Madsen *et al.* 1995). Therefore, both bones are always described as a single complex, commonly called the basisphenoid–parasphenoid complex (e.g. Madsen *et al.* 1995), the basisphenoid (e.g. Wilson 2005), or the parabasisphenoid (e.g. Balanoff *et al.* 2010), a term that is followed here. The parabasisphenoid (Fig. 13) serves as the floor of the braincase and forms the anterior part of the basal tubera, the basipterygoid process, the parasphenoid rostrum, and the anteriormost preserved floor of the brain cavity. This bone contacts the basioccipital posteriorly, laterosphenoid, and prootic dorsally, and exoccipital–opisthotic posterodorsally (Fig. 13).

As was noted above for the basioccipital, the parabasisphenoid is heavily fused with the basioccipital, leaving a small lateral fossa between them (Fig. 13). The parabasisphenoid forms the anterior one-third of the basal tubera, particularly the medial face (Fig. 13). In ventral view the parabasisphenoid forms a deep triangular medial fossa that contacts with the basioccipital (Fig. 13D). The basipterygoid processes, which are completely formed by the parabasisphenoid, follow the same angle of divergence as the basal tubera (45°). When the braincase is positioned in its presumed neutral position (i.e. with the lateral canal of the inner ear positioned horizontally; Schimtt 2012), the basipterygoid processes are posteroventrally inclined, forming an angle of 50° with respect to the horizontal plane. Whereas the basispterygoid processes are anteroposteriorly longer (1.04 cm) than medioventrally wide (0.76 cm) at their base, their distal end is wider (0.91 cm) than long (0.56 cm). The basipterygoid processes are relatively short (2.61 cm, measured at mid-length) and broad, being 2.9 times longer than the diameter at the base

(average ratio of the width and length = 0.9). The parasphenoid rostrum is anteriorly directed, running only slightly ventrally, diverging at an angle of slightly less than 10° from the horizontal plane.

The dorsal margin of the parabasisphenoid forms the floor of the neural cavity, which is pierced by two single foramina directly on the midline of the endocranial cavity floor. The foramen positioned posteriorly is very small and located slightly anterior to the pituitary fossa. We interpret this foramen as serving for the basilar artery, and it is also present in other sauropods in a similar position and communicating with the posterior wall of the pituitary fossa (e.g. *Plateosaurus*, *Spinophorosaurus*, *Giraffatitan*, *Bonatitan*; Janensch 1935–1936; Galton 1984, 1985; Knoll *et al.* 2012; Paulina Carabajal 2012). The largest and more anteriorly positioned foramen is used for the pituitary gland (the pituitary fossa or sella turcica), which is positioned close to the laterosphenoid–parabasisphenoid internal contact. The pituitary fossa is posteriorly bounded by the parabasisphenoid and seems to be completely inset in this bone. This fossa is posteroventrally directed from its dorsal opening and forms an angle of almost 60° with the horizontal plane. Two paired foramina pierce the parabasisphenoid anteriorly, and the external lateral surface of this bone communicates with the pituitary fossa. One pair of these foramina is also observed in other sauropods in the same position (e.g. Paulina Carabajal & Salgado 2007; Knoll & Schwarz 2009) and is interpreted as the foramina for the cranial nerve VI. The second pair of foramina is identified as a canal into the adenohypophysis; a canal in a similar position was recently described in some other sauropods (Paulina Carabajal 2012, fig. 3). The foramina for the cranial nerve VI are larger and more posterodorsally positioned than the canal into the adenohypophysis. The foramina for the carotid artery are recognized between the prootic and the basal tubera, entering the pituitary posteroventrally, as is also observed in some other sauropods (e.g. *Plateosaurus*: Galton 1985, fig. 7H; *Giraffatitan*: Janensch 1935–1936, fig. 117).

Ontogenetic changes. Besides slight size differences, the processes do not show any ontogenetic differences. DFMMh/FV 581.1 is morphotype A, as is DFMMh/FV 291.15. The elements indicate that both specimens most likely belong to fully grown individuals. In the case of DFMMh/FV 291.15 the occiput region and further cranial material have been found together with long bones, which are considered to be from an adult animal (see Sander *et al.* 2006).

Laterosphenoid–orbitosphenoid. Only the left laterosphenoid–orbitosphenoid (Fig. 13) is preserved in the braincase DFMMh/FV 581.1. The right laterosphenoid–orbitosphenoid was lost before or at the time of burial, as all the surrounding bones that articulate with these bones

show their articular surfaces, indicating the unfused condition of these elements. The laterosphenoid is discernible from the surrounding bones, as the sutures in lateral view are still visible, including the normally indistinguishable suture with the orbitosphenoid (Madsen *et al.* 1995). Therefore, both bones (laterosphenoid and orbitosphenoid) are described separately instead of as a complex. The laterosphenoid–orbitosphenoid suture is smooth but clearly visible as a small rough convexity (Fig. 13B, E). This suture extends from the parabasisphenoid, just above the foramen for cranial nerve VI, passing through cranial nerve III, probably bounding the anterior margin of cranial nerve IV (excluding its orbitosphenoid), and up to the middle of the laterosphenoid–orbitosphenoid dorsal contact for the frontal (Fig. 13B).

Posteriorly the laterosphenoid articulates with the prootic. A broad rectangular contact is visible on the right prootic in anterior view (Fig. 13C) and on the left prootic in lateral view (Fig. 13B). Additionally, the laterosphenoid contacts the supraoccipital posteromedially. Laterally the suture with the prootic runs from the parabasisphenoid up to the dorsal surface, passing through cranial nerve V, which is bounded within these two bones. Dorsally, the laterosphenoid contacts the parietal (posteriorly) and the frontal (anteriorly), both articular surfaces being separated by a shallow step at the level of the lateral expansion of the laterosphenoid (the crista antotica). The crista antotica is positioned just above the level of the trigeminal foramen (cranial nerve V) and is slightly posteriorly directed, and thus the laterosphenoid diverges from the paroccipital process at an angle of almost 30° (Fig. 13). The dorsal edge of the laterosphenoid serves as support for the anteroventral contact of the parietal, and thus forms the anteroventral wall of the supratemporal fenestra.

The left orbitosphenoid of specimen DFMMh/FV 581.1 is completely preserved and articulated with the laterosphenoid (posteriorly; see above) and the parabasisphenoid (ventrally). The posteroventral edge of the orbitosphenoid is just above cranial nerve VI. Above this, cranial nerve III is formed by the laterosphenoid (posteriorly) and the orbitosphenoid (anteriorly). Dorsolaterally, the orbitosphenoid seems to contact the laterosphenoid just anteriorly to cranial nerve IV, which is the smallest nerve foramen in this braincase. The dorsoventrally long cranial nerve III opens internally as a short foramen, which is situated above the pituitary fossa, and merged into the laterosphenoid–orbitosphenoid. Cranial nerve II opens anteriorly and, although the right orbitosphenoid is not preserved, the left and right foramina were in medial communication. Amongst basal sauropodomorphs, the orbitosphenoid is known only in *Massospondylus* and *Plateosaurus*, in which there is a single optic nerve (Galton & Upchurch 2004, fig. 12.4H, I). In contrast to basal sauropodomorphs (Yates 2007), the orbitosphenoid in sauropods is well ossified and has been described for

several taxa. In basal sauropods, the optic nerve is not medially divided but instead forms a single anterior foramen, as described for *Shunosaurus* (Chatterjee & Zheng 2002, fig.7), *Mamenchisaurus* (Ouyang & Ye 2002, fig. 6), and here for *Europasaurus*. In contrast, two optic foramina (left and right) are present in most neosauropods (*Amargasaurus*, *Nigersaurus*, *Camarasaurus*, *Giraffatitan*; Janensch 1935–1936; Salgado & Calvo 1992; Madsen *et al.* 1995; Wilson 2005; Sereno *et al.* 2007) and the closely related *Turiasurus* (Royo Torres & Upchurch 2012). A single, partially undivided, optical nerve described for *Suuwassea* was interpreted as an autapomorphic character (Harris & Dodson 2004; Harris 2006) but is also present in some specimens of *Diplodocus* (Osborn 1899; Berman & McIntosh 1978). The presence of a single optic foramen seems to be product of lack of ossification, which in *Europasaurus* could be the result of evolutionary dwarfing. Due to the current phylogenetic position of *Europasaurus*, the presence of a single optic foramen is considered an autapomorphic trait of this taxon, which is interpreted as a reversion to the plesiomorphic condition of basal sauropodomorphs.

Ontogenetic changes. Three complexes of the laterosphenoid–orbitosphenoid and a single laterosphenoid are preserved amongst the *Europasaurus* material. One element of MOS 1 is preserved, one of MOS 2, and two of MOS 3.

MOS 1 is recognized in DFMMh/FV 897. This fragmentary piece of a laterosphenoid lacks parts of the posterior region and the laterally arching, bony, wing-like lamina. The laterosphenoid bone is usually tightly fused with the orbitosphenoid. No fractures are visible on DFMMh/FV 897 that would suggest the bone was previously broken; instead, the laterosphenoid was not yet fused to the orbitosphenoid. Given its actual size and the fact that the bone surface shows little vascularization, it is of a much younger state than the others. The preservational condition does not give enough information about the foramen, since only the anterior margin for the trigeminal nerve (V) is preserved. It seems to be very robust, which is a character of morphotype B.

Element DFMMh/FV 785.4 is assigned to MOS 2. This robust bone has a mostly vascularized bone surface structure, and the isolated attachment facets are rugose and broad. It shows a clearly visible suture dorsally and ventrally of the trochlear nerve (IV) where the laterosphenoid meets the orbitosphenoid and extends further ventrally through the oculomotor nerve (III). The connection is still fragile and there is a gap at the ventral end of III, which should be closed in a fully grown individual. The foramen for IV is very large (main character for morphotype B), and that for III is slightly smaller. The foramen for the optic nerve (II) does not cut in deeply. Nerve V is much larger than that of DFMMh/FV 897.

The third MOS is represented by two substages. DFMMh/FV 291.16 (MOS 3.1) is incomplete and lacks the wing-like lamina of the laterosphenoid. There is no suture visible in this robust element and the two elements seem to be very well fused, with the foramen of III being fully closed. The sizes of IV and III are very similar to those of DFMMh/FV 785.4; II does not cut in deeply here either. Similarly to the two other morphotype B specimens above, V is relatively large. Bone surface structure is very smooth and has some rugose structures, especially at the broad attachment facets.

MOS 3.2 is observed in DFMMh/FV 581.1. This laterosphenoid–orbitosphenoid is the only one that is fused with most of the surrounding elements. It is complete and, contrary to the others, appears to be much more gracile, with slender attachment facets. The wing-like lamina, however, is much larger than in DFMMh/FV 785.4. Bone surface structure is smooth. The nerve for II cuts in very deeply. Interestingly, the foramen of IV (trochlear nerve) is very reduced, about the size of a pinhead. This element belongs to morphotype A but the small sample size means that it cannot be determined whether the exceedingly small foramen IV is a defining character of this morphotype or a pathological phenomenon.

Mandible

The mandible (Fig. 14) lacks only the articular. All other elements have been found at least twice, except for the splenial, which has been found only once and therefore is staged but not compared. From the three coronoids known in basal tetrapods (Romer 1956), only the intercoronoid is preserved in *Europasaurus*. The organizing principle for ordering the listed bone types proceeds from anterior to posterior on the lateral side, and from posterior to anterior on the medial side of the mandible.

Dentary. Fifteen dentaries (Fig. 14) were discovered amongst the *Europasaurus* material: eight are left elements (DFMMh/FV 033, 092, 093, 290, 290.11, 654, 1058.14, NMB 2207-R) and seven right elements (DFMMf/FV 034, 059, 094, 501, 653, 834.7, NMB 2207-R). The most completely preserved dentaries have 14 alveoli. Amongst some basal and derived camarasauromorphs there are between 12 and 13 teeth, one or two fewer teeth than in *Europasaurus* (e.g. *Camarasaurus* 12 or 13: Madsen *et al.* 1995; *Euhelopus* 13: Wilson & Upchurch 2009; *Nemegtosaurus* 13: Wilson 2005). In comparison, the brachiosaurids *Giraffatitan* (15: Janensch 1935–1936), *Abydosaurus* (14: Chure *et al.* 2010), and the skull referred to *Brachiosaurus* sp. (14: Carpenter & Tidwell 1998) each have one or two more teeth than *Europasaurus*. However, in basal sauropods the number of teeth is usually more than 20 (e.g. *Jobaria*, *Omeisaurus*: Sereno *et al.* 1999; Tang *et al.* 2001).
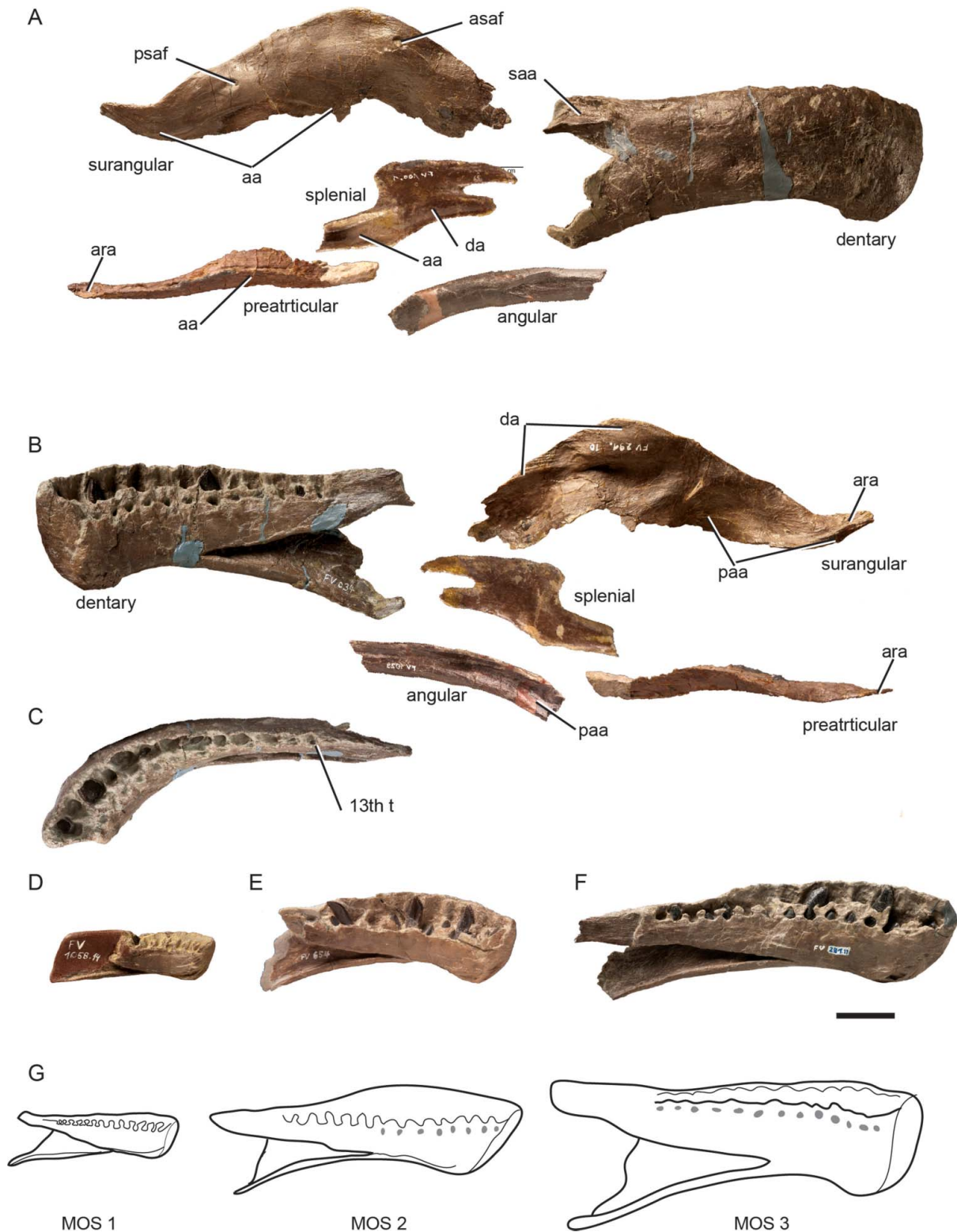
Figure 14. *Europasaurus holgeri* mandible bones. **A–C,** dentary (DFMMh/FV 034), angular (DFMMh/FV 1029; reversed), prearticular (DFMMh/FV 291.24), splenial (DFFMh/FV 100.1; reversed), and surangular (DFMMh/FV 291.10) in **A,** lateral, **B,** medial and **C,** dorsal views. **D–F,** medial views of the additionally dentaries; **D,** DFMMh/FV 1058.14; **E,** DFMMh/FV 654; **F,** DFMMh/FV 291.11. **G,** reconstruction of the different MOS detected amongst preserved dentaries in lateral view. Abbreviations: 13th t, thirteenth tooth; aa, angular articulation; ara, articular articulation; asaf, anterior surangular foramen; da, dentary articulation; paa, prearticular articulation; psaf, posterior surangular foramen; saa, surangular articulation. Scale bar represents 2 cm.

As in other sauropods, the articulated dentaries have a U-shaped symphysis in dorsal view (Fig. 14C), differing from the V-shaped mandibles of basal sauropodomorphs. The dorsoventral axis of the symphysis is slightly posteroventrally inclined, with a similar anterior edge of the dentary to that in *Camarasaurus* (Madsen *et al.* 1995, fig. 41; CM 11338) but not as straight as is in *Giraffatitan* (Janensch 1935–1936, fig. 50; MB.R. 2181.14). The anterior section of the dentary has a ventral expansion, starting around the fifth alveolus, and similar in shape to that observed in some specimens of *Camarasaurus* and *Giraffatitan*.

The lateral surface of the dentary is dorsoventrally convex and covered with numerous nutrient foramina, which are more abundant anteriorly and dorsally. A broad channel-like concave surface extends posterodorsally from around the third of the dentary up to the surface in which the angular articulates with the dentary. In the anterodorsal section of the dentary, tooth position is marked by regular convexities. Posteriorly, the dentary is divided into dorsal and ventral rami. This division starts between the last two teeth (DFMMh/FV 059) and slightly posterior to the last one (DFMMh/FV 034). The dorsal ramus seems to be more developed than the ventral ramus in DFMMh/FV 059 (which is the element that best preserves the posterior section of the dentary). This ramus has a well-marked and rough lateral surface that serves as attachment for the surangular (Fig. 14A). The ventral ramus is slightly shorter but more robust than the dorsal ramus, and its medial surface provides support for the angular. Although, the ventral ramus is not clearly divided in any of the preserved specimens, the available material is insufficient to fully confirm this. A divided posteroventral process is present in the brachiosaurids *Giraffatitan* and *Abydosaurus* (Chure *et al.* 2010), whereas a single posteroventral process is the plesiomorphic character present in all other non-brachiosaurid sauropods.

In medial view, each alveolus possesses rounded and well-marked nutrient foramina below it (Fig. 14A). Through these foramina, the crown of a second replacement tooth can be observed in the third and eighth alveolus of the element FVMMh/FV 034. The diameter of the alveoli decreases in size posteriorly. The nutrient foramina are completely enclosed, except for the ventral portion, by the interdental plates (as is evident when these are preserved). The union of the interdental plates forms the medial plate as in other sauropods (e.g. *Rapetosaurus*: Curry Rogers & Forster 2004). A well-developed, V-shaped Meckelian canal originates posteriorly from the dorsal and ventral rami and continues anteriorly up to the level of the sixth to eighth alveolus, varying between specimens. This fossa gives support to the prearticular and the splenial as in other sauropods. Anteroventrally, the Meckelian canal becomes abruptly narrow and a small and slender sulcus extends anteriorly from it. In more

ontogenetically advanced specimens, the Meckelian canal is short and far from the symphysis (see below).

Ontogenetic changes. The most important size-independent character is the closure during ontogeny of the Meckelian canal posterior to the symphysis between the third to sixth alveoli. Further characters are bone surface structure, fusion of the interdental wall above the nutrition foramen from anterior to posterior direction, as well as the deepening of the depression on the anterolateral side above the symphyseal bulge. Morphotype is defined by the presence or lack of the lingual plate of the interdental wall, morphotype A showing a complete interdental wall while morphotype B specimens lacking the lingual side but still showing laminae between the teeth in the labiolingual direction, which are part of the interdental wall. One element of MOS 1 is preserved, six of MOS 2, and eight of MOS 3.

DFMMh/FV 1058.14 represents MOS 1. This tiny dentary of morphotype A (Fig. 14F) shows an hvbs structure on both medial and lateral sides as well as the symphysis. The Meckelian canal is still open, up to the symphysis. The labial plate of the interdental wall above the nutrition foramen is present but is not yet fused. The depression on the anterolateral side is hardly visible in low-angle light.

The only specimen of morphotype A that is presumably of MOS 2 is DFMMh/FV 290; other elements staged with a MOS 2 are regarded as morphotype B (DFMMh/FV 092, DFMMh/FV 093, DFMMh/FV 094, DFMMh/FV 501 and DFMMh/FV 654). Both morphotypes show a moderately vascularized bone surface structure. In the morphotype A specimen, the lingual plate of the interdental wall is not yet entirely fused, whereas in morphotype B it is missing completely. The Meckelian canal in both morphotypes is not yet fully closed, leaving a small groove between alveoli 3–6. All specimens show an anterolateral depression.

Five specimens are assigned to the third MOS morphotype A (DFMMh/FV 033, 034, 291.11, 653 and NMB 2207-R), and two are assigned to morphotype B (DFMMh/FV 059 and 834.7). These elements show a smooth bone surface structure on their medial side, while the lateral side is partially rugose. In morphotype A the lingual plate of the interdental wall starts to fuse in the anteroposterior direction, while the lingual plate never fuses between alveoli 11–13 and 14 (DFMMh/FV 291.11, Fig 14D). In morphotype B the lingual wall is missing. The Meckelian canal in both morphotypes is closed posteriorly to the symphysis between alveoli 3–6. All specimens have a very deep anterolateral depression.

Surangular. Four surangulars have been found amongst the *Europasaurus* material (Fig. 14A). The surangular of *Europasaurus* resembles that of other camarasauromorphs in the way that it is dorsally bowed with a well-developed coronoid process (Wilson & Sereno 1998). The maximum

height of the surangular is reached just posteriorly to the anterior surangular foramen. As in most neosauropods the external mandibular fenestra is completely closed in *Europasaurus*, which differs from *Nigersaurus* (Sereno *et al.* 2007), an undescribed titanosaur from the Late Cretaceous of Patagonia, and titanosaur embryos (García *et al.* 2010). In lateral view, the surangular of *Europasaurus* has almost the same maximum anteroposterior length as the dentary length (excluding the ventral and dorsal processes). The anterolateral edge of the surangular is badly preserved in all specimens, and therefore it is unknown how much of its surface articulates with the posterior edge of the dentary.

Ontogenetic changes. The most important size-independent characters are the form of the dorsal ridge of the coronoid process and the absence or presence of a groove on the lateral side of the anterior surangular foramen anterior to it. Further characters include a crest positioned anterodorsally to the anterior surangular foramen on its medial side that attaches the posterodorsal branch of a dentary, another crest positioned above the posterior surangular foramen on the lateral side, and finely pronounced articular facets for the angular, articular and prearticular, when present. Of the surangulars, four disarticulated elements are preserved amongst the *Europasaurus* material: two belong to MOS 2 and two to MOS 3. No MOS could be determined that would justify staging as a juvenile.

DFMMh/FV 785.3 is interpreted as having MOS 2.1. This fragment consists of the contribution to the summit of the coronoid process with the preserved anterior surangular foramen. The apex of the coronoid process curves smoothly. The bone shows striations in the anteroposterior direction on both sides. A small groove in front of the anterior surangular foramen is barely visible at low angle light. There is no crest anterodorsally of the anterior surangular foramen on its medial side. This fragment, which lacks the ventral margin of the surangular, belongs to morphotype A. MOS 2.2 is observed in DFMMh/FV 838.3, a more complete specimen showing fewer striations. It lacks parts of the anteroventral margin and the posterior end. The summit is dented and much steeper anteriorly toward the anterior surangular foramen than in the other subadult specimen. No small groove in front of the anterior surangular foramen is visible in a low angle light. There are two crests, one on the medial side, anterodorsally to the anterior surangular foramen, and one laterally above the posterior surangular foramen. This surangular shows not very prominent articular facets for the angular, the articular and the prearticular. The specimen is assigned to morphotype B.

Two elements are interpreted as having the third MOS. DFMMh/FV 291.10 is a surangular that lacks only a very small part of the anteroventral margin. The form of the apex of the coronoid process is the same as in DFMMh/ FV 785.3. It also shows a hardly visible groove anterior to the anterior surangular foramen. No crest is present on the medial side, anterodorsally to the anterior surangular foramen, or laterally above the posterior surangular foramen. Prominent and rugose articular facets for the angular, the articular and the prearticular are visible. The bone surface is smooth rather than striated. This bone represents an adult specimen of morphotype A. DFMMh/FV 713 is the most complete specimen, lacking only a fragment of the anteroventral margin. It shows the dented, steep form of the coronoid process. The small groove in front of the anterior surangular foramen is absent, but two crests can be found: one on the medial side, anterodorsally to the anterior surangular foramen, and one laterally above the posterior surangular foramen. Therefore, it is regarded as morphotype B. This surangular has clearly visible, prominent, rugose articular facets for the angular, the articular and the prearticular.

Angular

Only two angulars (Fig. 14A) have been discovered amongst the *Europasaurus* material. The angular of *Europasaurus* is an elongated bone, which shows a thicker ventral part and a paper-thin lamella on the dorsal side. It is very reminiscent to the angular of *Camarasaurus* (Madsen *et al.* 1995) as well as *Giraffatitan* (Janensch 1935–1936). In both preserved specimens the posteroventral branch of the dentary fits in the lateral indentation. However, most of the posterior section is lacking in the angulars. While the dentary attaches at the anterior end, the dorsal part is mostly in contact with the surangular. The medial side contacts the splenial and prearticular, while the posterior part contacts the surangular and articular. Despite the small size of angular DFMMh/FV 291.34, this is also regarded as being of morphotype A. The larger angular DFMMh/FV 1029 does not differ significantly from the small one in its overall morphology, apart from its size. The larger angular seems to have been diagenetically deformed on the upper third of its dorsal lamella, which bends medially at a 90° angle after the lateral facet for the posteroventral branch of the dentary. DFMMh/FV 1029 has a smoother bone surface structure and is therefore assigned stage 3 and morphotype A (Fig. 14A).

Ontogenetic changes. The main size-independent characters used here are bone surface structure and the shape of the articular facet for the dentary on its lateral side.

DFMMh/FV 291.34 is an almost complete small and gracile specimen. The lateral and medial hvbs structure suggests a young ontogenetic stage; it is thus assigned to MOS 1. The arrowhead-shaped articular facet for the posteroventral branch of the dentary is very shallow and not well pronounced though already visible.

No MOS 2 was recognized, whereas DFMMh/FV 1029 represents MOS 3. In the older staged specimen, which lacks most of its anterior and posterior parts, the bone surface is only vascularized in a small area on the dorsolateral side, but has few striations in the posterior half of the lateral side. The overall appearance is very robust and the medial side is much deeper, featuring a clearly visible groove for the splenial and prearticular attachments. A deep and well-pronounced articular facet is present in the dentary attachment on the lateral side. The ventral rim seems to have become much thicker during ontogeny.

Prearticular

The prearticulars within the *Europasaurus* material are all incomplete and only the posterior parts of these bones are preserved ([Fig. 14](#)). All have the form of elongated cylinders. The posterior parts of the prearticulars are more reminiscent of those of *Giraffatitan* (Janensch [1935–1936](#)) than of *Camarasaurus* (Madsen *et al.* [1995](#)). The middle section of the prearticular has a narrow groove that becomes a flat facet posteriorly; this facet supports the relatively loose contact to the articular.

Ontogenetic changes. Size-independent characters are bone surface structure, the absence or presence of the longitudinal groove, and the depression on the ventral side of the dorsolateral ridge. The morphology does not justify a differentiation into more than one morphotype. Morphotype A seems most applicable here, since one of the prearticulars belongs to the holotype material. Two elements assigned to MOS 2 are preserved, and one to MOS 3. No MOS was determined that would justify a staging for a juvenile.

MOS 2 is observed in DFMMh/FV 837.4. This bone lacks most of its anterior section and the posterior articular facet. The bone surface shows pronounced growth patterns, such as a vascularized bone surface structure with three larger foramina on the dorsal and ventral sides. No development of a longitudinal groove is visible but there is a slight depression of the preserved middle section, namely the dorsolateral and ventromedial margin of the prearticular. The dorsolateral ridge is straight rather than convex on the ventral side. Another substage (MOS 2.2) is represented by DFMMh/FV 520. Although this specimen lacks its anterior part as well, it has a complete articular facet, which has a very rugose surface. The bone surface shows striations in the anteroposterior direction. The longitudinal groove is well developed but there is no depression.

DFMMh/FV 291.24 represents MOS 3. This specimen lacks the anterior section as well. The longitudinal groove is deep and the depression on the ventral side of the dorsolateral ridge is present. The bone surface is very irregular

with no vascularization visible, showing a well-pronounced articular facet.

Splenial

The splenial, also known as the opercular (Romer [1956](#)), is a very thin bone on the medial surface of the lower jaw ([Fig. 14A](#)). It is rarely preserved in sauropods (Madsen *et al.* [1995](#)). The preserved *Europasaurus* splenial has a form similar to a tuning fork. It is a thin, nearly flat lamina that consists of: (1) an anteroposteriorly elongated and dorsoventrally short ventral part, and (2) a dorsal flange which emerges at the dorsal margin of the ventral section. The splenial is very similar to that of *Giraffatitan* (Janensch [1935–1936](#)). Most of the lateral part of the splenial contacts the medial side of the dentary. The ventral part, especially the posterior process, is in contact with the angular.

Ontogenetic changes. DFMMh/FV 100.1 is considered to represent MOS 3 and is the sole splenial found amongst *Europasaurus* material, but only its anterior part is preserved. There are no juvenile characters, such as an hvbs structure, and it fits quite well into dentary DFMMh/FV 291.11. It is therefore, most likely, of the same ontogenetic stage (3) and probably the same morphotype (A).

Intercoronoid

The coronoids are three separate bony plates of the lower jaw that can be found in basal tetrapods (Romer [1956](#)). These three plates are usually named according to their position within the mandible (Laurin [1998](#); Sulej & Majer [2005](#); Wilson [2005](#)). The bone preserved here has been termed complementare [sic] by Janensch ([1935–1936](#)), or intercoronoid by Madsen *et al.* ([1995](#)), Barrett *et al.* ([2005](#)) and Martinez & Alcober ([2009](#)). This study will follow the latter terminology. The preserved intercoronoids amongst the *Europasaurus* material are incomplete. Every intercoronoid lacks the elongated anterior part. Only the posterior sections that cover the interdental plates at the medial side in the posterodorsal part of the dentary are preserved. The intercoronoid resembles that of *Camarasaurus* (Madsen *et al.* [1995](#)) as well as that of *Giraffatitan* (Janensch [1935–1936](#)).

Ontogenetic changes. Besides the bone surface structure, size-independent characters include the absence or presence of the depression on its posterolateral side, the elevation of the posteromedial side, and the degree of robustness. Due to incomplete preservation, the morphotype cannot be determined in either specimen. One element is assigned to MOS 1 and one to MOS 2.

DFMMh/FV 1083 represents MOS 1. This deformed, tiny and extremely thin element of the lower jaw is preserved as the posterior attachment to the medial side of

the posterodorsal branch of the dentary. Most of its anterior part is missing. This gracile element shows small grooves and striations in an anteroposterior direction and seems to represent an early juvenile stage. The lateral depression is scarcely visible, while the medial bulge is not. At first glance it appears to be a right intercoronoid, but it is actually a deformed left one.

The second MOS is observed in DFMMh/FV 789. This specimen is preserved in a similar manner as the more juvenile specimen but it lacks its most posterodorsal peak. About 75% of the anterior section is missing. Compared to the other specimen, it is more robust. The bone surface lacks the deep grooves and instead is vascularized near the dorsal margin of the lateral side and along the entire medial side. The lateral depression is very prominent and the medial elevation is pronounced.

Accessory skull elements, the hyoid apparatus

In the mostly cartilaginous hyoid apparatus of reptiles there are two pairs of ceratobranchials (Fürbringer 1922), of which only the ossified first ceratobranchial can be preserved (Romer 1956). The first ceratobranchial is the same element termed the thyrohyal bone (Gilmore 1925; Madsen *et al.* 1995) or first hypobranchial (Janensch 1935–1936). The *Europasaurus* material consists of three first ceratobranchials.

Ceratobranchial. These rod-like elements show a well-preserved anterior articular facet, which is rounded or triangular, while the posterior articular facet in the largest element is flattened. The ceratobranchials closely resemble those of *Giraffatitan* (Janensch 1935–1936). The ceratobranchials are not in contact with any other bone element and, therefore, are mostly isolated in the field if found at all. Only the most mature specimen is complete; the other two lack most of the anterior part beyond the dorsomedial inflection point. Size-independent characters used are bone surface structure, the presence or absence of the medial longitudinal groove, and the appearance of the articular facet on the lateral side of the posterior end. The morphology in all ceratobranchials is too similar for them to be divided into different morphotypes. All three MOS are present.

The first MOS is observed in element DFMMh/FV 1034.2. The smallest specimen shows a structure with very prominent striations. The incomplete specimen has a gently curved inflection point. The medial longitudinal groove is not yet present and the posterior articular facet is not well defined due to a mainly cartilaginous terminal articulation.

MOS 2 is represented by specimen DFMMh/FV 187, an incomplete intermediate ceratobranchial with a very shallow inflection point which is barely visible compared to the other two. The bone surface structure shows less

vascularization but a clearly visible striation pattern. As in the smallest specimen, the medial longitudinal groove is not present. The posterior articular facet is slightly rugose.

DFMMh/FV 288 is a complete ceratobranchial of MOS 3 that has a relatively smooth external surface. The medial longitudinal groove, which might have been tied to cartilaginous parts of the hyoid apparatus, is visible. The lateral side of the posterior end shows an irregular facet that was probably connected to cartilage as well.

Skull reconstruction

Having staged the bone elements and determined the morphotypes, it is possible to reassemble bone elements of presumed adult growth stages into a new skull reconstruction. This new reconstruction differs in many respects from that of Laven (2001), and is a slightly modified version of the reconstruction presented by Sander *et al.* (2006). The new skull reconstruction (Fig. 1) lacks only a few skull bones, none of which are represented in the currently available material of *Europasaurus*.

In contrast to the older reconstructions, the new reconstruction represents an adult skull. Although elements of different morphological stages could form the skull of non-adult specimens (e.g. due to differences in growth rates amongst different bones of the skull), the use of morphologically mature isolated bones ensures that the elements will not be undergoing any drastic change in shape or size. Not all of the separate bones from the specimens used for the reconstruction fit together perfectly. Therefore, they had to be scaled and fitted around a central element – the jugal – paying particular attention to the size of the articulation surface. Although the new skull reconstruction is reminiscent of that published by Sander *et al.* (2006), it differs in several aspects. Since the publication of Sander *et al.* (2006), newly recovered elements have been added, including lacrimal pieces, the ectopterygoid, and nasal elements, which fit very well with the skull. Several elements were modified, such as the surangular, angular, premaxilla and the jugal process of the maxillary. The new reconstruction of the frontal and postorbital along with the modified jugal produces a larger orbit. Based on the current interpretation of the premaxilla nasal process, along with the new nasal elements, the external nares become smaller and protrude less. As noted for the premaxilla description, the nasal process is reinterpreted as having a posterodorsal orientation, similar to other sauropods, and the premaxilla does not protrude and therefore is no longer considered an autapomorphic character of *Europasaurus*.

Teeth were added to the premaxilla, maxilla and dentary. The teeth were arranged very close to each other, with a slight overlap of their crowns anteriorly and more spacing posteriorly. This accommodation of the teeth is mainly based on specimens DFMMh/FV 580.1 and

896.7.4, which preserve most of their teeth in position but without bone (Régent 2011).

Furthermore, the occiput region was replaced in the base of the new braincase DFMMh/FV 581.1. The new squamosal DFMMh/FV 712.2 of stage 3 attaches so perfectly to braincase DFMMh/FV 581.1 that we assume they were similarly sized individuals. Additionally, the quadratojugal of the holotype (DFMMh/FV 291.25) fits very well with quadrate DFMMh/FV 062 and squamosal DFMMh/FV 712.2. Except for quadrate DFMMh/FV 062, the maxilla and the quadratojugal of the holotype as well as the pterygoid of DFMMh/FV 100.2 were used in the old and new reconstructions. Although the braincase DFMMh/FV 581.1, to which the squamosal and the quadrate fit perfectly, are not part of the holotype, they are probably of an individual that must have been fairly similar in size and shape.

Discussion

Dwarfing evolution of *Europasaurus*

Amongst sauropodomorphs most evolutionary developmental studies have focused on gigantism, and more recently on dwarfing (e.g. Sander *et al.* 2006; Pereda Suberiola & Galton 2008; Stein *et al.* 2010). Whereas the typical sauropod quadrupedal posture was suggested to have evolved through paedomorphosis (Reisz *et al.* 2005), the extremely large size of these animals is considered to have evolved through peramorphosis (Long & McNamara 1997; Sander *et al.* 2004). The existence of dwarf sauropods was recently proved thanks to the use of histological studies that indicates the non-juvenile condition of small forms such as *Europasaurus* (Sander *et al.* 2006) and *Magyarosaurus* (Benton *et al.* 2010; Stein *et al.* 2011). This diminution of size was regarded as a product of paedomorphic processes (Benton *et al.* 2010), as also suggested in the evolution of modern birds (Bhullar *et al.* 2012).

In the course of this study, we observed that the results of the histological studies conducted by Sander *et al.* (2006) were in concordance with the dwarfing of *Europasaurus* seen in the skull material. Besides microscopical studies of histology, macroscopical examinations of bones have also proven valuable in determining the relative age, i.e. skeletal maturity (e.g. Callison & Quimby 1984; Varricchio 1997; Tumarkin-Deratzian 2007). As originally noted by Sander *et al.* (2006), all of the *Europasaurus* individuals, which were classified as sub-adults to adults, were considerably smaller than their relatives. With this morphological study of individuals ranging from juveniles to adults, along with additional descriptions of the axial skeleton (Carballido & Sander 2014), *Europasaurus* is confirmed to be a dwarf sauropod.

The complete description presented here provides a large amount of information on the skull morphology of the dwarf sauropod *Europasaurus holgeri*. The comparisons made with relevant and closely related taxa resulted in the recognition of some unusual characters for a camara-sauromorph sauropod, some of them interpreted as autapomorphic traits of *Europasaurus*. Some of these characters are discussed here with respect to their distribution amongst Sauropodomorpha and sauropod juvenile specimens.

Large participation of the jugal to the ventral edge of the skull and to the ventral margin of the orbit. The ontogenetic series of *Europasauurs* jugals represented by juvenile (MOS 1) and adult elements (MOS 3) shows that the participation of the jugal to the ventral margin of the skull decreased during ontogeny. The presence of this character in a morphologically mature jugal of *Europasaurus* indicates that this character is retained in adult specimens. As noted above, large participation of the jugal to the ventral margin of the skull is a widespread character amongst basal sauropodomorphs. In contrast, amongst sauropods, the maxilla–quadratojugal contact precludes jugal participation to the ventral margin of the skull; *Shunosaurus* (Chatterjee & Zheng 2002) and *Europasaurus* (this paper) are the only exceptions. Titanosaur embryos also have the plesiomorphic condition for sauropodomorphs with a large participation of the jugal to the ventral edge of the skull (see García *et al.* 2010). Additionally, titanosaur embryos also have a wide participation of the jugal to the ventral margin of the orbit, an unusual character for a sauropod dinosaur, but present in *Europasaurus* (García *et al.* 2010) and also in basal sauropodomorph dinosaurs. Therefore, both characters are considered autapomorphic traits of *Europasaurus* (see Emended diagnosis above), which are reminiscent of the morphology observed in basal sauropodomorphs and titanosaur juvenile specimens.

Anteroposteriorly long and lateromedially wide frontals with reduced articulations for the frontal and prefrontal. Whereas the frontals of eusauropod dinosaurs are characterized by being wider than long, those of adult specimens of *Europasaurus* show the plesiomorphic character state for Sauropodomorpha (Wilson & Sereno 1998) and titanosaur embryos (García *et al.* 2010), i.e. frontals longer than wide. The reduced articular surface for the nasal and prefrontal, which is caused by the deep orbital rim, has not been described for any other sauropodomorph and is therefore recognized as a unique autapomorphic character of *Europasaurus*. The implications of this character are discussed below.

Presence of a postparietal fenestra. The adult braincase and parietals of *Europasaurus* (DFMMh/FV 581.1–3) have a well-developed postparietal fenestra. Amongst sauropodomorphs the presence of this fenestra has been reported for dicraeosaurid sauropods (Salgado & Clavo

1992; Upchurch 1998; Wilson 2002), the basal sauropod *Spinophorosaurus* (Knoll *et al.* 2012), and a titanosaur indet. from the Late Cretaceous of Argentina. Thus, its presence in *Europasaurus* is considered an autapomorphic character convergently acquired by these taxa. This character is not described for early juvenile sauropods as no evidence is available. Nevertheless, its presence in adult dicraeosaurid sauropods is interpreted as retention of the juvenile morphology, as this gap in the skull roof is usually found in juvenile tetrapods (Salgado 1996).

Single optic foramen (II). The optic foramen of *Europasaurus* is not medially divided, as it is in most neosauropods. Therefore, *Europasaurus* seems to have reverted to the plesiomorphic condition of having a single optic foramina seen in basal sauropodomorphs and basal sauropods. Amongst neosauropods the presence of a single optic foramen has been described only in the diplodocoids *Suuwassea* (considered an autapomorphy of this taxon: Harris 2006) and *Diplodocus* (in some specimens only: Berman & McIntosh 1978), and is thus considered another autapomorphy of *Europasaurus*. The presence of a single opening for the optical nerve could possibly be related to the lack of ossification in the presphenoid, which was suggested to be present in *Diplodocus* (Berman & McIntosh 1978) and more recently in *Rapetosaurus* (Curry Rogers & Foster 2004), although not preserved in the latter.

Evolution of dwarfism is considered a product of progenesis, a paedomorphic process that halted morphological and size changes at an early stage. As a result, the progenetic adult will be smaller than the ancestor and will retain juvenile characters (McNamara 1986). Several unusual characters for a neosauropod dinosaur were described for morphologically mature specimens of *Europasaurus*; most are reversions to the ancestral condition observed amongst basal sauropodomorphs, and/or are reminiscent of the condition of early juvenile or embryonic sauropods. Therefore, the aforementioned autapomorphic characters are considered further evidence of the paedomorphic evolution that caused the dwarfing documented in *Europasaurus* (see Sander *et al.* 2006; Stein *et al.* 2010; Benton *et al.* 2010).

Additionally to the autapomorphic characters proposed here, other morphological peculiarities of the *Europasaurus* skull are probably a result of the dwarf condition of this taxon (discussed below). The lack of fusion in many skull bones of *Europasaurus* is also regarded as a result of heterochronic processes, such as paedomorphosis, which could be linked to dwarfing. A similar pattern (juvenile characters and lesser degree of ossification) was reported for *Archaeopteryx* and the evolution of birds (Martin 1991; Bhullar *et al.* 2012). In *Europasaurus*, this can be seen especially in the bones building the braincase, as well as some dermal bones such as the frontal and the parietal.

Furthermore, as a consequence of insular evolution, the snout region shortens, and in regards to the frontal bone, the orientation of the orbits results in a frontalization of the eye sockets (Bover *et al.* 2008). Both patterns are common amongst several island taxa of mammals and birds (Köhler, pers. comm.). Regarding the frontals, the reason for *Europasaurus* to evolve this autapomorphic character remains unclear. Perhaps the change from more monocular (or wide field of view) to binocular vision resulted from less predation pressure on islands. The slightly stereoscopic or rather binocular visual field would also have improved spatial depth perception (Palombo *et al.* 2006).

Ontogenetic changes in *Europasaurus*. Although all the *Europasaurus* material comes from the same locality, most of the cranial elements cannot be associated to each other. Without articulated specimens and a large histological database of long bones and ribs that can be undoubtedly associated with specific cranial material, surface texture analysis is the only reliable diagnostic method to determine relative ontogenetic stages for disarticulated skull bones in dinosaurs (e.g. Tumarkin-Deratzian 2009). The utility of surface texture of dinosaur bone is much more reliable in juveniles than it is in older individuals (Tumarkin-Deratzian 2009). But the seemingly juvenile and subadult skull bones represent a minority of the specimens. The reason could be that preservation is poorer; typically, juvenile specimens are highly fragile and sometimes not even fully ossified in the skull material. Also, the skull elements cannot provide evidence for when sexual maturity was reached. Still, growth series could be established for single bone types in the skull, and due to the sample range, size-independent characters could be included in this study to support the arguments reflected by bone surface structure and texture.

Little is known about ontogenetic processes in the cranium of sauropods. Ontogenetic studies of embryonic skulls of titanosaurs (Chiappe *et al.* 2001, 2005; Salgado *et al.* 2005) and a juvenile *Diplodocus* (Whitlock *et al.* 2010) demonstrate intense morphological modifications during ontogeny and reveal possible correlations of certain features of the sauropod skull structure: changes in relative size of the cranial openings, especially the orbits, which become smaller (Varricchio 1997); relative enlargement, retraction and elevation of the external nares; increase in relative muzzle width (Rauhut *et al.* 2011); and elongation of the snout, which is usually short in juveniles (Varricchio 1997; Salgado *et al.* 2005, but see Ikejiri *et al.* 2005). The morphology and morphometry of cranial structures do not seem to change dramatically through ontogeny in *Europasaurus* but rather follow a more modest remodelling of the craniofacial skeleton, as described for *Camarasaurus* by Ikejiri (2004) and Ikejiri *et al.* (2005). In *Europasaurus*, fusion of skull bones is only observed in the partial braincases, the occiput region,

and also in those bones that usually fuse in late ontogeny and have bone surfaces indicating skeletal maturity, for example, the frontals and parietals (Madsen *et al.* 1995). The adult skull remains in a neotenic state, with prominent, distinctive juvenile features of the cranium still present, such as the autapomorphic characters.

The two different morphotypes of *Europasaurus*

Dimorphism can be recognized in adequate population samples of taxa by a divergence of biometric characters during ontogeny (Darwin 1871). Within Sauropodomorpha, dimorphism, with 'robust' and 'gracile' forms, has been documented in the postcranial material of the sauropodomorphs *Thecodontosaurus*, *Plateosaurus*, *Melanorosaurus* and *Neuquensaurus* (Isles 2009; Salgado *et al.* 2005; Otero 2010). Interestingly, these robust forms are less frequent than the gracile ones (see also Klein 2004). In *Europasaurus*, the more robust morphotype B also appears less frequently than the more gracile morphotype A.

Amongst sauropods, Klein & Sander (2008) recognized two morphotypes in *Camarasaurus*, one morphotype being small and the other large; it has been suggested that they either represent two separate species or different sexes. Sexual and size dimorphisms are abundant throughout extant vertebrate and invertebrate populations (Isles 2009). Several explanations, including the aforementioned ones, have been put forth to explain dimorphism in *Europasaurus*:

1. Ontogenetic differences. As the results have shown, there are ontogenetic differences within the skull elements of *Europasaurus*, but the frontal and the jugal illustrate that the two morphotypes appear in the same ontogenetic stages and are also more evident in ontogenetically young individuals. Therefore, the occurrence of the two different morphotypes must have another origin.

2. Sexual dimorphism. The differences in size and structural details may represent the two sexes in *Europasaurus*. One problem with trying to determine sexual dimorphic characters is that they are generally correlated with ontogeny (Ikejiri 2004). Determining the sex of sauropods remains a desirable but rather challenging quest (Chapman *et al.* 1997; Carpenter 1999). With statistical analyses of skeletal material hampered by small sample sizes and preservation bias (Isles 2009), sexual dimorphism has not yet been demonstrated unequivocally in any species of sauropod. Morphological differences at the species level that cannot be explained by ontogeny or sexual dimorphism, as suggested by Pagnac (1998), are considered to be due to intraspecific variation.

3. Individual variation. McIntosh *et al.* (1996), Ikejiri (2004) and Ikejiri *et al.* (2005) pointed out that several features in the skull transformation of *Camarasaurus* during ontogeny possibly reflect individual variations rather than exhibiting ontogenetic changes in the cranial elements.

4. Population variation. If the differences between the two morphotypes are not due to sexual or individual variation, another alternative explanation is that the smaller and gracile morphotype A and the larger and more robust morphotype B might represent different species or subspecies. There is a significant uncertainty about how much time was involved in the deposition of the layer where the *Europasaurus* material was found (Sander *et al.* 2006). So the factor of time plays a role and the changes in morphology could be due to chronological separation.

5. Although more unlikely, the *Europasaurus* material might also be from different islands in the same region, and therefore, geographical separation could have triggered dimorphism. The two morphotypes could also represent individuals of populations that exploited different ecological niches in response to different distributions of, for example, resources and competitors.

Of these hypotheses, the most likely explanations for the two morphotypes are either sexual dimorphism or a single species separated in time or space. Sexual dimorphism, however, has been rarely studied in sauropods (Ikejiri 2004; Ikejiri *et al.* 2005), and less so based on cranial elements alone. Sauropods lack substantial evidence from morphology (e.g. display structures), histology (e.g. medullary bone), and soft tissue preservation to suggest sexual dimorphism.

Although the presence of two species cannot be completely ruled out (see Carballido & Sander 2014), this is an unlikely explanation. First, all the collected material assigned to *Europasaurus* has minor morphological differences, which can be well explained as ontogenetic changes, not drastic changes which may suggest another taxon. Second, and most important, all the characters used here to diagnose *Europasaurus* are observed in all the diagnostic bones preserved and recovered from the quarry, as was also discussed for the axial elements (Carballido & Sander 2014). We presume *Europasaurus* is a single species but, unfortunately, the dataset is still insufficient enough to test any hypothesis, especially from cranial material alone.

Does a single specimen represent the holotype of *Europasaurus*?

All the cranial holotype material was assigned to an adult animal (Sander *et al.* 2006). Similarly, the axial and most of the skull elements were identified as adult specimens (Carballido & Sander 2014; and here). Three skull elements are assigned, with some uncertainty, to an adult

specimen and therefore indicate the presence of more than one specimen.

The smaller of the two angulars, DFMMh/FV 291.34, is less mature than most of the holotype material of the skull (which mostly corresponds to MOS 3) and also, and most importantly, from a specimen of a different size than the rest of the holotype. Therefore this element was excluded from the holotype, as it obviously represents another individual, less mature and smaller than the holotype. In a similar way, the laterosphenoid + orbitosphenoid (DFMMh/FV 291.16) was revealed to be morphotype B, and not morphotype A like the rest of the holotype skull material, and therefore excluded from the holotype material.

The exclusion of a less morphologically mature premaxilla is not as obvious. The premaxilla DFMMh/FV 291.18 is staged here as MOS 2 and is therefore morphologically less mature than most of the skull holotype material (of MOS 3). Nevertheless, the size difference between this premaxilla and the adult (MOS 3) maxilla of the holotype is not as evident. Currently, there is no evidence that all the skull bones have the same growth rate or that they will mature at the same moment in a single specimen. Conversely, due to allometries well documented in the vertebrate skull during its development from juvenile to adult, the different bones of the skull finish growing at different times. This will result in a single specimen with different MOS in different elements. The same was noted for the axial skeleton (Carballido & Sander 2014), in which neurocentral closure varied depending on the section (i.e. cervical, dorsal, caudal; Irmis 2007; Gallina 2011). Therefore, even though the MOS is different, we include the premaxilla as part of the holotype.

Conclusions

The dwarf sauropod *Europasaurus* provides the largest sample size of skull material for an ontogenetic study in any sauropod taxon. The information presented here not only offers more insights on the skull anatomy of the dwarfed sauropod *Europasaurus holgeri*, but also provides further information for skull reconstruction in this taxon, which was made on the basis of a single morphotype and with only morphologically mature elements. The presence of different ontogenetic stages amongst the *Europasaurus* material provides for the first time reliable information on the main skull transformations and anatomical changes in *Europasaurus*. Different morphological ontogenetic stages (MOS) with different relative age classes are determined for nearly every element. Two morphotypes, A and B, are recognized with the MOS. These two differently shaped morphotypes seem to differ only in their relative sizes, sharing the same combination of characters as well as autapomorphic traits as a whole. Morphotype B is the larger one of the two and seems to

be under-represented amongst the material, probably indicating population differences. The reason for the observed dimorphism, which is documented in the axial remains as well, remains problematical. Different hypotheses are presented here (e.g. sexual dimorphism, individual variation, two populations, or species separated in time or space). Finally, detailed descriptions and comparisons of each bone with closely related taxa, as well as with more basal and also derived sauropods, has led to the recognition of a large number of paedomorphic characters within the skull of *Europasaurus*. Some of the most prominent, distinctive features of the cranium are the extensive participation of the jugal to the ventral rim of the skull roof; the relatively large orbit in the adult (which remains in a neotenic state); the presence of parietal and postparietal foramina; and the relatively short snout of the adult. Along with the lack of fusion in many bones in the adult skull, these features reflect heterochronic processes related to dwarfing.

Supplemental data

Supplemental material for this article can be accessed here: http://dx.doi.org/10.1080/14772019.2013.875074

References

Alberch, P., Gould, S. J., Oster, G. F. & Wake D. B. 1979. Size and shape in ontogeny and phylogeny. *Paleobiology*, **5**, 296–317.

Allain, R. & Aquesbi, N. 2008. Anatomy and phylogenetic relationships of Tazoudasaurus naimi (Dinosauria, Sauropoda) from the late Early Jurassic of Morocco. *Geodiversitas*, **30**, 345–424.

Apesteguía, S. 2004. *Bonitasaura salgadoi:* a beaked sauropod in the Late Cretaceous of Gondwana. *Naturwissenschaften*, **91**, 493–497.

Balanoff, A. M., Bever, G. S. & Ikejiri, T. 2010. The braincase of *Apatosaurus* (Dinosauria: Sauropoda) based on Computed Tomography of a new specimen with comments on variation and evolution in sauropod neuroanatomy. *American Museum Novitates*, **3677**, 1–29.

Bandyopadhyay, S., Gillette, D. D., Ray, S. & Sengupta, D. P. 2010. Osteology of *Barapasaurus tagorei* (Dinosauria: Sauropoda) from the Early Jurassic of India. *Palaeontology*, **53**, 533–569.

Barrett, P. M., Upchurch, P. & Wang, X.–L. 2005. Cranial osteology of *Lufengosaurus huenei* Young (Dinosauria: Prosauropoda) from the Lower Jurassic of Yunnan, People's Republic of China. *Journal of Vertebrate Paleontology*, **25**, 806–822.

Benton, M. J., Csiki, Z., Grigorescu, D., Redelstorff, R., Sander, P. M., Stein, K. & Weishampel, D. B. 2010. Dinosaurs and the island rule: the dwarfed dinosaurs from Haţeg Island. *Palaeogeography, Palaeoclimatology, Palaeoecology*, **293**, 438–454.

Berman, D. S. & McIntosh, J. S. 1978. Skull and relationships of the Upper Jurassic sauropod *Apatosaurus* (Reptilia, Saurischia). *Bulletin of the Carnegie Museum of Natural History*, **8**, 1–35.

Bhullar, B-A. S., Marugán, J., Racimo, F., Bever, G. S., Rowe, T. B., Norell, M. A. & Abzhanov, A. 2012. Birds have paedomorphic dinosaur skulls. *Nature*, **487**, 223–226.

Bonaparte, J. F. 1986. The early radiation and phylogenetic relationships of sauropod dinosaurs, based on vertebral anatomy. Pp. 247–258 in K. Padian (ed.) *The Beginning of the Age of Dinosaurs*. Cambridge University Press, Cambridge.

Bonaparte, J. F. & Pumares, J. A. 1995. Notas sobre el primer craneo de *Riojasaurus incertus* (Dinosauria, Prosauropoda, Melanorosauridae) del Triasico superior de La Rioja, Argentina. *Ameghiniana*, **32**, 341–349.

Bover, P., Quintanab, J. & Alcoverc, J. A. 2008. Three islands, three worlds: paleogeography and evolution of the vertebrate fauna from the Balearic Islands. *Quaternary International*, **182**, 135–144.

Britt, B. B. & Naylor, B. G. 1994. An embryonic *Camarasaurus* (Dinosauria, Sauropoda) from the Upper Jurassic Morrison Formation (Dry Mesa Quarry, Colorado). Pp. 256–264 in K. Carpenter, K. Hirsch & J. R. Horner (eds) *Dinosaur eggs and babies*. Cambridge University Press, Cambridge.

Brochu, C. A. 1996. Closure of neurocentral sutures during crocodilian ontogeny: implications for maturity assessment in fossil archosaurs. *Journal of Vertebrate Paleontology*, **16**, 49–62.

Buffetaut, E., Suteethorn, V., Cuny, G., Tong, H., Le Leouff, J., Khansubha, S. & Jongautchariyakul, S. 2000. The earliest known sauropod dinosaur. *Nature*, **407**, 72–74.

Calvo, J. O. & Salgado, L. 1995. *Rebbachisaurus tessonei* sp. nov. a new Sauropoda from the Albian–Cenomanian of Argentina; new evidence on the origin of the Diplodocidae. *GAIA*, **11**, 13–33.

Calvo, J. O. & González Riga, B. J. 2003. *Rinconsaurus caudamirus* gen. et sp. nov., a new titanosaurid (Dinosauria, Sauropoda) from the Late Cretaceous of Patagonia, Argentina. *Revista Geológica de Chile*, **30**, 333–353.

Callison, G. & Quimby, H. M. 1984. Tiny dinosaurs: Are they fully grown?. *Journal of Vertebrate Paleontology*, **3**, 200–209.

Carpenter, K. & Tidwell, V. 2005. Reassessment of the Early Cretaceous sauropod Astrodon johnsoni Leidy 1865 (Titanosauriformes). Pp 78–114 in V. Tidwell & K. Carpenter (eds) *Thunderlizards: the sauropodomorph dinosaurs*. Indiana University Press, Bloomington and Indianapolis.

Carballido, J. L., Marpmann, J. S., Schwarz–Wings, D. & Pabst, B. 2012. New information on a juvenile sauropod specimen from the Morrison Formation and the reassessment of its systematic position. *Palaeontology*, **55**, 567–582.

Carballido, J. L., Pol, D., Cerda, I. & Salgado, L. 2011a. The osteology of *Chubutisaurus insignis* Del Corro, 1975 (Dinosauria: Neosauropoda) from the "middle" Cretaceous of central Patagonia, Argentina. *Journal of Vertebrate Paleontology*, **31**, 93–110.

Carballido, J. L., Rauhut, O. W. M., Pol, D. & Salgado, L. 2011b. Osteology and phylogenetic relationships of *Tehuelchesaurus benitezii* (Dinosauria, Sauropoda) from the Upper Jurassic of Patagonia. *Zoological Journal of the Linnean Society*, **163**, 605–662.

Carballido, J. L. & Sander, M. P. 2014. Postcranial axial skeleton of *Europasaurus holgeri* (Dinosauria, Sauropoda) from the Upper Jurassic of Germany: implications for sauropod ontogeny and phylogenetic relationships of basal Macronaria. *Journal of Systematic Palaeontology*, **3**, 335–387.

Carpenter, K. 1999. *Eggs, nests, and baby dinosaurs*. Indiana University Press, Bloomington, 372 pp.

Carpenter, K. & McIntosh, J. 1994. Upper Jurassic sauropod babies from the Morrison Formation. Pp. 265–278 in K. Carpenter, K. Hirsch & J. R. Horner (eds) *Dinosaur eggs and babies*. Cambridge University Press, Cambridge.

Carpenter, K. & Tidwell, V. 1998. Preliminary description of a *Brachiosaurus* skull from Felch Quarry 1, Garden Park, Colorado. *Modern Geology*, **23**, 69–84.

Carpenter, K. & Tidwell, V. 2005. Reassessment of the Early Cretaceous sauropod *Astrodon johnsoni* Leidy 1865 (Titanosauriformes). Pp 78–114 in V. Tidwell & K. Carpenter (eds) *Thunderlizards: the sauropodomorph dinosaurs.* Indiana University Press, Bloomington and Indianapolis.

Cerda, I. A., Pol, D. & Chinsamy, A. 2014. Osteohistological insight into the early stages of growth in *Mussaurus patagonicus* (Dinosauria, Sauropodomorpha). *Historical Biology*, **26**, 110–121.

Chapman, R. E., Weishampel, D. B., Hunt, G. & Rasskin–Gutman, D. 1997. Sexual dimophism in dinosaurs. Pp. 83–93. in D. L. Wolberg, E. Stump & G. D. Rosenberg (eds) *Dinofest International*. Academy of Natural Sciences, Philadelphia.

Chatterjee, S. & Zheng, Z. 2002. Cranial anatomy of Shunosaurus, a basal sauropod dinosaur from the Middle Jurassic of China. *Zoological Journal of the Linnean Society*, **136**, 145–169.

Chiappe, L. M., Salgado, L. & Coria, R. A. 2001. Embryonic skulls of titanosaur sauropod dinosaurs. *Science*, **293**, 2444–2446.

Chiappe, L. M., Jackson, F. D., Coria, R. A. & Dingus, L. 2005. Nesting titanosaurs from Auca Mahuevo and adjacent sites: understanding sauropod reproductive behavior and embryonic development. Pp. 285–302 in K. A. Curry Rogers

& J. A. Wilson (eds) *The Sauropods: Evolution and Paleobiology*. University of California Press, Berkeley.

Chure, D., Brooks, B. B., Whitlock, J. A. & Wilson, J. A. 2010. First complete sauropod dinosaur skull from the Cretaceous of the Americas and the evolution of sauropod dentition. *Naturwissenschaften*, **97**, 379–391.

Clauss, M. 2011. Sauropod biology and the evolution of gigantism: what do we know? Pp. 3–7 in N. Klein, K. Remes, C. T. Gee & P. M. Sander (eds) *Biology of the Sauropod Dinosaurs: Understanding the Life of Giants*. Indiana University Press, Bloomington and Indianapolis.

Coria, R. A. 1994. On a monospecific assemblage of sauropod dinosaurs from Patagonia: implications for gregarious behavior. *Gaia*, **10**, 209–215.

Curry Rogers, K. A. & Forster, C. A. 2001. The last of the dinosaur titans: a new sauropod from Madagascar. *Nature*, **412**, 530–534.

Curry Rogers, K. A. & Forster, C. 2004. The skull of *Rapetosaurus krausei* (Sauropoda: Titanosauria) from the Late Cretaceous of Madagascar. *Journal of Vertebrate Paleontology*, **24**, 121–144.

Curry Rogers, K. A. 2005. Titanosauria: a phylogenetic overview. Pp. 50–103 in K. A. Curry Rogers, K. A. & J. A. Wilson (eds) *The Sauropods: Evolution and Paleobiology*. University of California Press, Berkeley and Los Angeles.

Curry Rogers, K. A. & Forster, C. A. 2009. The postcranial osteology of Rapetosaurus krausei (Sauropoda: Titanosauria) from the Late Cretaceous of Madagascar. *Journal of Vertebrate Paleontology*, **29**, 1046–1086.

Darwin, C. 1871. *The Descent of Man, and Selection in Relation to Sex*. John Murray, London, 450 pp.

D'Emic, M. D. 2012. The early evolution of titanosauriform sauropod dinosaurs. *Zoological Journal of the Linnean Sociey*, **166**, 624–671.

Díez Díaz, V., Pereda Suberbiola, X. & Sanz, J. L. 2012. Juvenile and adult teeth of the titanosaurian dinosaur *Lirainosaurus* (Sauropoda) from the Late Cretaceous of Iberia. *Geobios*, **45**, 265–274.

Dong, Z. 1990. Sauropoda from the Kelameili Region of the Junggar Basin, Xinjiang Autonomous Region. *Vertebrata PalAsiatica*, **28**, 43–58.

Fastovsky, D. E. & Weishampel, D. B. 2005. *Sauropodomorpha: the big, the bizarre, and the majestic. Lifestyles of the huge and ancient*. 2nd edition. Cambridge University Press, Cambridge.

Foster, J. R. 2005. New juvenile sauropod material from Western Colorado, and the record of juvenile sauropods from the Upper Jurassic Morrison Formation. Pp. 141–153 in V. Tidwell & K. Carpenter (eds) *Thunder–Lizards: The Sauropodomorph Dinosaurs*. Indiana University Press, Bloomington.

Fürbringer, M. 1922. Das Zungenbein der Wirbeltiere insbesondere der Reptilien und Vögel. Nachgelassene Untersuchungen über die systematische Phylogenie mit besonderer Berücksichtigung der Wurzel der Säugetiere. *Abhandlungen der Heidelberger Akademie der Wissenschaften, Mathematisch–Naturwissenschaftliche Klasse*, **11**, 3–164.

Gallina, P. A. 2011. Notes on the axial skeleton of the titanosaur Bonitasaura salgadoi (Dinosauria-Sauropoda). *Annals of the Brazilian Academy of Sciences*, **83**, 235–246.

Gallina, P. A. & Apesteguía, S. 2011. Cranial anatomy and phylogenetic position of the titanosaurian sauropod *Bonitasaura salgadoi*. *Acta Paleontologica Polonica*, **56**, 45–60.

Gallina, P. A. 2011. Notes on the axial skeleton of the titanosaur *Bonitasaura salgadoi* (Dinosauria-Sauropoda). *Anais da Academia Brasileira de Ciências*, **83**, 235–246.

Galton, P. M. & Upchurch, P. 2004. Prosauropoda. Pp. 232–258 in D. B. Weishampel, P. Dodson & H. Osmólska (eds) *The Dinosauria*. University of California Press, Berkeley.

Galton, P. M. 1984. Cranial anatomy of the prosauropod dinosaur *Plateosaurus* from the Knollenmergel (Middle Keuper, Upper Triassic) of Germany. I. Two complete skulls from Trossingen/Württemberg with comments on the diet. *Geologica et Palaeontologica*, **18**, 139–171.

Galton, P. M. 1985. Cranial anatomy of the prosauropod dinosaur *Plateosaurus* from the Knollenmergel (Middle Keuper, Upper Triassic) of Germany. II. All the cranial material and details of soft–part anatomy. *Geologica et Palaeontologica*, **19**, 119–159.

García, R., Salgado, L., Coria, R. A. & Chiappe, L. M. 2010. Osteología embrionaria de saurópodos titanosaurios de Neuquén (Argentina): aspectos ontogenéticos y evolutivos. *Ameghiniana*, **47**, 409–430.

Gilmore, C. W. 1925. A nearly complete articulated skeleton of *Camarasaurus*, a saurischian from the Dinosaur National Monument, Utah. *Memoirs of the Carnegie Museum*, **10**, 347–384.

Gomani, E. M. 2005. Sauropod dinosaurs from the Early Cretaceous of Malawi, Africa. *Palaeontologia Electronica*, **1**, 37 pp.

Gow, C. E., Kitching, J. W. & Raath, M. A. 1990. Skulls of the prosauropod dinosaur *Massospondylus carinatus* Owen in the collections of the Bernard Price Institute for Palaeontological Research. *Palaeontologia Africana*, **27**, 45–58.

Harris, J. D. 2006. Cranial osteology of *Suuwassea emilieae* (Sauropoda: Diplodocoidea: Flagellicaudata) from the Upper Jurassic Morrison Formation of Montana, USA. *Journal of Vertebrate Paleontology*, **26**, 88–102.

Harris, J. D. & Dodson, P. 2004. A new diplodocoid sauropod dinosaur from the Upper Jurassic Morrison Formation of Montana, USA. *Acta Palaeontologica Polonica*, **49**, 197–210.

Hatcher, J. B. 1903. Osteology of *Haplocanthosaurus* with description of a new species, and remarks on the probable habits of the Sauropoda, and the age and origin of the *Atlantosaurus beds*. *Memoirs of the Carnegie Museum*, **2**, 1–72.

Hummel, J. & Clauss, M. 2011. Sauropod feeding and digestive physiology. Pp. 11–33 in N. Klein, K. Remes, C. T. Gee & P. M. Sander (eds) *Biology of the Sauropod Dinosaurs: Understanding the Life of Giants*. Indiana University Press, Bloomington.

Ikejiri, T. 2004. *Anatomy of Camarasaurus lentus (Dinosauria: Sauropoda) from the Morrison Formation (Late Jurassic), Thermopolis, Central Wyoming, with determination and interpretation of ontogenetic, sexual dimorphic, and individual variation in the genus*. Unpublished MSc thesis, State University, Fort Hays, 311 pp.

Ikejiri, T., Tidwell, V. & Trexler, D. 2005. New adult specimens of *Camarasaurus lentus* highlight ontogenetic variation within the species. Pp. 154–179 in V. Tidwell & K. Carpenter (eds) *Thunder–Lizards. The Sauropodomorph Dinosaurs*. Indiana University Press, Bloomington.

Irmis, R. B. 2007. Axial skeleton ontogeny in the Parasuchia (Archosauria: Pseudosuchia) and its implications for ontogenetic determination in archosaurs. *Journal of Vertebrate Paleontology*, **27**, 350–361.

Isles, T. E. 2009. The socio–sexual behaviour of extant archosaurs: implications for understanding dinosaur behaviour. *Historical Biology*, **21**, 139–214.

Janensch, W. 1935–1936. Die Schädel der Sauropoden *Brachiosaurus*, *Barosaurus* und *Dicraeosaurus* aus den Tendaguru–Schichten Deutsch–Ostafrikas. *Palaeontographica*, **2** (Supplement to 7), 147–298.

Klein, N. 2004. *Bone histology and growth of the prosauropod dinosaur Plateosaurus engehardti Meyer 1837 from the Norian bonebeds of Trossingen (Germany) and Frick (Switzerland)*. Unpublished PhD thesis, University of Bonn, 128 pp.

Klein, N. & **Sander, M.** 2008. Ontogenetic stages in the long bone histology of sauropod dinosaurs. *Paleobiology*, **34**, 247–263.

Knoll, F., Witmer, L. M., Ortega, F., Ridgely, R. C. & **Schwarz–Wings, D.** 2012. The braincase of the basal sauropod dinosaur *Spinophorosaurus* and 3D reconstructions of the cranial endocast and inner ear. *PLoS ONE*, **7**, e30060.

Knoll, F. & **Schwarz-Wings, D.** 2009. Palaeoneuroanatomy of *Brachiosaurus*. *Annales de Paléontologie*, **95**, 165–175.

Ksepka, D. T. & **Norell, M. A.** 2010. The illusory evidence for Asian Brachiosauridae: new material of *Erketu ellisoni* and a phylogenetic reappraisal of basal Titanosauriformes. *American Museum Novitates*, **3700**, 1–27.

Laurin, M. 1998. The importance of global parsimony and historical basis in understanding tetrapod evolution. Part I. Systematics, middle ear evolution and jaw suspension. *Annales des Sciences Naturelles*, **1**, 1–42.

Laven, T. 2001. *Kraniale Osteologie eines Sauropoden (Reptilia, Saurischia) aus dem Oberjura Norddeutschlands und dessen phylogenetische Stellung*. Unpublished Diploma thesis, Johannes–Gutenberg–Universität, 171 pp.

Lehmann, T. M. & **Coulson, A. B.** 2002. A juvenile specimen of the sauropod dinosaur *Alamosaurus sanjuanensis* from the Upper Cretaceous of Big Bend National Park, Texas. *Journal of Paleontology*, **76**, 156–172.

Long, J. A. & **McNamara, K. J.** 1997 Heterochrony. Pp. 311–317 in P. J. Currie & K. Padian (eds) *Encyclopedia of dinosaur*. Academic Press, San Diego.

Madsen, J. H., McIntosh, J. S. & **Berman, D. S**. 1995. Skull and atlas–axis complex of the Upper Jurassic sauropod *Camarasaurus* Cope (Reptilia: Saurischia). *Bulletin of the Carnegie Museum of Natural History*, **31**, 1–115.

Mahammed, F., Läng, E., Mami, L., Mekahli, L., Benhamou, M., **Bouterfa, B. Kacemi, A., Chérief, S. A., Chaouati, H.** & **Taquet, P.** 2005. The 'Giant of Ksour', a Middle Jurassic sauropod dinosaur from Algeria. *Comptes Rendus Paleovol*, **4**, 707–714.

Mannion, P. D. & **Upchurch, P.** 2010. Completeness metrics and the quality of the sauropodomorph fossil record through geological and historical time. *Paleobiology*, **36**, 283–302.

Mannion, P. D. 2011. A reassessment of *Mongolosaurus haplodon* Gilmore, 1933, a titanosaurian sauropod dinosaur from the Early Cretaceous of Inner Mongolia, People's Republic of China. *Journal of Systematic Palaeontology*, **9**, 355–378.

Mannion, P. D., Upchurch, P., Barnes, R. N. & **Mateus O.** 2013. Osteology of the Late Jurassic Portuguese sauropod dinosaur *Lusotitan atalaiensis* (Macronaria) and the evolutionary history of basal titanosauriforms. *Zoological Journal of the Linnean Society*, **168**, 98–206.

Martin, V. 1991. Mesozoic birds and the origin of birds. Pp. 485–540 in H. P. Schultze & L. Trueb (eds) *Origins of the higher groups of tetrapods*. Cornell University, Ithaca.

Martin, V. 1994. Baby sauropods from the Sao Khua Formation (Lower Cretaceous) in Northeastern Thailand. *Gaia*, **10**, 147–153.

Martin, V., Buffetaut, E. & **Suteethorn, V.** 1994. A new genus of sauropod dinosaur from the Sao Khua Formation (Late Jurassic or Early Cretaceous) of northeastern Thailand. *Comptes Rendus, l'Académie des Sciences de Paris*, **319**, 1085–1092.

Martin, V., Suteethorn, V. B. & **Buffetaut, E.** 1999. Description of the type and referred material of *Phuwiangosaurus sirinhornae* Martin, Buffetaut and Suteethorn, 1994, a sauropod from the Lower Cretaceous of Thailand. *Oryctos*, **2**, 39–91.

Martinelli, A. G. & **Forasiepi, A. M.** 2004. Late Cretaceous vertebrates from Bajo de Santa Rosa (Allen Formation), Río Negro province, Argentina, with the description of a new sauropod dinosaur (Titanosauridae). *Revista de Museo Argentino Ciencias Naturales*, **6**, 257–305.

Martinez, R. N. & **Alcober, O. A.** 2009. A basal sauropodomorph (Dinosauria: Saurischia) from the Ischigualasto Formation (Triassic, Carnian) and the early evolution of Sauropodomorpha. *PLoS ONE*, **4**, e4397.

Mateer, N. J. & **McIntosh, J. S.** 1985. A new reconstruction of the skull of *Euhelopus zdanskyi* (Saurischia:Sauropoda). *Bulletin of the Geological Institutions of the University of Uppsala, new series*, **11**, 25–132.

McIntosh, J. S., Miles, C. A., Cloward, K. C. & **Parker, J. R**. 1996. A new nearly complete skeleton of *Camarasaurus*. *Bulletin of Gunma Museum of Natural History*, **1**, 1–87.

McNamara, K. J. 1986. A guide to the nomenclature of heterochrony. *Journal of Paleontology*, **60**, 4–13

Monbaron, M., Russell, D. A. & **Taquet, P.** 1999. *Atlasaurus imelakei* n. g., n. sp., a brachiosaurid–like sauropod from the Middle Jurassic of Morocco. *Comptes Rendus de l'Académie des Sciences Series IIA, Sciences de la Terre et des Planètes*, **329**, 519–526.

Nowinski, A. 1971. *Nemegtosaurus mongoliensis* n. gen., n. sp., (Sauropoda) from the uppermost Cretaceous of Mongolia. *Palaeontologica Polonica*, **25**, 57–81.

Osborn, H. F. 1899. A skeleton of *Diplodocus*. *Memoirs of the American Museum of Natural History*, **1**, 189–214.

Otero, A. 2010. The appendicular skeleton of Neuquensaurus, a Late Cretaceous saltasaurine sauropod from Patagonia, Argentina. *Acta Palaeontologica Polonica*, **55**, 399–426.

Ouyang, H. & **Ye, Y.** 2002. *The first mamenchisaurian skeleton with complete skull:* Mamenchisaurus youngi. Chengdu, Sichuan Science and Technology Press, 88 pp. [In Chinese with English summary].

Pagnac, D. C. 1998. *Variation within the pectoral region and its implications concerning species level taxonomy of the North American sauropod, Camarasaurus Cope*. Unpublished MSc thesis, South Dakota School of Mines and Technology, 192 pp.

Palombo, M. R., Bover, P., Valli, A. F. M. & **Alcover, J. A.** 2006. The Plio–Pleistocene endemic bovids from the Western Mediterranean islands: knowledge, problems and perspectives. *Hellenic Journal of Geosciences*, **41**, 153–162.

Paulina Carabajal A. & **Salgado, L.** 2007. El basicráneo de un titanosaurio (Dinosauria, Sauropoda) del Cretácico Superior del norte de Patagonia: descripción y aportes al conocimiento del oído interno de los dinosaurios. *Ameghiniana*, **44**, 109–120.

Paulina Carabajal, A. 2012. Neuroanatomy of titanosaurid dinosaurs from the Upper Cretaceous of Patagonia, with comments on endocranial variability within Sauropoda. *The Anatomical Record*, **295**, 2141–2156.

Paulina Carabajal, A., **Carballido J. L.** & **Currie, P.** In press. Braincase neuroanatomy and neck posture of *Amargasaurus cazaui* (Sauropoda: Dicraeosauridae) and its implications for understanding head posture in sauropods. *Journal of Vertebrate Paleontology*.

Pereda-Suberbiola, X. & **Galton, P. M.** 2009. Dwarf dinosaurs in the latest Cretaceous of Europe?. Pp. 263–272 in Colectivo Arqueológico-Paleontológico Salense (ed.) *Actas, IV*

Jornadas Internacionales sobre Paleontología de Dinosaurios y su Entorno. Salas de los Infantes (Burgos, Spain).

Pol, D. & **Powell, J. E.** 2007. Skull anatomy of *Mussaurus patagonicus* (Dinosauria: Sauropodomorpha) from the Late Triassic of Patagonia. *Historical Biology*, **19**, 125–144.

Powell, J. E. 1992. Osteologia de *Saltasaurus loricatus* (Sauropoda-Titanosauridae) del Cretácico Superior del Noroeste argentine. Pp. 165–230 in J. L. Sanz & A. D. Buscalioni (eds) *Los Dinosaurios y su Entorno Biotico*. Instituto "Juan de Valdes", Cuenca.

Rauhut, O. W. M., **Fechner, R.**, **Remes, K.** & **Reis, K.** 2011. How to get big in the Mesozoic: the evolution of the sauropodomorph body plan. Pp. 119–149 in N. Klein, K. Remes, C. T. Gee & P. M. Sander (eds) *Biology of the Sauropod Dinosaurs: Understanding the Life of Giants*. Indiana University Press, Bloomington and Indianapolis.

Régent, V. 2011. *Die Bezahnung des Zwergsauropoden* Europasaurus holgeri *aus dem Oberjura Norddeutschlands – ontogenetische und funktionelle Muster*. Unpublished Diploma thesis, University of Bonn, 102 pp.

Reisz, R. R., **Scott, D.**, **Sues, H. D.**, **Evans, D. C.** & **Raath, M. A.** 2005. Embryos of an Early Jurassic prosauropod dinosaur and their evolutionary significance. *Science*, **309**, 761–764.

Remes, K. 2006. Revision of the Tendaguru sauropod dinosaur *Tornieria africana* (Fraas) and its relevance for sauropod paleobiogeography. *Journal of Vertebrate Paleontology*, 26, 651–669

Remes, K. 2009. Taxonomy of Late Jurassic diplodocid sauropods from Tendaguru (Tanzania). *Fossil Record*, **12**, 23–46.

Romer, A. S. 1956. *The Osteology of the Reptiles*. University of Chicago Press, Chicago. Illinois, 772 pp.

Royo Torres, R. & **Upchurch, P.** 2012. The cranial anatomy of the sauropod *Turiasaurus riodevensis* and implications for its phylogenetic relationships. *Journal of Systematic Palaeontology*, **10**, 553–583.

Salgado, L. & **Calvo, J. O.** 1992. Cranial osteology of *Amargasaurus cazaui* Salgado and Bonaparte (Sauropoda, Dicraeosauridae) from the Neocomian of Patagonia. *Ameghiniana*, **29**, 337–346.

Salgado, L. 1996. The macroevolution of the Diplodocimorpha (Dinosauria; Sauropoda): a developmental model. *Ameghiniana*, **36**, 203–216.

Salgado, L., **Coria, R.** & **Calvo, J. O.** 1997. Evolution of titanosaurid sauropods. I: phylogenetic analysis based on the postcranial evidence. *Ameghiniana*, **34**, 3–32.

Salgado, L. & **Azpilicueta, C.** 2000. Un nuevo saltasaurino (Sauropoda, Titanosauridae) de la provincia de Río Negro (Formación Allen, Cretácico Superior), Patagonia, Argentina. *Ameghiniana*, **37**, 259–264.

Salgado, L., Garrido, A. C., Cocca, S. E. & **Cocca, J. R.** 2004. Lower Cretaceous rebbachisaurid sauropods from Cerro Aguada del León (Lohan Cura Formation), Neuquén Province, Northwestern Patagonia, Argentina. *Journal of Vertebrate Paleontology*, **24**, 903–912.

Salgado, L., Coria, R. A. & **Chiappe, L. M.** 2005. Osteology of the sauropod embryos from the Upper Cretaceous of Patagonia. *Acta Palaeontologica Polonica*, **50**, 79–92.

Salgado L., **Canudo J. I.**, **Garrido A.** & **Carballido J. L.** 2012. Evidence of gregariousness in Rebbachisauridae (Dinosauria, Sauropoda, Diplodocoidea) in the Early Cretaceous of Neuquén (Rayoso Formation), Patagonia, Argentina. *Journal of Vertebrate Paleontology*, **32**, 603–613

Sampson, S. D., Ryan, M. J. & **Tanke, D. H.** 1997. Craniofacial ontogeny in centrosaurine dinosaurs (Ornithischia: Ceratopsidae): taxonomic and behavioral implications. *Zoological Journal of the Linnean Society*, **121**, 293–337.

Sander, P. M., **Klein, N.**, **Buffetaut, E.**, **Cuny, G.**, **Suteethorn, V.** & **Le Loeuff, J.** 2004. Adaptive radiation in sauropod dinosaurs: Bone histology indicates rapid evolution of giant body size through acceleration. *Organisms, Diversity & Evolution*, **4**, 165–173.

Sander, P. M., Christian, A., Clauss, M., Fechner, R., Gee, C. T., Griebeler, E.–M., Gunga, H.–C., Hummel, J., Mallison, H., Perry, S. F., Preuschoft, H., Rauhut, O. W. M., Remes, K., Tütken, T., Wings, O. & **Witzel, U.** 2010. Biology of the sauropod dinosaurs: the evolution of gigantism. *Biological Reviews*, 86, 117–155.

Sander, P. M. & **Clauss, M.** 2008. Sauropod gigantism. *Science*, **322**, 200–201.

Sander, P. M. & **Klein, N.** 2005. Developmental plasticity in the life history of a prosauropod dinosaur. *Science*, **310**, 1800–1802.

Sander, P. M., Klein, N., Stein, K. & **Wings, O.** 2011. Sauropod bone histology and its implications for sauropod biology. Pp. 276–302 in N. Klein, K. Remes, C. T. Gee & P. M. Sander (eds) *Biology of the Sauropod Dinosaurs: Understanding the Life of Giants*. Indiana University Press, Bloomington and Indianapolis.

Sander, P. M., Mateus, O., Laven, T. & **Knötschke, N.** 2006. Bone histology indicates insular dwarfism in a new Late Jurassic sauropod dinosaur. *Nature*, **441**, 739–741.

Sereno, P. C., Beck, A. L., Dutheil, D. B., Larssen, H. C. E., Lyon, G. H., Moussa, B., Sadleir, R. W., Sidor, C. A., Varricchio, D. J., Wilson, G. P. & **Wilson, J. A.** 1999. Cretaceous sauropods from the Sahara and the uneven rate of skeletal evolution among dinosaurs. *Science*, 286, 1342–1347.

Schulte, P., Alegret, L., Arenillas, I., Arz, J. A., Barton, P. J., Bown, P. R., Bralower, T. J., Christeson, G. L., Claeys, P., Cockell, C. S., Collins, G. S., Deutsch, A., Goldin, T. J., Goto, K., Grajales–Nishimura, J. M., Grieve, R. A. F., Gulick, S. P. S., Johnson, K. R., Kiessling, W., Koeberl, C., Kring, D. A., MacLeod, K. G., Matsui, T., Melosh, J., Montanari, A., Morgan, J. V., Neal, C. R., Nichols, D. J., Norris, R. D., Pierazzo, E., Ravizza, G., Rebolledo–Vieyra, M., Reimold, W. U., Robin, E., Salge, T., Speijer, R. P., Sweet, A. R., Urrutia–Fucugauchi, J., Vajda, V., Whalen, M. T. & **Willumsen, P. S.** 2010. The Chicxulub asteroid impact and mass extinction at the Cretaceous–Paleogene boundary. *Science*, 327, 1214–1218.

Schwarz, D., Ikejiri, T., Breithaupt, B. H., Sander, P. M. & **Klein, N.** 2007. A nearly complete skeleton of an early juvenile diplodocid (Dinosauria: Sauropoda) from the Lower Morrison Formation (Late Jurassic) of north central Wyoming and its implications for early ontogeny and pneumaticity in sauropods. *Historical Biology*, **19**, 225–253.

Schmitt, A. D. 2012. *The inner ear of diplodocoid and basal macronarian sauropods: vestibular adaptation and paleobiological implications*. Unpublished Diploma thesis, University of Bonn, 82 pp.

Seeley, H. G. 1887. The classification of the Dinosauria. *Geological Magazine*, **3**, 562.

Sereno, P. C., Wilson, J. A., Witmer, L. M., Whitlock, J. A., Maga, A., Ide, O. & **Rowe, T. A.** 2007. Structural extremes in a Cretaceous dinosaur. *PLoS ONE* **2**: e1230. doi:10.1371/journal.pone.0001230.

Stein, K., Csiki, Z., Rogers, K. C., Weishampel, D. B., Redelstorff, R., Carballido, J. L. & **Sander, P. M.** 2010. Small body size and extreme cortical bone remodeling indicate phyletic dwarfism in *Magyarosaurus dacus*

(Sauropoda: Titanosauria). *Proceedings of the National Academy of Sciences of the United States of America*, **107**, 9258–9263.

Stein, K., **Csiki, Z.**, **Curry-Rogers, K.**, **Weishampel, D. B.**, **Redelstorff, R.**, **Carballido, J. L.** & **Sander, P. M.** 2010. Small body size and extreme cortical bone remodeling indicate phyletic dwarfism in Magyarosaurus dacus (Sauropoda: Titanosauria). *Proceedings of the National Academy of Sciences of the United States of America*, **107**, 9258–9263.

Sues, H.–D., Reisz, R., Hinic, S. & **Raath, M. A.** 2004. On the skull of *Massospondylus carinatus* Owen, 1854 (Dinosauria: Sauropodomorpha) from the Elliot and Clarens Formations (Lower Jurassic) of South Africa. *Annals of Carnegie Museum*, **73**, 239–257.

Sulej, T. & **Majer, D.** 2005. The temnospondyl amphibian *Cyclotosaurus* from the Late Triassic of Poland. *Palaeontology*, **48**, 157–170.

Suteethorn, S., Le Loeuff, J., Buffetaut, E., Suteethorn, V., Talubmook, C. & **Chonglakmani, C.** 2009. A new skeleton of *Phuwiangosaurus sirindhornae* (Dinosauria, Sauropoda) from NE Thailand. *Geological Society of London, Special Publications*, **315**, 189–215.

Tang, F., Jin, X., Kang, X. & **Zhang, G.** 2001. [*Omeisaurus maoianus* a complete Sauropoda from Jingyan, Sichuan]. *Research works of Natural History Museum of Zhejiang*, **10**, 1–127. [In Chinese with English summary].

Tschopp, E. & **Mateus, O.** 2013. The skull and neck of a new flagellicaudatan sauropod from the Morrison Formation and its implication for the evolution and ontogeny of diplodocid dinosaurs. *Journal of Systematic Palaeontology*, **11**, 853–888.

Tumarkin-Deratzian, A. R. 2007. Fibrolamellar bone in wild adult Alligator mississippiensis. *Journal of Herpetology*, **41**, 341–345.

Tumarkin–Deratzian, A. R. 2009. Evaluation of long bone surface textures as ontogenetic indicators in centrosaurine ceratopsids. *The Anatomical Record*, **292**, 1485–1500.

Upchurch, P. 1995. Evolutionary history of sauropod dinosaurs. *Philosophical Transactions of the Royal Society of London B*, **349**, 365–390.

Upchurch P. 1998. The phylogenetic relationships of sauropod dinosaurs. *Zoological Journal of the Linnean Society*, **124**, 43–103.

Upchurch, P., Barrett, P. M. & **Dodson, P.** 2004. Sauropoda. Pp. 259–322 in D. B. Weishampel, P. Dodson & H. Osmólska (eds) *Dinosauria*. University of California Press, Berkeley.

Upchurch, P., **Mannion, P. D.**, **Benson, R. B. J.**, **Butler, R. J.** & **Carrano, M. T.** 2011. Geological and anthropogenic controls on the sampling of the terrestrial fossil record: a case study from the Dinosauria. *Special Publications of the Geological Society of London*, **358**, 209–240.

Varricchio, D. J. 1997. Growth and embryology. Pp. 282–288 in P. J. Currie & K. Padian (eds) *Encyclopedia of Dinosaurs*. Academic Press, San Diego.

von Huene, F. 1932. Die fossil Reptil-Ordnung Saurischia, ihre Entwicklung und Geschichte. *Monographen zur Geologie und Palaeontologie*, **4**, 1–361.

Wedel, M. J. & **Taylor. P. M.** 2013. Neural spine bifurcation in sauropod dinosaurs of the Morrison Formation: ontogenetic and phylogenetic implications. *PalArch's Journal of Vertebrate Palaeontology*, **10**, 1–34.

Whitlock, J. A., Wilson, J. A. & **Lamanna, M. C**. 2010. Description of a nearly complete juvenile skull of *Diplodocus* (Sauropoda: Diplodocoidea) from the Late Jurassic of North America. *Journal of Vertebrate Paleontology*, **30**, 442–457.

Whitlock, J. A. 2011. A phylogenetic analysis of Diplodocoidea (Saurischia: Sauropoda). *Zoological Journal of the Linnean Society*, **161**, 872–915.

Wilson, J. A. 2002. Sauropod dinosaur phylogeny: critique and cladistic analysis. *Zoological Journal of the Linnean Society*, **136**, 215–275.

Wilson, J. A. 2005. Redescription of the Mongolian sauropod *Nemegtosaurus mongoliensis* Nowinski (Dinosauria: Saurischia) and comments on Late Cretaceous sauropod diversity. *Journal of Systematic Palaeontology*, **3**, 283–318.

Wilson, J. A. & **Sereno, P. C**. 1998. Early evolution and higher–level phylogeny of sauropod dinosaurs. *Journal of Vertebrate Paleontology*, **18**, 1–68.

Wilson, J. A. & **Upchurch, P.** 2003. A revision of *Titanosaurus* Lydekker (Dinosauria – Sauropoda), the first dinosaur genus with a "Gondwanan" distribution. *Journal of Systematic Palaeontology*, **1**, 125–160.

Wilson, J. A. & **Upchurch, P.** 2009. Redescription and reassessment of the phylogenetic affinities of *Euhelopus zdanskyi* (Dinosauria: Sauropoda) from the Early Cretaceous of China. *Journal of Systematic Palaeontology*, **7**, 199–239.

Witmer, L. M. & **Ridgely, R.** 2009. New insights into the brain, braincase, and ear region of *Tyrannosaurus* (Dinosauria, Theropoda), with implications for organization and behavior. *The Anatomical Record*, **292**, 1266–1296.

Witmer, L. M., Ridgely, R. C., Dufeau, D. L. & **Semones, C.** 2008. Using CT to peer into the past: 3D visualization of the brain and ear regions of birds, crocodiles, and nonavian dinosaurs. Pp. 67–87 in H. Endo & R. Frey (eds) *Anatomical Imaging: Towards a New Morphology*. Springer–Verlag, Tokyo.

Woodruff, D. C. & **Fowler, D.** 2012. Ontogenetic influence on neural spine bifurcation in Diplodocoidea (Dinosauria: Sauropoda): A critical phylogenetic character. *Journal of Morphology*, **273**, 754–764.

Yates, A. M. 2007. The first complete skull of the Triassic dinosaur *Melanorosaurus* Haughton (Sauropodomorpha: Anchisauria). *Special Papers in Palaeontology*, **77**, 9–55.

Yates, A. M. & **Kitching, J. W.** 2003. The earliest known sauropod dinosaur and the first step towards sauropod locomotion. *Proceedings of the Royal Society, Series B*, **270**, 1753–1758.

Zaher, H., Pol, D., Carvalho, A. B., Nascimento, P. M., Riccomini, C., Larson, P., Juarez–Valieri, R., Pires–Domingues, R., Silva, N. J. & **Campos, D. A.** 2011. A complete skull of an Early Cretaceous sauropod and the evolution of advanced titanosaurians. *PLoS ONE*, **6**, e16663.

Zheng, Z. 1991. Morphology of the braincase of *Shunosaurus*. *Vertebrata PalAsiatica*, **29**, 108–118. [In Chinese with English summary].